universität wien

MASTERARBEIT / MASTER'S THESIS

Titel der Masterarbeit / Title of the Master's Thesis

„The N-end rule pathway in *Arabidopsis thaliana*"

verfasst von / submitted by

Telser Theresia, BSc

angestrebter akademischer Grad / in partial fulfilment of the requirements for the degree of

Master of Science (MSc)

Wien, 2020 / Vienna, 2020

Studienkennzahl lt. Studienblatt / degree programme code as it appears on the student record sheet:	UA 066 834
Studienrichtung lt. Studienblatt / degree programme as it appears on the student record sheet:	Masterstudium Molekulare Biologie
Betreut von / Supervisor:	Univ.-Prof. Mag. Dr. Andreas Bachmair

Acknowledgements

First, I would like to thank my supervisor Univ.-Prof. Mag. Dr. Andreas Bachmair for giving me the opportunity to work on this interesting project. I am very thankful for the knowledge and experience he gave to me, for his encouragement and patience.

Further, I would like to thank Nikola Winter and Lilian Nehlin for their support and guidance from the very beginning. They were amazing colleagues with a great deal of patience and readiness for help. They supported me during this time in the lab and outside, took over for me when I did not make it to the lab. Help was always there when it was needed.

My sincere thanks go to Marie-Therese Kurzbauer and Fabian Künzl for their help and advices for microscopy; and to Silvia and Lisi for the great time together.

My lifetime thanks to my family. Most of all I want to express my deep gratitude to my parents, Otto and Monika, and to my sister Daniela for all their constant support and encouragement through all the years of my studies. Danke für alles!

Contents

I. Abstract

Plants as sedentary organisms cannot escape stressful situations. Therefore, they are more dependent on transcriptional control, posttranslational modifications and protein homeostasis to maintain an intact metabolism and to react to changes in their environment. Two important protein degradation pathways and their regulation play an essential role in this process, the autophagy and the ubiquitin-26S proteasome degradation pathways.

The N-end rule degradation pathway as part of the ubiquitin-proteasome system sets the half-life of a peptide in relation to its N-terminal amino acid. Two N-recognins in plants are known, PRT1 and PRT6, which lead to the degradation of primary destabilizing amino acids. The binding protein of Leu and Ile, also belonging to this category of amino acids, has not yet been identified.

The present work deals with the characterization of possible candidates as N-recognin for Leu and Ile N-terminal peptides discovered in an EMS-induced mutant screening. ATG10 as part of the autophagy cascade showed the strongest correlation between a homozygous genotype and the stabilization of the reporter construct L-GUS. The frequently discussed candidate BIG was also examined in an ONPG assay. A certain activity could not be detected for this protein, although a stabilization of the L-GUS construct could be shown in a T-DNA insertion line concerning exon 5 of the protein.

In addition to the characterization of N-recognin candidates, the establishment of tandem fluorescence timers was aimed at to enable a temporal and spatial investigation of the protein degradation pathway at the cellular level. Since the first experiment did not lead to an expression of the constructs, it was not possible to study transformed plants of the second experiment due to time constraints.

II. Zusammenfassung

Pflanzen als sessile Organismen können Stresssituationen nicht entfliehen. Somit sind sie stärker auf Transkriptionskontrolle, posttranslationale Modifikationen und Proteinhomöostase angewiesen, um einen intakten Metabolismus aufrecht zu erhalten und um auf Veränderungen in ihrer Umwelt reagieren zu können. Zwei wichtige Proteinabbauwege und deren Regulation spielen dabei eine essenzielle Rolle, zum einen die Autophagie, zum anderen das Ubiquitin-26S-Proteasom-System

Der N-end rule Abbauweg als Teil des Ubiquitin-Proteasom-Systems setzt die Halbwertszeit eines Peptids in Abhängigkeit zu seiner N-terminalen Aminosäure. Zwei N-recognine in Pflanzen sind bekannt, PRT1 und PRT6, die zum Abbau von primären destabilisierenden Aminosäuren führen. Das Bindeprotein von Leu und Ile, ebenfalls zu dieser Kategorie von Aminosäuren zählend, wurde bisher noch nicht identifiziert.

Die vorliegende Arbeit befasst sich mit der Charakterisierung von möglichen Kandidaten als N-recognin für Leu und Ile N-terminale Peptide, die infolge eines EMS induzierten Mutatenscreenings entdeckt wurden. ATG10 als Teil der Autophagie- Kaskade zeigte dabei die stärkste Korrelation zwischen einem homozygoten Genotyp und der Stabilisierung des Reporterkonstrukts L-GUS. Ebenso wurde der häufig diskutierte Kandidat BIG in einem ONPG assay untersucht. Eine bestimmte Aktivität konnte für dieses Protein jedoch nicht nachgewiesen werden, obwohl in einer T-DNA Insertionslinie, betreffend das Exon 5 des Proteins, eine Stabilisierung des L-GUS Konstrukts nachgewiesen werden konnte.

Neben der Charakterisierung von N-recognin Kandidaten wurde die Etablierung von Tandem Fluoreszenz Timern angestrebt, um eine zeitliche und räumliche Untersuchung des Proteinabbauwegs auf zellulärer Ebene zu ermöglichen. Da der erste Versuch zu keiner Expression der Konstrukte führte, war es auf Grund von zeitlichen Beschränkungen nicht mehr möglich, transformierte Pflanzen des zweiten Versuchs zu untersuchen.

III. Abbreviations

A. thaliana	*Arabidopsis thalian*
A. tumefaciens	*Agrobacterium tumefaciens*
AIM	ATG8-interacting motif
ALP	Autophagy-lysosome pathway
APC	Anaphase-promoting E3 complex
ASA1	Attenuated shade avoidance1
AUX	Auxin transporter proteins
BC	Back cross
Brtz	Bortezomib
BTB	Bric-a-brac-tramtrack-broad complex
c16/cand16	Candidate 16
CAB	Chlorophyll a/b binding proteins
CDS	Coding sequence
CIS1	CO_2 insensitive 1
CMA	Chaperone-mediated autophagy
Col-0	Columbia-0
ConA	Concanamycin A
CP	Core particle
CRD	Cysteine rich domain
CRL	Cullin-RING ligases
CRM1	Corymbosa1
CUL	Cullin
dCAP	Derived Cleaved Amplified Polymorphic Sequence
DDB	DNA damage-binding
Dex	Dexamethasone
DNA	Desoxyribonucleic acid
dNTP	Desoxyribonucleic acid triphosphate
DOC1	Darkoverexpression of CAB1
DUB	Deubiquitylating enzymes
E. coli	*Escherichia coli*
EMS	Ethyl methanesulfonate
FP	Fluorescence Protein

GFP	Green Fluorescence Protein
GUS	β-Glucuronidase
HECT	Homology to E6-AP C-Terminus
HRP	Horse Radish Peroxidase
IBR	InBetweenRING
JA	Jasmonate
LAX	Auxin-like proteins
LeuOMet	Leucine O-Methyl Ester:
L-GUS	β-glucuronidase with N-terminal Leu
LHC	Light harvesting complex
LPR1	Low phosphate-resistant root1
MetAP	Methionine aminopeptidase
NBP	NPA binding protein
NPA	N-1-naphthylphthalamic acid
ONPG	Ortho-Nitrophenyl-β-galactoside
PAS	Phagophore assembly site
PAT	Polar auxin transport
PCD	Programmed cell death
PCR	Polymerase Chain Reaction
PIN	PIN-FORMED
PRT	Proteolysis
PTM	Posttranslational modification
RBR	Ring between Ring
RING	Really interesting new gene
RP	Regulatory particle
S. cerevisiae	*Saccharomyces cerevisiae*
SA	Salicylic acid
SCF	S-phase kinase-associated protein 1 – Cullin 1 – F-box
sfGFP	Superfolder Green Fluorescence Protein
tFT	Tandem fluorescent protein timer
TIR3	Transport-inhibitor Response3
Ub	Ubiquitin
UBA	Ubiquitin Activating Enzyme
UBC	Ubiquitin Conjugating Enzyme
UBR	Ubiquitin Recognition (component)

UMB1	Umbrella1
UPS	Ubiquitin-26S proteasome system
WT	Wildtype
YFP	Yellow Fluorescence Protein
βgal	β-galactosidase

IV. List of tables

V. List of figures

1 Introduction

1.1 Protein homeostasis in plants

Plants as sessile organisms are more dependent on transcriptional control and post-translational modifications (PTMs) to respond to changes in their environment and to adapt to stress situations than organisms that can move and escape. Also, during different developmental stages PTMs such as methylation, acetylation, phosphorylation and ubiquitination are essential for cell division and growth (Shu and Yang, 2017; Vierstra, 2009).

One crucial point for maintaining protein homeostasis is the control of stability and half-life of proteins to regulate the abundance of key regulatory proteins and enzymes. In eukaryotes, two major pathways are known to be essential, 1) the autophagy-lysosome pathway (ALP) and 2) the ubiquitin-26S proteasome pathway (UPS) (Dikic, 2017).

ALP is responsible for the degradation of potentially dangerous cell components like insoluble protein aggregates, dysfunctional proteins or organelles and for proteins involved in cellular stress responses (Chen et al., 2019).

Three different types are distinguished, all delivering their cargo to the lytic vacuole i) micro-autophagy, ii) macro-autophagy and iii) chaperone-mediated autophagy (CMA).

In this work, the main focus is on macro-autophagy, described as the major form and referred to as autophagy. Proteins intended for degradation are included in double-membrane vesicles called autophagosomes. This formation of a phagophore starts at the phagophore assembly site (PAS) and expands to sequester the cargo into these vesicles. Delivered to the vacuole, the outer membrane fuses with the tonoplast and releases the inner membrane and cargo into the acidic compartment. This single membrane vesicle is now called autophagic body. The degradation there is mediated by hydrolases and proteases (Kim et al., 2012, Chen et al., 2019).

Micro-autophagy in plants on the other hand is poorly understood. Here, the membrane of the vacuole invaginates the cargo intended for degradation, forming a vesicle in the inside; whereas the existence of the third type, CMA, has not been proven yet in plants (van Doorn and Papini, 2013).

During starvation conditions, autophagy acts as nonselective degradation pathway to mobilize nutrients, during programmed cell death (PCD) induced by pathogens or senescence as recycling machinery. As well as mediating unspecific degradation processes, it also can be

selective in recognising the cargo by specific receptors binding to Atg8 required for the formation and expansion of autophagosomal membranes. These receptors such as AtNBR1 (At4g24690) are characterized by the ATG8-interacting motif (AIM) (van Doorn and Papini, 2013, Chen et al., 2019).

The UPS on the other hand removes short-lived, misfolded or damaged proteins. Furthermore, it is connected to the regulation of cellular pathways such as cell cycle, proliferation, survival or apoptosis due to its impact on the regulation of transcription and cell signalling. Its important role in protein turnover is reflected in the genome of *Arabidopsis thaliana*, a plant model organism. Over 6% of the genome are connected to the UPS (Downes and Vierstra, 2005).

For long time, it was assumed that these two protein turnover systems ALP and UPS are distinct and don't interact, but an extensive communication between the two degradation pathways is pivotal for protein homeostasis. Especially studies in mammalian cells have shown that one interface is the mTOR protein kinase, a key activator in starvation conditions. During nutrient replenishment it inhibits autophagy and induces the formation of proteasomes, during starvation it acts on contrary to mobilize nutrients stored as proteins to provide amino acids for essential metabolic functions (Dikic, 2017). An overload in the UPS mediated degradation leads to an increase of autophagy, while in long term inhibition of the autophagic machinery, UPS can cope (Shaid et al., 2013). In plant cells, the detailed interactions are not fully enlightened, but an increase of proteasome activity has been observed in *atg* mutants and vice versa, an increase in proteasomal activity was shown if autophagy is inhibited (Wang and Schippers, 2019).

Another point of intersection of selective autophagy and UPS mediated degradation is the substrate labelling. In both pathways, the protein meant to be degraded can be tagged with ubiquitin (ub), a small ubiquitous protein. This process is called ubiquitylation or ubiquitination.

In this work, the focus is set on the UPS system in plants to elucidate its function and impact on the metabolism with special attention to the N-end rule pathway, a subgroup determining the half-life of a protein via its N-terminus.

1.2 The UPS in plants

Ubiquitin (Ub) is a 76 amino acids long protein of 8.5kDa (Figure 1 A). It is highly conserved in eukaryotes with only two or three amino acids difference between mammals, plants and yeast (Callis, 2014). Its structure is described as ubiquitin fold (Pickart and Eddins, 2004), a β-grasp fold characterised by four β-strands and one α-helix (Figure 1 B) (Burroughs et al. 2007).

For ubiquitination, an isopeptide bond is formed between the ε-amino group of a lysine within the target protein and the C-terminal glycine of Ub.

Besides these Glycine-Lysine linkages, Ub can also be conjugated through the methionine residue located at the N-terminus forming linear chains (Vierstra, 2009, Shaid et al. 2013). So far, there is no proof for an existence of this kind of ubiquitination in *A. thaliana* (Walsh and Sadanandom, 2014).

The seven internal Lys residues as possible acceptation sites for further Ub moieties, define the ubiquitination code and allow the formation of various chains. Linkages formed at the positions Lys48 and Lys63 are the most abundant. Lys48 chains are leading to the degradation through the 26S proteasome, K63 concatenations are connected to selective autophagy and signalling (Erpapazoglou et al., 2014, Romero-Barrios and Vert, 2017). Besides proteolysis-dependent functions, ubiquitination as a reversible PTM acts in diverse signalling cascades; for example, mono-ubiquitination at Histone H2A (H2Aub1) and Histone H2B (H2Bub1) is a hallmark of epigenetic changes in eukaryotes leading to transcriptional repression or activation (Feng and Shen, 2014).

Deubiquitylating enzymes (DUBs) are hydrolases cleaving ubiquitin moieties from the target contributing to the repeated use of the small protein and preventing it from degradation. Around 50 different DUBs have been identified in *Arabidopsis.* Located at the proteasome, these enzymes allow the recycling of the Ub and shortening Ub chains (Isono and Nagel, 2014).

On the cellular level, three different Ub pools are distinguished: i) free Ub, ii) activated Ub bound to enzymes via a thioester and iii) conjugated Ub, bound to the ε-amino group of a Lys on proteins (Clague et al., 2015).

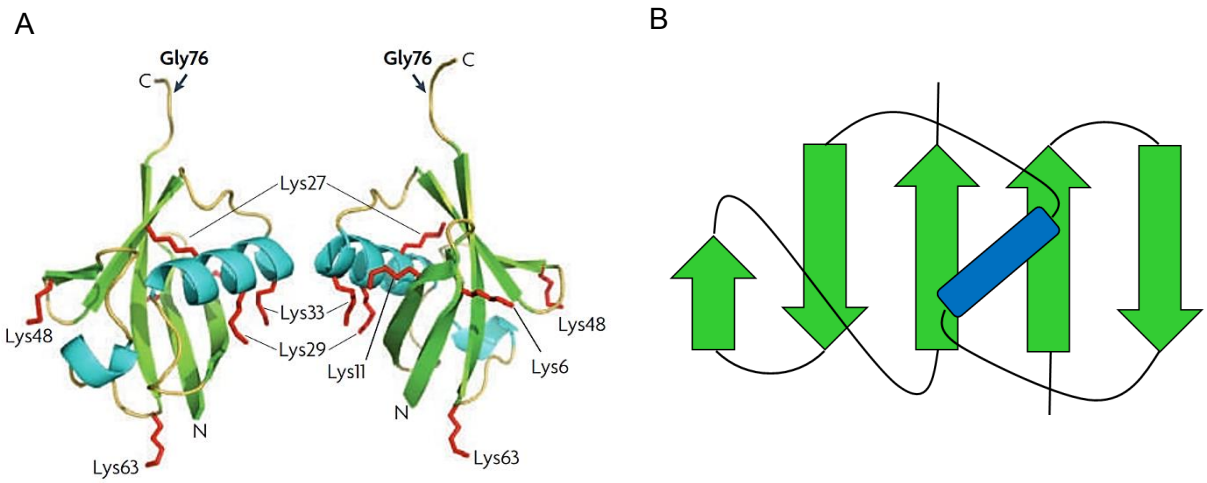

Figure 1 Ubiquitin. A) 3D structure of Ub. Between Gly76 and the ε-amino group of a Lys an isopeptide bond is formed leading to the ubiquitination of the target protein. Here, the seven Lys residues as possible target sites for concatenation are shown. Lys48 and Lys 63 are the most common target sites for ubiquitination leading to the degradation through the UPS or ALP pathway. In plants, Lys27 has not been described as Ub linkage site. (Callis, 2014). Figure reprinted from Vierstra (2009) B) ribbon model of the β-grasp fold (Ubiquitin-like) as a combination of five antiparallel β-strands and a single α-helix. Figure based on Burroughs et al. (2007).

Three categories of proteins play the major role in regulating the identification of a substrate and its ubiquitination leading to its degradation through the 26S proteasome (Figure 2).

The enzymatic cascade starts with a Ub activating enzyme, called E1 or UBA. Using an ATP molecule, a thioester linkage between a Cys on the active site of E1 and the Gly76 on the C-terminus of a Ub molecule is formed. In *Arabidopsis*, the two known E1s are encoded from the two genes AtUBA1 and AtUBA2 having about 80% amino acid sequence identity. Through the high conservation of the UPS system in eukaryotes, the two proteins show also a high sequence similarity to E1s identified in other organisms (Hatfield et al., 1997).

This Ub binding leads to structural rearrangements in the E1, increasing the binding affinity of a ubiquitin conjugating enzyme, E2 or UBC. After binding, a transesterification leads to the transfer of the ubiquitin from E1 to E2, releasing E1 (Clague et al., 2015). In *Arabidopsis*, 37 different UBCs have been identified so far. In these proteins (Vierstra, 2009), a ~150-200 amino acid long region is conserved, the so called UBC domain (Kraft et al., 2005). It comprises the active Cys accepting the Ub from the E1. E2s are also responsible for the elongation of Ub chains and concatenations, some are lacking the ability of chain initiation (Ye and Rape, 2009).

The activity of ubiquitin ligases (E3) defines the last step in the cascade by identifying and marking the substrate with ub molecules on a Lys residue. Numerous hormone receptors act as ubiquitin ligases, so the ubiquitin system has an essential impact in the regulation of signalling cascades or the plant metabolism leading to the degradation of key proteins. More than 1000 different ubiquitin ligases are predicted in *Arabidopsis* referring to its high specificity and importance in protein homeostasis (Mazzucotelli et al., 2006).

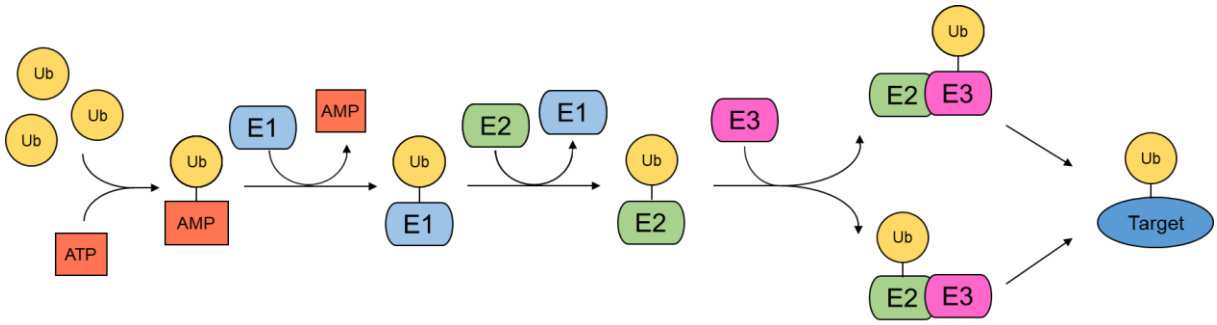

Figure 2 The Ubiquitin-26S proteasome system. In the initial reaction, Ub is activated in an ATP-consuming reaction forming a high energy thioester bond between the Cys in the active site of E1 and the Gly76 at the C-terminus of Ub. As consequence from the resultant structural changes, an E2 accepts the Ub through a transesterification reaction. Depending on the category of the E3, Ub is either accepted from the E2 as interim target, or it is directly transferred from the E2 to the ε-amino group of Lys on the protein target site mediated by the E3.
This process of ubiquitination is either reversible by cleaving off the UB moiety by the action of DUBs or leads to the degradation of the target protein through the 26S proteasome. Here, DUBs process polyUb chains into Ub monomers, and together with the amino acids from the degraded protein, they are released from the proteasome and are re-used.
Figure modified according to Vierstra (2009) and Shu and Yang (2017).

Three main categories of E3s can be classified. Depending on their E2 interaction sites and the presence of different domains they are named HECT (Homology to E6-AP C-Terminus) E3 ligases, RING (Really interesting new gene)/U-box E3 ligases (Mazzucotelli et al., 2006) and, as a combination between HECT and RING/U-box E3 ligases, RING-BetweenRING-RING (RBR) E3 ligases.

i) HECT E3 ligases (Figure 3A)

Only seven known E3 ligases belong to this class of single polypeptides in *Arabidopsis* comprising a HECT domain as UBC interaction site. Ub interacts directly by being attached covalently to a Cys residue at the HECT domain, forming a thioester intermediate before being transferred to the Lys residue on the target protein (Vierstra, 2009).

ii) RING or U-box E3 ligases (Figure 3B)

A much larger group of E3s is characterized by a RING or the structurally similar U-box domain forming the E2 interaction site. RING motifs contain eight Cys or His residues stabilized by two zinc ions, while U-box motifs are formed by hydrogen bonding networks within the ~70 amino acids long domain (Ohi et al., 2003). In contrast to HECT E3s, none of these Ub ligases interacts with a Ub covalently but forms the adaptor between a E2 and the target, mediating the transfer of the Ub from the E2 to the protein to be marked for degradation (Mazzucotelli et al., 2006).

Monomeric enzymes of this class comprise both domains for the interaction with a E2 and the target, while four different types of multimeric RING/U-box ligases named Cullin-RING ligases

(CRLs) can be distinguished. They are built according to the modular principle comprising a Cullin (Cul) protein forming the adaptor between a RING domain protein as the E2 interaction site, and a variable polypeptide giving the substrate specificity allowing the formation of many E3s using few components. Additionally, a range of other subunits can be attached. In Arabidopsis, four classes of Cullins are present, CUL 1, 3, 4 and APC 2. (Shu and Yang, 2017, Mazzucotelli et al., 2006). CRLs are highly dynamic and disassemble after the ubiquitination of the target protein (Vierstra, 2009).

Four different types of CRLs can be distinguished according to their substrate receptors and CUL backbones:

- S-phase kinase-associated protein 1 – Cullin 1 – F-box (SCF) complex forms the biggest group of RING/U-box ligases. The important subunits for the substrate specificity are the so called F-box proteins (>700 genes identified in *Arabidopsis*) recognizing and binding to the different target proteins leading to their degradation. The subunit Arabidopsis Skp1-related (ASK) mediates the interaction between CUL1 and the F-box protein.
- BTB E3s (bric-a-brac-tramtrack-broad complex) interact via their BTB domain with the target protein. It contains CUL3. 80 different E3s are part of this category.
- DDB E3s (DNA damage-binding) via their DWD domain with the substrate and are linked via CUL4 to the RING domain protein. This category comprises 85 members.
- The anaphase-promoting E3 complex (APC) is the smallest category and differs in its structure, the complex comprises ~10 core proteins and a variable number of regulatory proteins. It is highly conserved throughout the eukaryotes, being essential for the regulation of the cell cycle by mediating the degradation of cyclins. It contains APC 2, is distant member of the Cullin protein family (Mazzucotelli et al., 2006; Vierstra, 2009).

iii) RBR E3 ligases (Figure 3C)

E3 ligases of the RBR type are multidomain proteins containing numerous RING domains. They are characterized by the supradomain RBR and consist of three consecutive protein domains. RING1 is liked via an InBetweenRING (IBR) domain to RING2. RING1 is the E2 interaction site. The C-terminal RING2 shows sequence similarities to known RING domains, but it is structurally different from conservative RING domains. It possesses one Cys as acceptance site for Ub (Spratt et al., 2014, Walden and Rittinger, 2018). In plants, little is known about the function of RBR E3 ligases, 42 genes are predicted to encode RBR-type proteins. This class of E3 ligases is subdivided into 4 families (Marín, 2010).

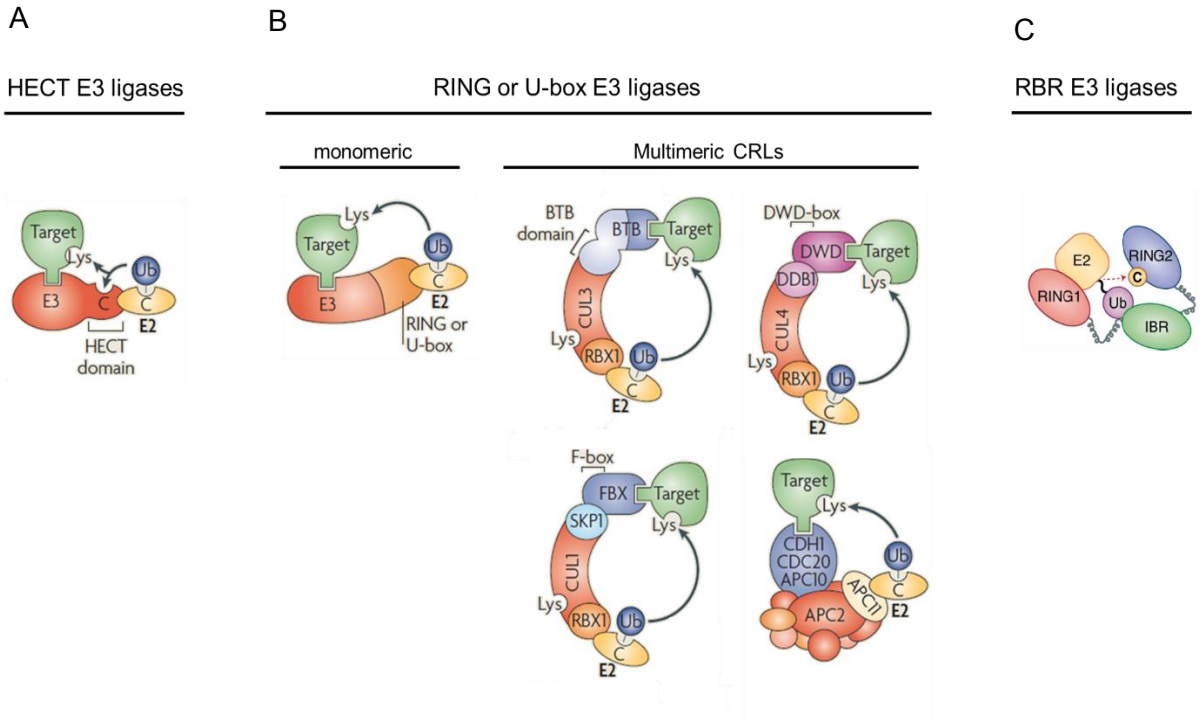

Figure 3 Plant ubiquitin ligases. A) HECT E3 ligases are single polypeptides and characterized by their HECT domain. They accept the Ub chain forming a convalent bond before transferring it to the target protein. Their most important functions are connected to abiotic stress response and and plant development such as leaf senescence and trichome formation. B) RING or U-box E3 ligases are defined by their E2 interacting domain called RING or U-box domain. According to their composition, they are divided into monomeric and multimeric protein complexes. In monomerics, the E2 and the target recognition site are located on the same protein. Multimeric CRLs comprise four distinct categories according to their target recongition domain and Cullin backbone. BTB complexes as well as DDB ligases are associated with all developmental stages and abiotic stress responses. SCF complexes are essential in stress response, hormone signaling and plant development, for example mediating the degradation of Auxin repressors. APC complexes as regulators of the cell cycle promoting the transitions during mitotic progression, primarily known in yeast and animals, but less well known in plants. According to the structure, it can be seen as outsider compared to BTB, DDB and SCF complex missing a cullin and RBX1 (Shu and Wang, 2017). C) RBR E3 ligases as hybrids between the RING and HECT type are multimeric proteins. They are characterized by two RING domains connected by a IBR domain, forming a RBR supradomain.
Figure modified from Vierstra (2009) and Walden and Rittinger (2018).

The degradation of ubiquitinated proteins occurs at the 26S proteasome, a tubular complex consisting of a central core particle (CP) flanked by two regulatory particles (RP) present in the nucleus and cytosol. Hydrolases for the degradation of the proteins are located at the inside and associated DUBs prevent Ub from being degraded. The rate of protein degradation by the UPS is not determined by the amount of ubiquitinated substrate, but it is dependent on the abundance and degradative capacity of proteasomes present in the cell (Vierstra, 2009, Clague et al., 2015).

1.3 The N-end rule pathway in plants

The N-end rule pathway is part of the UPS and relates the in vivo half-life of peptides and proteins to the different amino-terminal amino acids (Gibbs et al., 2014). To be recognized as

a substrate for the degradation through this pathway, pre-proproteins are processed by proteases or the initiator amino acid Met of a protein is cleaved off by Methionine aminopeptidases (MetAPs), exposing new N-terminal residues. This step does not automatically lead to the formation of a new degradation substrate, the properties of the neighbouring residues are as important as the accessibility of the N-terminus for a binding protein called N-recognin. Furthermore, the presence of a nearby Lys as possible ubiquitination site is essential (Dissmeyer et al., 2017).

Fulfilling these conditions, amino terminal amino acids are classified according to their stability into primary, secondary and tertiary destabilizing residues (Figure 4).

Primary destabilizing residues confer a short half-life and are directly recognized by a specific ubiquitin ligase E3 (Graciet et Wellmer, 2010).

In plants, so far, two different N-recognins have been identified which differ in the binding affinity according to the basic and hydrophobic properties of the amino acids at the N-termini. PROTEOLYSIS1 (PRT1) binds to primary destabilizing residues type II comprising bulky hydrophobic N-termini, leading to the degradation of substrates with the aromatic amino terminal residues Phe, Tyr and Trp. Leu and Ile, also part of this category, are not bound by PRT1 and the specific N-recognin has not been found yet. PRT1 was the first identified Ubiquitin Protein Ligase of the plant N-end rule pathway. It was found by positional cloning and the two comprised RING finger domains allow the interaction with UBCs (E2s). It contains also a ZZ-domain, a Zn^{2+} binding domain mediating different protein-protein interactions (Potuschak et al., 1998, Stary et al., 2003).

The class of primary destabilizing residues type I comprising the basic amino termini Arg, Lys and His is recognized by PRT6. This E3 was identified due to sequence similarities to the UBR domain (Ubiquitin recognition domain) of UBR1, the only N-recognin in yeast. This highly conserved domain mediates the interaction with the basic N-termini, leading to their degradation. PRT6 comprises also a RING domain to allow binding of E2s (Garzon et al., 2007).

Into the category secondary destabilizing residues fall the two N-termini Glu and Asp. They are converted to a primary destabilizing residue by R-transferases attaching an Arg to the N-terminus. In plants exist two different Arg-tRNA-protein transferases, AtATE1 and 2, encoded by two closely related genes (Graciet et al., 2010, Yoshida et al., 2002).

N-termini of the category tertiary destabilizing amino-termini are very stable and require different modifications for the transformation into a secondary destabilizing residue, followed by the conversion into primary destabilizing residues. Cys is oxidized through a chemical reaction requiring NO and O_2, while Asn and Gln are deamidated either by AtNTAN1 or AtNTAQ1, two N-terminal amidohydrolases converting them into Asp and Glu, secondary destabilizing residues (Graciet et al., 2010).

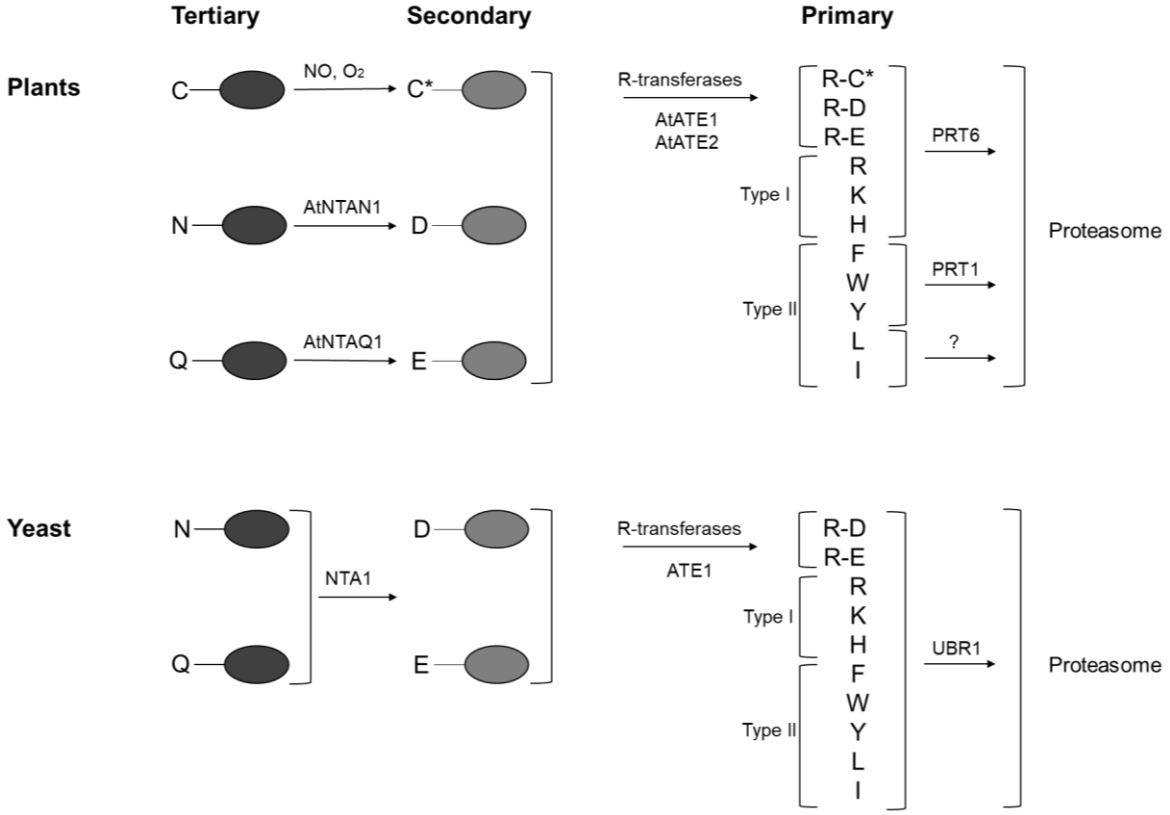

Figure 4 The N-end rule pathway in plants and yeast. In both systems, N-terminal amidohydrolases (NTAs) are converting the tertiary destabilizing residues Asn and Gln into the secondary Asp and Glu. In plants, additionally to Asn and Gln also Cys belongs to this category and is oxidized. R-transferases (AtATE1 and 2 in *Arabidopsis*, ATE1 in yeast) form from secondary primary destabilizing residues. So far, two N-recognins were identified in *Arabidopsis*: PRT6 mediating the degradation of type I primary destabilizing residues comprising arginylated Cys, Glu and Asp and the basic amino acids Arg, Lys and His, and PRT1 binding to type II of hydrophobics Phe, Trp and Tyr. The N-recognins of Leu and Ile, part of type II primary destabilizing residues, has not been found yet.
In yeast, UBR1 is the only known N-recognin leading to the degradation of primary destabilizing residues by the proteasome. Cys is not part of tertiary destabilizing residues because NO for the oxidation is absent in *S. cerevisiae* (Hu et al., 2005).

For better understanding of the experimental conditions and results, the yeast N-end rule is described briefly (Figure 4). The tertiary destabilizing residues Gln and Asn, in contrast to higher eukaryotes, are recognized by the same N-terminal hydrolase NTA1 (Graciet et al., 2010). Cys on the other hand is not part of this category because yeast lacks NO and N-terminal Cys oxidases (Hu et al., 2005). As mentioned, only one N-recognin, UBR1, is known

in yeast comprising a UBR and a ClpS homology region. The UBR domain binds to the basic residues of Type I primary destabilizing residues Arg, Lys and His, the Clps homology region, its homolog in animal is called N-domain, mediates the interaction with the bulky hydrophobic Type II primary destabilizing residues Phe, Trp, Tyr, Leu and Ile (Tasaki et al., 2009). So, in a yeast strain lacking an intact ORF of UBR1 (ΔUBR1), all peptides with a primary destabilizing residue at the N-terminus are stabilized.

1.4 Putative complementation group PRT13

As mentioned before, N-recognins for the N-termini Leu and Ile have not been identified yet. To detect possible N-recognins, a genetic screen was performed. Seeds of a transgenic line of *Arabidopsis thaliana* in the background of ecotype Columbia-0 (Col-0) comprising a reporter L-glucuronidase (L-GUS) (Figure 5) integrated in the genome were treated with Ethyl methanesulfonate (EMS) to obtain a set of different mutations. By whole genome sequencing, mutated genes were identified and by individual analysis the different possible candidates were selected and clustered into complementation groups for further investigations.

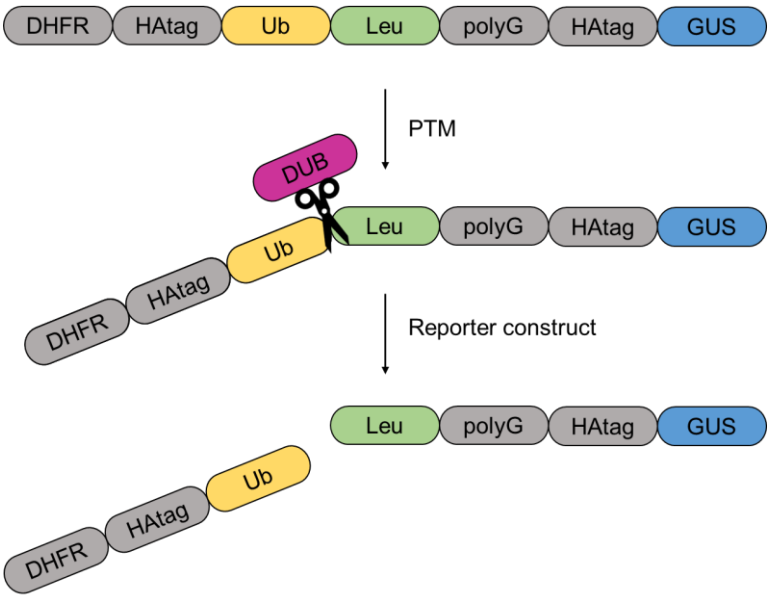

Figure 5 L-GUS reporter construct. This construct, transformed into *A. thaliana,* is used for the characterization of the stability of Leu N-termini in seedlings in an *in vivo* GUS-stain. Co-translationally, DUBs cleave off the DHFR-HAtag-Ub fragment setting free the Leu amino terminus.

The reporter integrated in the genome reveals an essential role of the mutated gene in the Leu N-end rule pathway. Co-translationally, DUBs cleave after Ub and the peptide with the N-terminal Leu is set free. The coupled β-glucuronidase acts as reporter in the *in vivo* staining detecting the stability of the protein depending on its N-terminus. If this GUS staining is negative, meaning the seedling appears white, the construct has been degraded and the

investigated mutated plant gene is not involved in the degradation of proteins with Leu-N-termini. In contrast, the seedling appears blue if the construct is not degraded, the protein is stabilized. Therefore, the enzyme is active and it can be assumed that the mutated gene has an important role in the degradation of peptides with Leu as N-terminus (Figure 6).

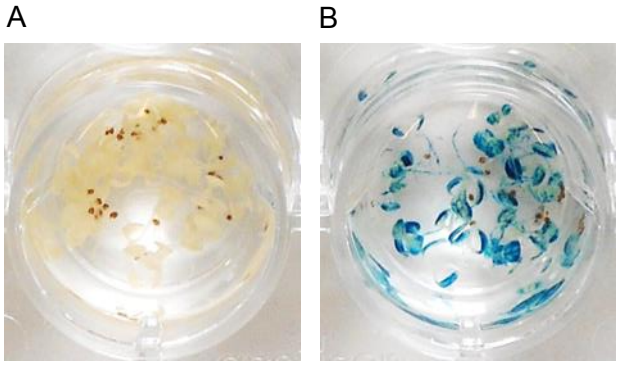

Figure 6 *In vivo* GUS stain in *Arabidopsis* seedlings expressing the L-GUS reporter construct. A) After PTMs, if the newly exposed Leu N-terminus leads to degradation according to its role as primary destabilizing residue in the plant N-end rule pathway, the coupled GUS enzyme is unstable and not active. No blue colour is detectable in the GUS stain and the seedlings appear white. B) On the contrary, if the reporter protein is stabilised in combination with a mutated Leu N-recognin candidate gene, the GUS is active, leading to blue colour formation in the staining assay (right picture). Picture kindly provided by Winter Nikola.

Plants grown from the EMS-treated seeds with a positive GUS staining were selfed to enhance or to reduce the phenotype causing mutation. One plant showing a blue phenotype after the selfing event was assigned the complementation group PRT13. It was backcrossed (BC) with WT Col-0 carrying the L-GUS construct (WT L-GUS) to get rid of undesired mutations and to confirm the mutations in the candidate genes. In the F2 generation, a GUS stain was performed, while the F3 (BC1F3) was backcrossed to the WT L-GUS plants. In this work, progenies from the generation BC1F3 x L-GUS (named BC2F3) were genotyped and the following genes as part of the complementation group PRT13 were investigated:

1) BIG (At3g02260), the EMS treatment caused a mutation on position c.13493C>T (=p.Ala4498Val). Its known functions are described in chapter 1.5.2 BIG in more detail.
2) Autophagy related 10 (Atg10) (At3g07525) with the mutation on position c.514C>T (=p.Pro172Ser). As described, autophagy is a highly regulated process and highly conserved in eukaryotes. Atg10 is an E2-like enzyme involved in the development of an autophagic vesicle to an autophagosome (Kim et al., 2012).
3) F-box protein (At3g13680) mutated at position 1171A>G (p.Arg391Gly).
4) Protein phosphatase 2A (PP2A) B' (At3g09880) with a G>A mutation at position 520 (p.Glu174Lys). The protein plays an important role in the response of the two plant hormones abscisic acid (Waadt et al., 2015) and brassinosteroids (Wang et al., 2016),

as well as in the cohesion of the two sister chromatids during meiosis in *Arabidopsis* (Yuang et al., 2018).

1.4.1 Experimental design

The candidate genes were characterized either by sequencing or by Derived Cleaved Amplified Polymorphic Sequences (dCAPs). This method takes advantage of the single nucleotide polymorphism (SNP) caused during the EMS treatment and the specificity of restriction enzymes. The corresponding gene fragment was amplified via PCR and incubated for the digest. Depending on the presence or absence of the restriction enzyme recognition site, the mutant can be determined according to the pattern present after the gel separation (Neff et al., 1998).

1.5 Putative candidates of Leu N-recognin in *Arabidopsis*

Identified in the genetic screen as the two additional putative candidates for a Leu N-recognin in *Arabidopsis*, an F-box protein (At3g12350) named candidate 16 (cand16/ c16) and BIG (At3g02260), were also characterized during this work.

1.5.1 Candidate 16

Not much is known about this F-box protein (At3g12350). In a genetic microarray-screening identifying repressed or induced genes after phosphate starvation, a twofold transcriptional increase of cand16 was identified as a response to this nutrient depletion. It was declared as a putative transcription factor (Müller et al., 2007) and it has similarity to the SKP1 interacting partner 2 (At5g67250), another F-box protein associated with the auxin signalling pathway (Schwager et al., 2007). Two different splicing variants are known, in this work referred as long and short cand16.

1.5.2 BIG

BIG (At3g02260) is, like its name implies, one of the biggest proteins found in *Arabidopsis*. Its genomic region located at the top of chromosome 3 covers 17.5kb, its CDS comprises approximately 15200 nucleotides and the functional protein with its 5098 amino acids has a molecular weight of 566 kDa. Four splicing variants are known. In spite of its huge size, direct binding partners were not identified yet.

BIGs role as possible N-recognin for Leu N-termini was suggested after a BLASTP search against the mouse UBR4, an E3 ligase, identifying a UBR domain at amino acid position ~ 1560 with similarity to the UBR domain found in the yeast UBR1 and in the PRT6 of *Arabidopsis*. Next to this first cysteine-rich putative zinc finger domain (CRD1), a second highly conserved zinc finger (CRD2) at position ~3440 was identified. Additionally, a ZZ-domain mediating protein-protein interactions has been found at amino acid position ~2590 (Gil et al., 1991, Graciet et Wellmer, 2010).

BIG is predicted to be the plant homolog of the mammalian UBR4 and of the protein PUSHOVER found in *Drosophila melanogaster*. Sticking out is the enormous size of all three proteins ranging from 560kDa (Pushover) to 570kDa (UBR4). Additionally, they show highly similar regions at the C-terminus in a length of over 3000 amino acids. Also, the two CRDs found in BIG are detected in PUSHOVER, but this latter protein is lacking the ZZ-domain (Gil et al., 1991).

PUSHOVER belongs to the calossin protein family, a group of integral membrane proteins acting as calmodulin binding partners. Genetic studies have associated its function with male reproduction, nonrecombinant chromosome segregation in female meiosis, synaptic transmission in photoreceptor cells and perineurial glial growth mediating signal transmission (Richards et al., 1996, Sekelsky et al., 1999, Muday et Murphy, 2002). UBR4 belongs to the group of seven identified mammalian E3 ubiquitin ligases containing a UBR box similar to the plant N-recognin PRT6 and the yeast N-recognin UBR1. Further studies are necessary to determine if UBR4 itself is an E3 ligase or if it is a substrate recognition subunit as a part of an E3 complex. So far, no ubiquitination site has been identified (Tasaki et al., 2005).

To summarize, the function of these three homologous proteins can be briefly described as regulators of signalling pathways in response to hormones, neurotransmitters or exogenous signals.

Despite no identification of a direct binding partner or a clear molecular function in *Arabidopsis*, some impacts of BIG on diverse cellular processes were found in mutation screens. The most revealing alleles and their associated role are listed below:

- *Transport-inhibitor response3* (*tir3*): auxin metabolism (Ruegger et al., 1997)
- *big-j588*: auxin-mediated organ growth (Guo et al., 2012)
- *Corymbosa1* (*crm1*): auxin-dependent growth of pedicels and internodes (Yamaguchi et al., 2007)
- *Low phosphate-resistant root* (*lpr1*): auxin-mediated pericycle cell activation (López-Bucio et al., 2005)

- *Dark overexpression of CAB1 (doc1*): cellular light response (Li et al., 1993)
- *Attenuated shade avoidance1* (*asa1*): shade avoidance response (Kanyuka et al., 2003)
- *Umbrella1* (*umb1*): reduced cytokinin sensitivity (Kanyuka et al., 2003)
- *CO_2 insensitive 1 (cis1):* CO_2 dependent stomata regulation (He et al., 2018)

BIG was mapped by Gil et al. (2001) in an experiment confirming the allelism of *doc1* and *tir3,* describing it as a major actor in the polar auxin transport (PAT) in *Arabidopsis*. Mainly associated with this pathway, its proposed role in this hormone signalling is described in more detail compared to other identified functions.

Auxin as a plant hormone has a broad spectrum of effects in embryogenesis, all types of organogenesis, maintenance of the root meristem, differentiation of the vascular tissue, elongation growth of hypocotyl and root, formation of lateral roots, apical dominance, fruit ripening and growth response to environmental factors. From its synthesis site in the meristem of the shoot apex in the aerial parts of the plant, it is carried via the polar auxin transport system to the roots. Two transportation routes are known, 1) parenchymal and 2) via the phloem. For the cell-to-cell transport in the parenchyma, Auxin transporter proteins (AUX) and Auxin-like proteins (LAX) act as Auxin-influx-carrier, and PINFORMED proteins (PIN) as Auxin-efflux-carrier. On this way, two kinds of auxin concentration gradients appear in the plant, one over a long distance, basipetal in the shoot and acropetal in the root, and one over short distance within a cell. This local auxin gradient is the most important condition for cell differentiation and developmental processes (Blakeslee et al., 2005, Petrášek and Friml, 2009).

As suggested by Gil et al. (2001), BIG plays an important role in this PAT. One important point in discovering was the treatment with N-1-naphthylphthalamic acid (NPA), an auxin transport inhibitor, blocking the cellular efflux of auxin by binding to the NPA binding protein (NBP) associated to PIN1. *tir3* mutants, plants with an altered response to this NPA treatment, show a reduction of NBPs and a reduced PAT from the inflorescence to the roots (Gil et al., 2001). So, NBP must have a positive effect on the PAT, and as a mutated BIG shows the same effects as a NPA treatment, it is positively connected to this plant hormone transport. This results in a strong connection between NBP and BIG, suggesting BIG may be required for the expression, localization or stabilization of NBP (Ruegger et al., 1997, Gil et al., 2001).

The phenotype of the *tir3* allele shows a reduction of all elongating organs like inflorescence and siliques and a near absence of the formation of lateral roots as a consequence of the local decreased auxin concentration. This lack in hormone transport leads to a reduced cell length in the stems of the mutants compared to wildtype plants; however, in roots, the cell number

rather than cell length is changed, strengthening the dependence of the cell division in the roots from auxin (Ruegger et al., 1997). This dwarf phenotype with delayed flowering was also described by Guo et al. (2013). They investigated another allele of BIG, named *big-j588* with a mutation located in CRD1 (UBR domain) substituting one Cys by a Tyr. A reduction of this efflux carrier was found affecting the auxin gradients. They suggested that BIG may influence the abundance of PIN1 by regulating its transcription and confirmed the reduction in cell size in the epidermal cells and the reduction of cell number in the roots as Ruegger et al. (1997) had published. Another BIG allele, *crm1*, found by Yamaguchi et al. (2007) reinforced its connection to the auxin signalling. Affecting the cell elongation in pedicels and internodes, a corymb-like inflorescence phenotype appears (Yamaguchi et al., 2013). Because of the inducing effect of the auxin pathway on the gibberellin synthesis and promoting the degradation of its repressors, mutations in BIG also affect the signalling and status of this phytohormone in *Arabidopsis* (Desgagné-Penix et al., 2005).

In addition to the link to auxin signalling, BIG is associated with different physiological processes and stress regulations. The *cis1* allele connects the huge protein to the stomatal regulation preventing a closure after a sensed increase in the CO_2 concentration (He et al., 2018). During low P-conditions, the formation of lateral roots is promoted to increase the uptake. In a screen identifying mutants defective in this adaption, another BIG allele was found named *lrp1* (López-Bucio et al., 2005).

The *umb1* allele was found in a screen identifying plants with decreased cytokinin sensitivity in root growth inhibition (Kanyuka et al., 2001), *asa1* in a screen identifying suppressors of phytochrome-mediated shade avoidance. *asa1* reduced all aspects of the shade avoidance response normally characterized by elongated stems and petioles, reduced apical dominance and early flowering (Smith and Whitelam, 1997). Both mutants showed the same phenotype as *tir3* plants, mapping led to the confirmation of being allelic (Kanyuka et al. 2003).

The connection of BIG to light response was made by *doc1* mutants. CAB (chorophyll a/b-binding) proteins bind pigments in the light harvesting complex (LHC) of the photosystems and are regulated by the amount of light hitting the plant. At high light levels CAB genes are expressed in green parts of the plants as well as under low light levels in dark-grown seedlings. Mutations in the *doc1* locus lead to a high expression of CAB genes also in the dark (Li et al., 1993).

BIG acts also as an interaction point between the jasmonate (JA) and salicylic acid (SA) signalling, both are highly linked to the plant immune response, JA predominantly against herbivores and SA against biotrophic pathogens. Under stress-free conditions JA synthesis is downregulated by BIG. BIG mutants lead to a disbalance between the two phytohormones because of a de-repression of JA synthesis, reducing the plant resistance against fungal

pathogens and increasing it against herbivores by reducing the attractivity of the plant for the insects. (Zhang et al., 2018). Furthermore, this latter author suggests that the mutual negative regulation of BIG and JA is responsible for the decreased PAT observed in BIG mutants. The increase of JA, caused by the loss of repression through BIG, inhibits the intracellular trafficking of the auxin export proteins PIN, reducing the auxin transport.

Summarizing, BIG is strongly connected to the PAT, and to cellular light and stress responses through an impact on the hormones JA, gibberellins and ethylene. It was the first key protein evidencing the connection between the light response and hormone signalling pathways (Gil et al., 2001) and by affecting the C/N ratios, it connects also the nutrient management to these pathways (Zhang et al., 2019). Causing a disbalance between SA and JA, BIG has an important influence on the plant immunity, decreasing the resistance against fungi, while increasing it against herbivores.

1.5.3 Further candidates

In addition to cand16 and BIG, three more constructs were investigated to detect possible N-terminal binding i) a fragment of BIG, ii) a fragment of BIG C-terminally fused to the F-box of Ufo1, an F-box protein of *S. cerevisiae*, and iii) the UBR domain of PRT6 C-terminally fused to Ufo1 F-box.

As described, BIG comprises a ZZ-domain involved in protein-protein interactions and two putative CRDs, a UBR and a zinc-finger domain. Previous experiments testing the binding affinity of the ZZ-domain in a yeast-two hybrid assay to L and R N-termini did not give a result (performed by Nikola Winter). Now, besides the complete BIG protein, also a larger fragment including this previously investigated putative ZZ-domain at amino acid position ~2600 should be tested for N-recognin activity. This BIG fragment covers the protein sequence from position 2160-3419 and may improve folding kinetics and stability compared to the previously used smaller fragment. Additionally, this whole fragment is C-terminally fused to the yeast F-box of Ufo1.

As a further control construct comprising the Ufo1 F-box fused to the C-terminal UBR domain of the PRT6, the N-recognin for type I destabilizing residues, was established. It was developed to test the combination of the yeast F-box for the recognition of the substrates and the UBR domain of PRT6 from *Arabidopsis*, mediating the interaction with basic amino termini.

1.5.4 βgal-based assays

In the experiments, the binding affinity of the candidate proteins to Leu-N-termini should be tested. Method of choice to identify a possible interaction partner of a Leu N-terminus promoting its degradation via the N-end rule pathway was the ONPG (ortho-nitrophenyl-β-D-galactopyranoside) assay performed in the yeast *S. cerevisiae*. The β-galactosidase (β-gal) is the key enzyme of this reaction. It was fused to different N-termini, in our case Phe, Leu, Met, Arg, Ser and Val, to test the stability of the ensuing protein in combination with the appropriate candidate ligase. ONPG serves as substrate for the galactosidase, the amount of the product o-nitrophenol, visible as yellow colour, can be detected photometrically (Figure 7). If the tested protein does not promote the degradation of the X-β-galactosidase in this system, the enzyme is stabilized, and a high accumulation of the enzymatic product can be detected at wavelength 420nm. In contrast, if the candidate mediates the degradation of the protein with a respective N-terminus, low activity of the β-galactosidase is present in the system.

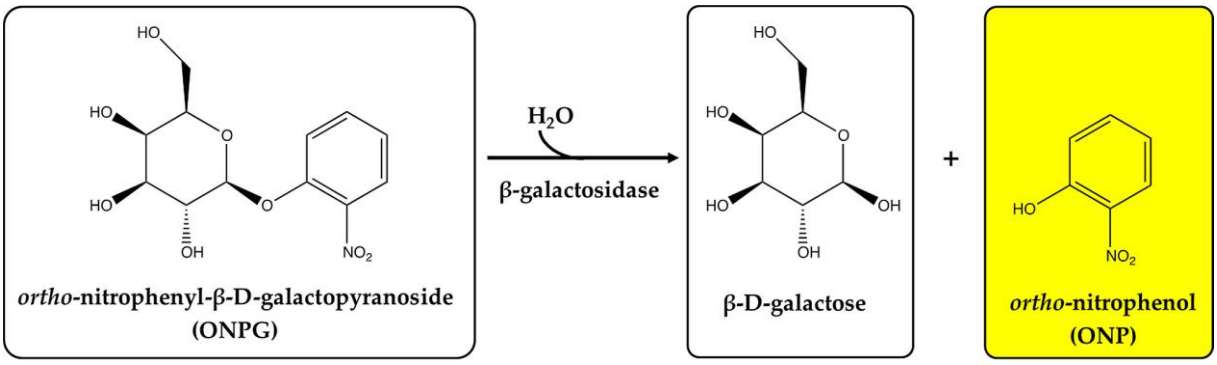

Figure 7 ONPG assay. The reporter enzyme βgal converts the substrate ONPG into β-D-galactose and o-nitrophenol (ONP). The amount of ONP can be detected photometrically (wavelength 420nm) calculating therefrom the specific activity of the enzyme by which the stability of the coupled N-terminus can be determined.
Figure from Labus (2018).

The assay will be performed in two different yeast strains. In SUS13, the UBR1 gene encoding the only known N-recognin in yeast is deleted, lacking the ability to degrade substrates with primary destabilizing first residues. The other strain used in ONPG assays, CB80, is a WT form of *S. cerevisiae*. At the end of the practical work, the generation of a new strain was started. The UBR1 gene in the WT strain CB80 should be disrupted by the insertion of a kanamycin resistance module (KanMX cassette) mediated by CRISPR. So, further assays can be performed in two isogenic strains differing exclusively in the functionality of UBR1.

1.6 The development of tandem fluorescent timers

Tandem fluorescent timers (tFT) can define the cellular abundance and age of a certain protein or peptide through time-dependent change in colour. The idea behind is to combine the advantages of two fluorescence proteins, that are united into one ORF, for *in vivo* studies of the proteome. They should differ in their maturation times, have a well-separated emission spectrum and a difference in pKa values. Depending on the combinations and their specific pKa values the subcellular localization in the acidic vacuole or compartment can be defined. As they differ in their folding kinetics, the approximate lifetime of the tagged protein of interest in the cytoplasm can be determined (Khmelinskii et al., 2012, Khmelinskii and Knop, 2014).

As the focus of this work is set on the N-end rule pathway, the two fluorophores were linked to a N-terminal ubiquitin fusion construct comprising a DHFR, Ub and a triplet coding for the differing N-termini. By the same principle as for the L-GUS construct used previously to identify candidates for putative Leu N-recognins, DUBs are cleaving co-translationally, exposing the new N-terminus, either Arg, Leu or Met (Figure 8). The stability of the released tFT constructs is depending on the newly exposed amino acid, Met as stable and Arg and Leu as primary destabilizing residues according to the N-end rule pathway.

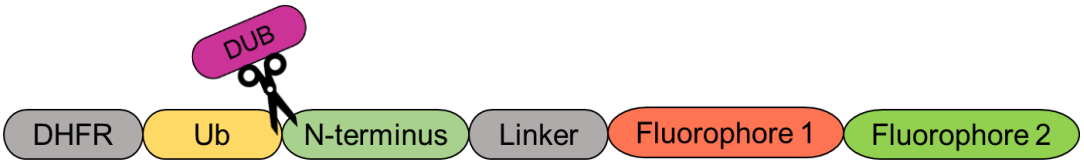

Figure 8 General overview of a tFT construct. It consists of a DHFR and Ub, followed by the specific N-terminus This ubiquitin fusion protein is linked to the two fluorophores. In a PTM event, DUBs cleave behind the Ub, releasing the tFT construct. Its stability is dependent on the specific N-terminus. In the linker, an HAtag is localised, facilitating immunological detection of the transgene on the protein level.

Established tFT constructs comprise a red (RFP), in this work mCherry or mScarlet-I, and a green fluorescent protein (GFP), superfolder GFP (sfGFP), yellow fluorescent protein (YFP) or mNeonGreen. As mentioned, they are tagged to the protein of interest to investigate its subcellular localization and lifespan. In general, the red variants fold slower than the green variants. If a red and a green signal are detectable, it reflects a longer lifespan of the fusion protein (Khmelinskii et al., 2012, Zhang et al., 2019).

mCherry matures in a two-step folding process, the first step is completed within 17 min, the second leading to an active fluorescent protein within 30 min. The mature protein has a pKa value of ~4.5 (Shaner et al., 2004, Merzlyak et al., 2007). mScarlet-I is a newly developed synthetic RFP defined by a high photostability, high molecular brightness, a maturation time of

about 36 min and a pKa of 5.4 (Bindels et al., 2017). As mentioned, the GFPs are characterized by a fast maturation time compared to the reds and they are even visible when tagged to proteins with short lifetime: sfGFP (pKa 5.9) emits light already six min after translation (Roberts et al., 2016). The more pH sensitive YFP has 7 min folding time (pKa 7.0) (Wachter et al., 1998). mNeonGreen, due to the low sequence similarities not called as GFP variant, folds within 10 min. This protein is resistant to bleaching and very bright, its pKa is at ~5.7 (Pédelacq et al., 2006).

As a well-established tFT construct adapted for plants, the combination of mCherry-sfGFP has been tested (Zhang et al., 2019). In more acidic organelles like lysosomes with a pH of around 5.0, mCherry is still active, while sfGFP emit no light as its β barrel structure is inactivated (Roberts et al., 2016). If both fluorescent proteins are active because of the stability of the N-terminus and in a compartment with pH above 6.0, the spectra will overlap. With the calculation of the ratio between the red and the green fluorescence intensities (redFP/greenFP ratio of intensities) the age of the protein can be defined (Khmelinskii et al., 2012).

So, the approximate lifespan of the proteins can be detected as well as their subcellular location.

In a first attempt, three different novel reporter constructs were established differing in their combinations of fluorescent proteins. The proteins were tagged to a construct (Figure 8) comprising of DHFR, Ub and the three different N-termini Met, Arg and Leu; Met as stable and Arg and Leu as primary destabilizing residues are known from the plant N-end rule pathway. The binary vector pV-Top, obtained from Ian Moore, was used comprising the promotor pOP6 inducible by Dexamethasone (Dex), a glucocorticoid (Moore et al., 2006).

1) Tandem fluorescent protein timer (tFT): the combination of mCherry and sfGFP was developed in the Markus Wirtz lab at the University of Heidelberg (Zhang et al., 2019)
2) Autophagic flux reporter: YFP and mCherry, received from Yasin Dagdas
3) Scarlet-I construct: mScarlet-I and mNeonGreen, developed in the Bachmair lab

The nine constructs were transformed into the *Arabidopsis* WT Columbia-0 and plant line 6-1-1. In this work, the second generation (T2) of Hygromycin resistant plants were investigated for the expression of the transgenes.

In a second cloning strategy, the combination of the different fluorescent proteins was abandoned for the use of three vectors differing in their promoters. Only the iScarlet – mNeonGreen fluorophores were taken. This combination with a very similar pKa is not well suited for cellular location, but its big advantages are the difference in the maturation kinetics, and both are very bright and photostable, highly important if the tagged protein should be detected in cells containing chlorophyll.

1.7 Aim of the work

The N-end rule pathway as part of the UPS relates the half-life of polypeptides to their N-termini, those are recognized by specific binding proteins called N-recognins. So far, N-recognins for Leu and Ile, N-termini of the type II primary destabilizing residues comprising bulky hydrophobic amino acids, in *Arabidopsis thaliana* are not identified yet. The aim of this Thesis is to test putative candidates, above all BIG and cand16, in an enzymatic activity assay define their possible roles in the N-end rule pathway in plants. Furthermore, the correlation between mutations in genes belonging to the putative complementation group PRT13 and a stabilized L-GUS construct in seedlings detected in a GUS stain should be determined by sequencing or dCAPs.

To detect the cellular localization of the N-end rule mediated degradation of the N-termini Met, Arg and Leu, tFT constructs should be developed consisting of the two fluorophores mScarlet-I and mNeonGreen. Three plasmids differing in their promotors were used to increase the spatial and temporal control of transgene expression. Apart from this, the translational products of previously established tFTs in the combinations mCherry-sfGFP and YFP-mCherry should be investigated to define subcellular localizations and, according to the different folding kinetics of the fluorophores, the lifespan of the proteins should be estimated.

2 Material and Methods

2.1 Material

2.1.1 Bacterial strains

Escherichia coli (E. coli) DH5α:

Genotype: *F– φ80lacZΔM15 Δ(lacZYA-argF)U169 recA1 endA1 hsdR17(rK–, mK+) phoA supE44 λ– thi-1 gyrA96 relA1*

E. coli DH10β:

Genotype*: F– mcrA Δ(mrr-hsdRMS-mcrBC) φ80lacZΔM15 ΔlacX74 recA1 endA1 araD139 Δ(ara-leu)7697 galU galK λ– rpsL(StrR) nupG*

Agrobacterium tumefaciens (A. tumefaciens) GV3101

2.1.2 Yeast strains

Saccharomyces cerevisiae (S. cerevisiae) SUS13:

Genotype: *Mata trp1-1 ura3-52 his3-Δ200 leu2-3,-112 can1-100 GAL+ ubr1-Δ1::LEU;*

S. cerevisiae CB80:

Genotype*: Mata ura3-52 leu2-3,-112 trp1-1 his3-Δ200 Gal+.*

2.1.3 Plant lines

Arabidopsis thaliana (A. thaliana):

- Wildtype (WT): Columbia-0 (Col-0)
- Plant line S7: 35S::LhGR2, activator line for the two component system of chemically inducible gene expression, expressing the synthetic transcription factor LhGR2 under the CaMV35S promoter (35S).
- Plant line 6-1-1: pRPS5A::LhGR2, also an activator line like plant line S7, but expressing LhGR2 under a ribosomal protein promoter, contains an internal GUS construct.

2.1.4 Used vectors

For standard cloning:

pICH41308: was used as high copy empty building vector adapted for the method of Golden Gate cloning of the BIG gene. It was obtained from Karolin Delker from the Leibniz Institute for Plant Biochemistry Halle. It conveys Spectinomycin resistance.

pACYC177: this vector was used for the fragment by fragment assembly of the BIG CDS by the method of In-Fusion cloning. A low copy plasmid was taken because of the possibility of toxicity of the huge protein in *E. coli.* It contains both a Kanamycin and an Ampicillin resistance gene.

For plant transformation:

pV-Top: This Dexamethasone-inducible binary vector is part of a two-component system, for the activation of the transgenes in plants the synthetic transcription factor LhGR2 is needed. Therefore, it must be transformed in an activator plant line like S7 or 6-1-1. It carries a Kanamycin resistance marker for the selection in bacteria and a Hygromycin marker for plants, and encodes a β-glucuronidase for GUS stain.

pBIBpOpTev-c1: This vector, inducible by Dexamethasone is a binary vector and requires, as the pV-Top vector due to the two-component system, an activator plant line. It carries a Kanamycin resistance marker for the selection in bacteria and a Hygromycin marker for plants. It was constructed in the Bachmair lab.

pBIN AR_Sat5_tFT: This plasmid carries a tFT construct comprising mCherry and sfGFP under the CaMV35S promoter, built by and obtained from the Markus Wirtz group from the Ruprecht-Karls-University in Heidelberg. It was used for comparison in the development of novel tFT constructs consisting of the two fluorophores mScarlet-I and mNeonGreen. It contains a Kanamycin resistance gene for the selection in bacteria.

pNIGEL07: This vector is part of the Wave lines created in the Niko Geldner lab at the Department of Plant Molecular Biology at the University of Lausanne comprising a Ubi10 promoter. It possesses an Ampicillin resistance gene for bacterial selection and a BASTA resistance gene for plant selection. For the successful replication in *Agrobacterium,* it requires the pSoup helper plasmid selecting on Tetracycline.

For yeast transformation:

YCplac22: Into this ARS1-CEN4 yeast vector, the different candidates for a Leu N-recognin in plants to be tested in an ONPG assay, are cloned. The cloning was performed in *E. coli* with the selection marker Ampicillin and yeast transformants are selected on -Trp1 medium (Gietz and Sugino, 1988).

pUB23: The 2micron vector carries the different X-β-gal constructs under a lacZ promoter. Their stabilities have to be tested in combination with the different candidates for Leu N-recognin in plants in an ONPG assay. As selection marker in yeast it carries URA3 (Bachmair et al., 1986).

2.1.5 Oligonucleotides

All primers and oligonucleotides used in this work for PCRs and sequencing were purchased from Microsynth AG (Balgach, Switzerland).

2.1.6 Antibodies

Anti-HA High Affinity IgG antibody (Roche): This monoclonal antibody derived from rat was used in the detection of the tFT constructs in plants of the T2 generation as primary antibody.

Anti-rat IgG antibody (GE Healthcare): This antibody produced in goat was conjugated to a horse radish peroxidase (HRP) and used to visualize the primary antibodies derived from rat as the Anti-HA High Affinity IgG antibodies.

2.1.7 Buffer, Media and Antibiotics

2.1.7.1 Buffer

Unless otherwise noted, chemicals are stored at room temperature

Bortezomib: working concentration: 5µM (stock: 10mM in DMSO, stored at -20°C)

Zebularine: working concentration: 80µM (stock: 20mM in DMSO, stored at -20°C)

Dexamethasone: working concentration: 10µM (stock: 10mM in DMSO, stored at -20°C)

Leucine O-Methyl Ester: working concentration: 10mM (stock: 1M in 2% gal SD medium 0.2M K-P-buffer pH 7.0, stored at 4°C)

Phenylmethylsulfonyl fluoride (PMSF): 40mM in Isopropanol (stored at -20°C)

Protein extraction buffer:
90mM Hepes pH 7.4 (stock: 1M)
2% SDS (stock: 10%)
30mM DTT (stock: 1M, stored at -20°C)
20µg/ml Pepstatin (stock: 1mg/ml in methanol, stored at 4°C)
Protease Inhibitor Cocktail (Sigma P9599) in DMSO (stored at -20°C)
prepare fresh before use

10X PBS:
27mM KCl
1.37M NaCl
100mM Na_2HPO_4
20mM KH_2PO_4
pH 7.2-7.6

4X sample loading buffer:
50mM Tris pH 6.8
12.5mM EDTA
2% SDS
10% Glycerol
1% β-Mercaptoethanol
0.02% Bromophenol Blue (stored at 4°C)

5X SDS-PAGE running buffer:
1M Glycine
125mM Tris
0.5% SDS

1X PBS-T:
addition of 0.05% Tween-20 to 1X PBS

Transfer buffer:
190mM Glycine
25mM Tris
0.05% SDS
20% Ethanol

Z-buffer:
62mM Na_2HPO_4
45.8mM NaH_2PO_4
10mM KCl
1mM $MgSO_4$
0,27% β-Mercaptoethanol
store at 4°C

10X TE buffer:
0.1M Tris-HCl
10mM EDTA
pH 7.5

TE/LiOAc buffer:
0.1M LiOAc (stock: 1M)
1X TE buffer (stock: 10X)

PEG/LiOAc solution:
60µl TE buffer (stock: 10X)
60µ LiOAc (stock: 1M)
10µl ssDNA (stock: 10mg/ml, stored at -20°C, boiled for 5 min)
470µl PEG (stock: 50%, prepare fresh)
For 1 transformation reaction (V=600µl)

ONPG solution: 4mg/ml in Z-buffer
prepare fresh before use

Breaking buffer: 100mM Tris-Cl pH 8.0
1mM DTT (stored at -20°C)
20% Glycerol

GUS staining solution: 50mM Sodium phosphate buffer pH 7.0 (500mM stock)
1mM Potassium Ferricyanide (100mM stock)
1mM Potassium Ferrocyanide (100mM stock)
0,1% Triston X-100 (20% stock)
1mM X-Gluc in 50:50 MeOH:DMSO (100mM stock, stored at -20°C)
prepare fresh

TFB buffer: 10mM Pipes
15mM CaCl2
250mM KCl
pH 6.7
addition of 55mM $MnCl_2$
store at 4°C

Plant DNA extraction buffer: 200mM Tris pH 8.8 (1M stock)
250mM NaCl (5M stock)
25mM EDTA (0.5M stock)
0.5% SDS (10% stock)

2.1.7.2 Media

Fill up to 1l with ddH_2O

LB medium: 10g Bactotryptone
5g Yeast extract
10g NaCl
For plates: 15g Agar

SOB medium: 20g Bactotryptone
5g Bacto yeast extract
10mM NaCl
2.5mM KCl

YEB medium: 5g Tryptone
5g Peptone
1g Yeast extract
5g Sucrose
pH 7.2-7.3 with NaOH
addition after autoclaving: 10mM $MgSO_4$

SD medium: 1.9g Yeast nitrogen base (w/o amino acids)
5.0g $(NH_4)_2SO_4$
pH 5.6 - 5.8 with NaOH

For plates: 20g agar
addition after autoclaving: 100ml 10X Dropout mix

YPD medium: 10g Bactoyeast extract
20g Bactopeptone (Casein)
pH 5.8 with NaOH
For plates: 20g Agar
addition after autoclaving: 50ml 40% Glucose

MS medium: 4.3g Murashige Skoog salts incl. Nitsch vitamins, stored at 4°C
10g Sucrose
0.5g MES
pH 5.7 with 1M KOH
For plates: 3g Gelrite

2.1.7.3 Antibiotics

Ampicillin: Working concentration: 100mg/l (stock: 100mg/ml in H_2O, prepare fresh)

Kanamycin: Working concentration: 25-50mg/l (stock: 50mg/ml in H_2O, stored at -20°C)

Spectinomycin: Working concentration: 50mg/l (stock: 50mg/ml in H_2O, stored at -20°C)

Vancomycin: Working concentration: 400mg/l (stock: 100mg/ml in H_2O, stored at -20°C)

Hygromycin: Working concentration: 15mg/l (stock: 50mg/ml in PBS, stored at 4°C)

Carbenicillin: Working concentration: 125mg/l (stock: 50mg/ml in H_2O, prepare fresh)

Tetracycline: Working concentration: 12.5mg/l (stock: 12.5mg/ml in Ethanol, stored at -20°C)

Gentamicin: Working concentration: 25mg/l (stock: 50mg/l in H_2O, stored at -20°C)

Rifampicin: Working concentration: 25-50mg/l (stock: 50mg/ml in DMSO, stored at -20°C)

2.2 Methods

2.2.1 Molecular Biology

2.2.1.1 Polymerase chain reaction (PCR)

Below (Table 1, 2, 3, 4, 5, 6) the standard conditions of PCR reactions using different polymerases are listed. For genotyping bacteria, plants and yeast, the GoTaq® (Promega, USA) and the OneTaq DNA polymerase (New England Biolabs, NEB, USA) were used. For the amplification of inserts for molecular cloning, the Q5 High Fidelity DNA Polymerase (NEB) comprising a 3´→ 5´ exonuclease activity was taken to reduce the error rate compared to the other two used DNA polymerases.

- GoTaq® DNA Polymerase (Promega)

Table 1: PCR reactions of the GoTaq® DNA Polymerase for a final volume of 25µl or 50µl.

Component [concentration]	**Final volume [concentration]**	**Final volume [concentration]**
5X Green GoTaq® Reaction Buffer	5µl	10µl
dNTPs [2mM]	2.5µl [0.2mM]	5µl [0.2mM]
5' primer [10µM]	1µl [0.4µM]	2.5µl [0.5µM]
3' primer [10µM]	1µl [0.4µM]	2.5µl [0.5µM]
DNA template	1µl (<200ng)	2µl
GoTaq® DNA Polymerase [5u/µl]	0,1µl	0.5µl
H_2O	14.4µl	27.5µl
Total reaction	25µl	50µl

Table 2: Standard thermal cycling conditions for GoTaq® DNA Polymerase mediated PCR amplification.

Step	**Temperature**	**Time**
Initial denaturation	95°C	2 min
Denaturation	95°C	30 sec
Annealing	Primer specific	30 sec
Elongation	72°C	1 min/kb
Repeat 30 times (colony-PCR) or 35 times (genotyping)		
Final elongation	72°C	5 min

- OneTaq DNA Polymerase (NEB)

Table 3: PCR reaction set-up of the OneTaq DNA Polymerase for a final volume of 25µl or 50µl.

Component [concentration]	**Final volume [concentration]**	**Final volume [concentration]**
5X Green GoTaq® Reaction Buffer	5µl	10µl
dNTPs [2mM]	2.5µl [0.2mM]	5µl [0.2mM]
5' primer [10µM]	1µl [0.4µM]	2.5µl [0.5µM]
3' primer [10µM]	1µl [0.4µM]	2.5µl [0.5µM]
DNA template	1µl (<20ng)	2µl
OneTaq DNA Polymerase [5u/µl]	0,1µl	0.5µl
H_2O	14.4µl	27.5µl
Total reaction	25µl	50µl

The 5X Green GoTaq® Reaction Buffer from Promega is used instead of the suggested 5X OneTaq reaction buffer from NEB because of better results and less background bands.

Table 4: Standard thermocycling conditions for OneTag DNA polymerase.

Step	**Temperature**	**Time**
Initial denaturation	94°C	2 min
Denaturation	94°C	30 sec
Annealing	Primer specific	30 sec
Elongation	68°C	1 min/kb
Repeat 30 times (colony-PCR) or 35 times (genotyping)		
Final elongation	68°C	5 min

- Q5 polymerase (NEB)

Table 5: PCR reactions of the Q5 High Fidelity DNA Polymerase for a final volume of 50µl.

Component [concentration]	**Final volume [concentration]**
5X Q5 Reaction Buffer	10µl
dNTPs [2mM]	5µl [0.2mM]
5' primer [10µM]	2.5µl [0.5µM]
3' primer [10µM]	2.5µl [0.5µM]
DNA template	2µl (<10ng)
Q5 High Fidelity DNA Polymerase [2u/µl]	0.5µl
H_2O	27.5µl (17.5µl for pVTOP + R-Dagdas_YFP-mCherry constructs)
5X Q5 High GC Enhancer	10µl (for pVTOP + Dagdas_YFP-mCherry constructs only)
Total reaction	50µl

Due to sequence similarities in the two fluorophores mCherry and YFP used in the Autophagic flux reporter constructs promoting unspecific primer binding, the PCR conditions were adapted. The extension time was prolonged to 10 minutes for 15 cycles and the reaction mix was adjusted by addition of 5X Q5 High GC Enhancer (NEB).

Table 6: Thermocycling conditions for the Q5 High Fidelity DNA polymerase.

Step	**Temperature**	**Time**
Initial denaturation	98°C	30 sec
Denaturation	98°C	10 sec
Annealing	Primer specific[1]	30 sec
Elongation	72°C	20-30 sec/kb
Repeat 5-25 times[2]		
Final elongation	72°C	2 min

[1]If a two-step PCR is performed for the amplification of the inserts for In-Fusion cloning, [2] 5 cycles run on a lower annealing temperature depending on the length of the regions of the primers homolog only to the insert, followed by 25 cycles on a higher annealing temperature given full homology.

An overview of the specific melting temperatures of the primer pairs is given in Table 12.

PCR fragments and linearized vectors separated on a 1.2% TAE gel were purified using the Wizard® SV Gel and PCR Clean-Up System (Promega). The elution from the columns was performed with 35µl ddH_2O, heated to 60°C after 10 min incubation.

2.2.1.2 Restriction digest

In Table 7 the standard reactions for restriction digests are listed. For control digests for the integrity of plasmids, 500ng purified DNA were incubated with 2U restriction enzyme for 2.5 – 3 hours in a 30µl reaction. To prepare linearized vector for cloning reactions, 3µg plasmid were digested with 2 – 30U enzyme and incubated overnight in 50µl volume. Buffers and incubation temperatures were chosen according to the enzyme supplier's suggestions.

For dCAPs, 7-10µl unpurified PCR product was used for the digest if the restriction enzyme was compatible with the PCR reaction.

Table 7 Standard restriction digest reactions

Component [concentration]	**Final volume [concentration]**	**Final volume [concentration]**
10X restriction enzyme buffer	3µl	5µl
DNA / PCR product	500ng / 7-10µl	3µg
Restriction enzyme	0.2µl [2U]	0.2µl – 3µl [2 – 60U]
H_2O	Up to 30µl	Up to 50µl
Total reaction	30µl	50µl

2.2.1.3 Sequencing

Samples to be sequenced were sent to LGC (Berlin), DNA and oligos were prepared according to the guidelines of the company.

2.2.1.4 In-Fusion Cloning

The generation of constructs via the Gibson cloning strategy was performed using the In-Fusion® HD Cloning Kit developed from Takara (France). It allows to clone one or more different inserts into a linearized vector. The ability of the DNA polymerase from the vaccinia virus to recognize complementary regions is used to fuse the insert(s) and the vector during a recombination event to a new plasmid (Irwin et al., 2012). To generate the required 15 bp extensions for homology, a specific primer design is necessary for the amplification of the inserts attaching the overhangs.

The method of In-Fusion® Cloning allows to clone one or more inserts into a linearized vector. To generate the required 15 bp extensions for homology, a specific primer design is necessary for the amplification of the inserts attaching the overhangs in a PCR reaction.

Table 8 Ingredients for an In-Fusion reaction.

Component	**Final volume**
5X In-Fusion HD Enzyme Premix	2µl
Linearized vector	50-200ng
PCR fragment (insert)	50-200ng
H_2O	Up to 10µl
Total reaction	10µl

The two-step PCRs for the amplification of the inserts (Table 12) were performed using the Q5® High-Fidelity DNA Polymerase with standard conditions, the linearization of the vector occurred by a restriction digest with one or two restriction enzymes. After the separation on a

1.2% TAE gel the purification was carried out according to the Wizard Plus SV Gel and PCR Clean_Up System (Promega). The elution from the columns happened with 35µl ddH_2O, heated to 60°C after 10 min incubation. The molar ratios of digested vector:insert(s) were calculated according to the In-Fusion molar ratio calculator with the ratio 1:2. At least 50ng DNA were used for each component. The reaction (Table 8) was incubated for 15min at 50°C, then put on ice and used for transformation into bacteria.

2.2.1.5 Golden Gate assembly

The *in vitro* cloning allows the assembly of multiple DNA fragments into a single plasmid using type II restriction enzymes and T4 DNA-ligase simultaneously. This type of restriction enzymes cut outside of their recognition sequence and does not generate palindromic overhangs. The loss of the restriction sites after the ligation ensures the correct orientation of the fragments (Engler and Marillonnet, 2013).

Table 9 Golden Gate reaction for undigested building vector.

Component [concentration, supplier]	**Amount molar ratio 1:1 (2:1)**
Each fragment	40fmol
Building vector pICH41308	40fmol (20fmol)
T4 DNA ligase [1U/µl, Roche]	1µl
10X T4 DNA ligase buffer (Roche)	2µl
Restriction enzyme BpiI [10U/µl, NEB]	1µl
Restriction enzyme BsaI [10U/µl, NEB]	1µl
H_2O	Up to 20µl
Total reaction	20µl

In the reaction comprising a linearized building vector, the volume of the restriction enzyme BsaI was replenished with H_2O.

The BIG CDS was obtained divided in four fragments from Carolin Delker from the Martin Luther University Halle-Wittenberg together with two building vectors, i) pAGM1287 without the possibility of a stop codon at the C-terminus of the CDS and ii) pICH41308 with a stop codon. The ligation reaction (Table 9) for the Golden gate cloning strategy to obtain the full CDS of BIG in the building vector pICH41308 was set up in two different molar ratios vector:insert 1:1 and 1:2. For each molar ratio, two different reactions were set, one with BsaI linearized building vector pICH41308, and one with undigested vector and BsaI in the ligation reaction. The reactions were incubated for 50 cycles 2 min at 37°C to 3 min at 16°C with the final inactivation steps at 50°C for 5min and at 80°C for 5min.

2.2.1.6 Western blot

30µl protein extract, stored at -80°C, were boiled in sample loading buffer for 5 min at 95°C and ran on a 12% SDS-PAGE (Table 10) at 80V in SDS-PAGE running buffer. After equilibration of gel and PVDF membrane in transfer buffer, the proteins were transferred to the PVDF membrane via wet blotting at 50 V for 1 h. After disassembling the blot, the membrane was rinsed twice in PBS. A Ponceau S stain was performed incubating it for few minutes in the Ponceau dye to verify the presence of proteins, the destaining happened with deionized H_2O. After rinsing the blot twice in PBS-T, the membrane was blocked for 40min in PBS-T 5% non-fat dried milk powder, moderately shaking at room temperature. The incubation with the primary antibody Anti-HA High Affinity from rat in a concentration 1:1000 in PBS-T occurred overnight at 4°C. The blot was rinsed once in PBS-T and washed 3x5 min in 25ml PBS-T. Afterwards the incubation with Anti-rat antibody (1:5000) in PBS-T was performed for 2 h at room temperature. The blot was rinsed in PBS-T and washed 3x for 5 min in 25ml PBS-T, rinsed once in PBS and washed for 5 min in PBS. The detection of the proteins was performed by chemiluminescence using WesternBright Sirius HRP substrate by Advansta. (ChemiDoc MP Imaging System, Bio-Rad Laboratories).

Table 10 Ingredients for a stacking and a 12% resolving gel, 1mm thickness.

	For stacking gel	For 12% resolving gel
Component [concentration]	**Final volume [concentration]**	**Final volume [concentration]**
Acrylamide [30%, mix 29:1]	330µl [5%]	2000µl [15%]
Tris-Cl pH 6.8 [1M]	250µl [50mM]	
Tris-Cl pH 8.8 [1M]		1950µl [390mM]
SDS [10%]	20µl [0.01%]	50µl [0.01%]
Bromophenol Blue	20µl	
APS [10%]	20µl [0.01%]	50µl [APS]
TEMED	2µl	4µl
H_2O	1358µl	946µl
Total reaction	2ml	5ml

2.2.2 Work with *Escherichia coli*

2.2.2.1 Preparation of competent cells

Bacteria were streaked out on an LB-agar plate to obtain fresh colonies. One single colony was inoculated in 250ml SOB medium containing 10mM $MgCl_2$ and 10mM $MgSO_4$ and grown at 37°C to an OD600 between 0,45-0,75. The cells were cooled down immediately in an ice bath and harvested for 10 min at 4°C 2500 rpm (rotor: Fiberlite F12-6 x 500, 152mm radius,

ThermoScientific). The pellet was resuspended on ice in 80ml TFB buffer. After an incubation time of 10 min, the cells were harvested for 10 min 4°C at 2500 rpm and resuspended in 20ml TFB buffer. 1.5ml DMSO were added and after an incubation time of 10 min, aliquots of 200µl cells were shock frozen in liquid nitrogen and stored at -80°C. For usage, the cells were thawed on ice.

2.2.2.2 Transformation

5-10µl In-Fusion or Golden Gate reactions were incubated with 200µl competent *E. coli* cells for 30 min on ice. All cloning reactions were transformed into the bacterial strain DH5α, except the construct YCplac22 + BIG_CDS into DH10β because of the size of the transformed plasmid. The heat shock treatment was performed at 42°C for 90 sec, followed by a 2 min chill on ice. 800µl SOC media were added and the reactions were incubated at 37°C shaking at 600 rpm for 1 hour. The reactions were pelleted for 3 min 3000 rpm (centrifuge: 5424/5424R, rotor: FA-45-24-11, Eppendorf), the supernatant was discarded, and the pellet was resuspended in the few µl of remaining liquid. Via the beads-methods the cells were plated on LB agar plates containing the specific antibiotic for selection of the plasmid.

2.2.2.3 Verifying constructs and plasmid preparation

As a first screening for the presence of a successful cloning reaction and transformation into *E. coli,* a colony-PCR was performed. A single colony was i) resuspended in 100µl H_2O and incubated for 10 min at 95°C, 1µl was used as PCR template, or ii) directly resuspended in the PCR reaction. Primer pairs were chosen to amplify the vector-insert border regions, or for the amplification of specific regions within the insert.

Positive colonies were inoculated in LB medium containing the specific antibiotic for the selection of the transgene. The purification of plasmids from *E. coli* was performed applying the PureYield™ Plasmid Miniprep System (Promega). The elution of prepared vector from 4ml liquid culture from the columns was carried out with 35µl ddH_2O, heated to 60°C. For low copy vectors, plasmids were isolated from 250ml cultures using the PureYield™ Plasmid Midiprep System (Promega). With 600µl ddH_2O, the plasmids were eluted from the columns.

At least one control restriction digest was performed to exclude rearrangements or deletions in the plasmid. Clones tested positive up to this point were confirmed by Sanger sequencing performed by LGC (Berlin).

2.2.3 Work with *Agrobacterium tumefaciens*

2.2.3.1 Preparation of competent cells

A single colony was inoculated in 20ml LB + Rifampicin + Gentamicin (if the selection for the pSoup helper plasmid was necessary, Tetracycline was added too) and at 30°C 600 rpm. 200ml LB + antibiotics were inoculated with 10ml of the overnight culture, growing to OD600 of ca. 0.6. The culture was cooled down immediately in an ice bath and the cells were harvested by centrifugation at 7500 g 4°C for 12 min followed by a washing step in 300ml sterile ice-cold H_2O. The pellet harvested in a further centrifugation step at 7500 g 4°C for 12 min was resuspended in 300ml ice-cold sterile 10% glycerol and harvested again. The cells were resuspended in 5ml ice-cold 10% glycerol and shock frozen in liquid nitrogen in 200µl aliquots. They were stored at -80°C.

2.2.3.2 Transformation

100-500ng plasmid DNA and 100µl competent cells *Agrobacterium* cells, thawed on ice, were briefly mixed in electroporation cuvettes chilled on ice. The transformation by electroporation was carried out using the electroporator GenePulser®BioRad with the settings 1.7kV, 25µF and 200Ω resistance. After the pulse, 1ml SOC medium was added and the reaction was transferred into a fresh tube. The cells were incubated at 30°C for 2h shaking at 600 rpm. Between 10-100µl were plated on LB agar-plates containing the antibiotics for the selection of the plasmid and incubated at 30°C in the dark.

2.2.3.3 Plasmid Preparation

For the verification of the colony comprising the correct plasmid without any rearrangements, the plasmid was purified from 4ml liquid medium. The PureYield™ Plasmid Miniprep System (Promega) was adapted, incubating the cell lysate for 10 min instead of 5 min with the enzyme alkaline protease. The neutralization solution was chilled on ice before stopping the reaction of the protease. The elution of the purified vector from the columns was carried out with 35µl 60°C ddH_2O.

To ensure the integrity of the plasmid purified from *Agrobacterium*, 50-100ng DNA were back-transformed into 50-200µl competent *E. coli* using the heat shock method. Grown colonies were investigated by different restriction digests to exclude rearrangements or deletions.

2.2.4 Work with *Saccharomyces cerevisiae*

2.2.4.1 Transformation

Yeast transformation of plasmids was performed according to the small-scale lithium-acetate method. An overnight culture from a single colony grown in the appropriate SD medium was diluted to OD600 0.25 in YPD and cultured at 30°C shaking at 250 rpm to OD600 0.2-0.3. The cells were harvested at 2000 rpm for 2 min at room temperature and washed in 25-50ml TE buffer. The pellet was resuspended in 1.5ml of freshly prepared TE/LiOAc buffer. 100µl yeast competent cells and 600µl PEG/LiOAc solution were added to the prepared DNA. For the transformation of a single plasmid, 100ng DNA in a volume of ca. 15µl H_2O were used; for a co-transformation, the molar ratio of the two plasmids was adjusted to 1:1 for 100ng each in 20µl H_2O.

The reaction was vortexed for 15-20 sec and incubated for 30 min at 30°C shaking at 600 rpm. 70µl DMSO were added and gently mixed by inversion. Afterwards, a heat shock reaction was performed at 42°C for 10-15min, the cells were cooled for 2 min on ice. The reaction was centrifuged 1 min at 2000 rpm (centrifuge: 5424/5424R, rotor: FA-45-24-11, Eppendorf), the pellet was washed in 500µl TE buffer and resuspended in 200-500µl TE buffer. The cells were plated on SD-plates containing the specific amino acid drop out mix for the selection of the desired transformant. The plates were incubated at 30°C for 2-3 days.

2.2.4.2 DNA preparation for colony-PCR

A colony was resuspended in 100µl 20mM LiOAc 1% SDS, vortexed for 10 sec and incubated at 70°C for at least 5 min. 300µl 96% EtOH were added and vortexed shortly. The reaction was pelleted at 15000 g for 3 min and the supernatant discarded. The pellet was washed with 500µl 70% EtOH and 500µl EtOH abs. After drying for 10 min, it was resuspended by adding 100µl H_2O and incubated for 10 min at 55°C shaking to dissolve the DNA. To obtain the template for the PCR, the reaction was spun down for 1 min at 15000 g and the supernatant was transferred into a fresh tube.

For the verification of the different N-termini of the X-beta-gal constructs after yeast transformation, a colonyPCR was performed to amplify the region covering the N-termini.

PCR was performed under standard conditions (OneTaq, 25µl reaction) with primer pair 1722_uplacIseq2 and 219_URA3dn. To verify the correct N-terminus, the purified fragment was sent for sequencing with primer 1722-lacIseq2.

2.2.4.3 Development of a yeast strain deficient in the UBR1 gene

To establish another *S. cerevisiae* strain besides SUS13, with deleted UBR1 gene, the WT strain CB80 was mutated to obtain an isogenic strain for equal conditions in the experiments.

The amplification of the UBR1 KanMX gene disruption cassette by PCR (primer 1919-UBR113Bsi + 1935-UBR6790Spe, template: UBR1-KanMX-UBR1, Q5 DNA polymerase) was followed by a gel purification. The CRISPR construct was amplified with primer pair 2076-yUBR_Fw1 + 2077-yUBR_Rv1, Q5 DNA polymerase, as template pRCC-N was used, a yeast CRISPR vector established from Generoso et al. (2016).

3 different transformation reactions using the small-scale lithium acetate method were set:

1) CB80: 20µl unpurified CRISPR PCR product + 3.5µg UBR1 KanMX disruption cassette PCR product
2) CB80: 3.5µg UBR1 KanMX disruption cassette PCR product, filled up to 15µl with H_2O
3) CB80 comprising the BIG CDS in YCplac22 vector: 3.5µg UBR1 KanMX disruption cassette PCR product, filled up to 15µl with H_2O

The transformed cells were incubated for 2 h in YPD on 30°C 600 rpm as regeneration step before plating on YPD with 200mg/l Geneticin (G418). ColonyPCRs (standard conditions with GoTaq® DNA polymerase) were performed to detect the insertion of the UBR1 KanMX gene disruption cassette by homologous recombination into the UBR1 locus:

For the detection of the wildtype form of UBR1:

1) Primer pair 1878-UBR1Bsi113 + 1989-UBR1_840-820 (upper border)
2) Primer pair: 1992-UBR1_5942-5964 + 1881-UBR1Spe6790 (lower border)

For the detection of the disrupted UBR1 gene:

3) Primer pair 1878-UBR1Bsi113 + 1871-KanMXup1 (upper border)
4) Primer pair 1872-KanMXdn1 + 1881-UBR1Spe6790 (lower border)

2.2.4.4 ONPG assay

For the induction of the Ub-X-βgal genes under the galactose-inducible GAL10 promoter, a single yeast colony was inoculated in 0.1% glucose 2% galactose (≥99% ROTH) SD medium before growing in 2% galactose only SD medium. SD-media used for the ONPG assays comprised 2% galactose (≥99%) and no glucose and the specific amino acid drop out mixes for the selection of the plasmids. All assays were carried out as duplicates or triplicates and performed at least two times in independent measurements.

An overnight culture, grown in the appropriate medium for the selection of the plasmid, was diluted to OD600 0.25 in the specific SD medium and grown to OD600 0.8-1. 10ml were harvested by centrifugation at 900 rcf 4°C for 5 min, the pellet was resuspended in 250µl breaking buffer. The cells were kept on ice from this time on. The cells were stored at -20°C and for the assay thawed on ice. Glass beads were added until they nearly reached the level of the meniscus of the liquid. 12.5µl PMSF were added and crude extracts were produced by vortexing six times in 15-second bursts. 250µl breaking buffer were added and mixed by shortly vortexing. The liquid was withdrawn and clarified by centrifugation for 15 min max. speed. The supernatant was transferred into a fresh tube. To perform the assay, 900µl Z-buffer were mixed with 50µl extract and the volume was adjusted to 1ml with 50µl breaking buffer, the samples were incubated for 5 min at 28°C. 200µl ONPG solution were added to start the reaction. As soon as a yellow colour developed, the reactions were terminated by the addition of 500µl Na_2CO_3. The optical density was measured at OD420. The protein concentration of the extract was determined in a Bradford assay performed in duplicates.

The specific activity of βgal in each extract was expressed according to the formula (Equation 1) in nmoles/minute/mg protein:

Equation 1 Formula for the specific activity of the βgal in the extracts in the ONPG assay

$$\text{specific activity} = \frac{\text{OD420} \times 1.7}{0.0045 \times \text{protein concentration} \times \text{extract volume} \times \text{time}}$$

OD420	Optical density of o-nitrophenol
1.7	Correction for reaction volume
0.0045	Optical density of 1 nmol/ml solution of o-nitrophenol
Protein concentration [mg/ml]	
Extract volume	Volume of extract assayed [ml]
Time [min]	

2.2.4.4.1 Inhibition of the Leu-N-end rule pathway

An overnight culture grown in the selective medium was diluted to OD600 0.25 and grown to OD600 0.5. At this time, Leu-OMet to a final concentration of 10mM was added. The cultures were grown to OD600 0.8-1, and an ONPG assay was performed.

2.2.5 Work with *Arabidopsis thaliana*

2.2.5.1 Sterilization of *Arabidopsis* seeds

10mg pulverized Bayrochlor was dissolved in 100µl H_2O and 900µl 96% EtOH were added to prepare a sterilization solution. Seeds in the volume of approximately 50µl were incubated for 10 min in 1ml sterilization solution, shaking moderately. The solution was discarded, and the seeds were washed 3 times with 1ml 96% EtOH. After the third washing step, as much EtOH as possible was removed and the seeds were dried in the clean bench for several hours until they were not sticking together anymore.

2.2.5.2 DNA extraction from plants

For the plant sample collection, a small young leaf of each plant (about 20-200mg) or a whole seedling, shock frozen and kept in liquid nitrogen, was ground with 1 metal bead (2.8 mm stainless steel) for 5 min with max. speed in the Qiagen TissueLyser II. After pulverization, the plant material was homogenized in 700µl DNA extraction buffer and centrifuged for 15 min, max. speed at room temperature. 600µl supernatant were added to 600µl isopropanol, inverted and centrifuged for 10 min, max. speed. The supernatant was discarded, and the pellet washed with 1ml 70% EtOH. After centrifugation for 5 min, max. speed, the supernatant was removed and 1ml 96% EtOH was added. The supernatant was removed, the pellet was dried for 10 min by tube inversion. The pellet was resuspended in 100µl H_2O and incubated for 10 min shaking at 55°C. The DNA concentration was measured by NanoDrop (260nm). Isolated DNA samples were used as templates for the PCR-based genotyping.

2.2.5.3 *Agrobacterium* mediated transformation

For the first attempt for developing novel reporter constructs using the pV-Top vector and the three different combinations of fluorophores, mCherry+sfGFP, YFP+mCherry, iScarlet+mNeonGreen, plant lines S7 and 6-1-1 were used. For the second attempt using the vectors pNIGEL07 the plant line WT Col_0, and for pBIBpOpTev-c1 the line 6-1-1 were used.

The plant lines were seed sterilized and sown on soil:perlite (4,5:1) mixture. For stratification, the seeds were stored for three days at 4°C and afterwards grown under standard conditions. The first bolts were clipped to promote the formation of secondary shoots.

The transformation of five weeks old plants starting to bloom was carried out using the floral dip method. An *Agrobacterium* overnight culture grown in YEB 10mM $MgSO_4$ and the specific antibiotic for selection of the transgene, for the pNIGEL constructs additionally Tetracycline,

was resuspended in 5% sucrose solution and 0,02% Silwet Gold. This added surfactant reduced the surface tension of the cells, facilitating the intrusion of the bacteria to increase the transformation rate (Clough and Bent, 2008). The plants were dipped into the solution for 30 sec, to prevent dehydration they were put into the dark and covered with plastic bags overnight. If the dip was carried out twice, the treatment was repeated after 7 days.

For the three pNIGEL07 constructs, a mixture of several colonies obtained from a previous transformation were inoculated as overnight culture because the *Agrobacterium* strain comprising the confirmed plasmid was not propagated at the timepoint of plant transformation.

2.2.5.4 Selection and Dexamethasone induction

The selection of the T1 plant generations was performed on MS-plates including the antibiotic according to the specific vector resistance and Vancomycin. Between 10 and 28 resistant plants of each construct of each plant line were transferred to soil. For the induction of the transgenes in the T2 generation, seeds were stratified at 4°C in liquid MS medium + Hygromycin. After 2 days, the medium was exchanged for MS medium including Dexamethasone and cultivated at standard conditions.

2.2.5.5 Genotyping

For PCR-based genotyping of plant material, the region of interest of extracted DNA was amplified and analysed, or fluorophores were detected under the fluorescence microscope.

PRT13:

The genotyping of the putative complementation group PRT13 comprising possible candidates of the N-recognin for Leu-N-termini was performed by dCAPs or sequencing of the candidate PCR fragments. The aim was to detect a correlation between a defined positive GUS staining and a co-segregating mutation in the candidate genes. Three possible candidates were investigated during this Thesis:

- ATG10 (At3g07525). Method of choice: dCAPs
  amplification of the fragment: 25µl PCR reaction, standard conditions with GoTaq® polymerase with primer pair 2073-prt13BspH + 2074-prt13dn1
  restriction enzyme: BspHI (NEB), CutSmart buffer
  separation on 2.5% TBE gel
- F-box protein (At3g13680). Method of choice: sequencing

Amplification of the fragment: 50µl PCR reaction, standard condition with ONETaq polymerase with primer pair 2187-13_3g1368dn1 + 2188-13_3g1368up1
Sequencing with primer 2187-13_3g1368dn1

- PP2A B' (At3g09880). Method of choice: sequencing
  Amplification of the fragment: 50µl PCR reaction, standard condition with ONETaq polymerase with primer pair 2185-13_3g0988dn1 + 2186-13_3g0988up1
  Sequencing with primer 2185-13_3g0988dn1 and 2186-13_3g0988up1

Novel reporter constructs (tFT constructs):

The detection of the artificial transcription factor LhGR2 by PCR (GoTaq, standard conditions) was carried out with primer pair 1560-LhGRIIdn1 and 1562-LhGRIIup2, for the pV-Top comprising the different combinations of the fluorophores, primer pair 955A-GUSupup and 1599-DHFRq1up was chosen.

Roots of 8-day old seedlings of the T2 plant generation of the tFT constructs in the pV-Top vector transformed into *Arabidopsis* selected on Hygromycin and induced by Dexamethasone were scanned under the fluorescence microscope for the presence of the red and yellow fluorophores.

For the detection of red fluorophores mScarlet and mCherry, the filter setting 561/688nm was selected, for YFP 488/561nm. The samples were not screened for mNeonGreen. So far, this fluorescence protein has not been tested in plants, and as a first screening for the presence of the tFT constructs standard fluorophores were preferred.

2.2.5.6 Detection of β glucuronidase activity (GUS stain)

Sterilized seeds were sown in liquid ½ MS medium. After 2 days, the medium was exchanged to ½ MS containing Hygromycin, Dexamethasone and Zebularine. 8-9 days later an *in vivo* GUS stain was performed.

After the fixation of the seedlings in 80% ice cold acetone by vacuum infiltration, they were rinsed with 50mM Na-P-buffer pH 7. The GUS staining solution, containing the substrate X-gluc was vacuum infiltrated for 10 min and incubated in the dark at 37°C overnight. The seedlings were rinsed with water, the destaining in 70% EtOH was repeated until the tissue was bleached white.

2.2.5.7 Protein extraction

9 days old *Arabidopsis* seedlings were dried, shock frozen and kept in liquid nitrogen. Manually, the plants were crushed with an ice-cold spatula. The samples were ground with 1 metal bead (2.8mm stainless steel) in the Qiagen TissueLyser II, velocity 28 for 2 min. The shaker was stopped every 20 sec.

After the lysis, the plant tissue was homogenized in 100µl protein extraction buffer and vortexed until it was liquid. The samples were boiled at 95°C for 6 minutes and pelleted for 10 min 20000 g at room temperature. The proteins in the supernatant were transferred into a fresh tube, frozen in liquid nitrogen and stored at -80°C until a Western blot was performed.

3 Results

3.1 Putative complementation group PRT13

The EMS-induced mutations on chromosome 3 were genotyped with the aim to detect a correlation between a positive blue GUS staining and mutations in the candidate genes for possible Leu N-recognins in *Arabidopsis* present in the putative complementation group PRT13. The blue developed colour in the *in vivo* staining proved the stabilization of the reporter enzyme GUS coupled to the primary destabilizing N-terminus Leu. All four candidate genes investigated in this experiment, BIG, ATG10, a F-box protein and PP2A B', are annotated on one arm of chromosome 3.

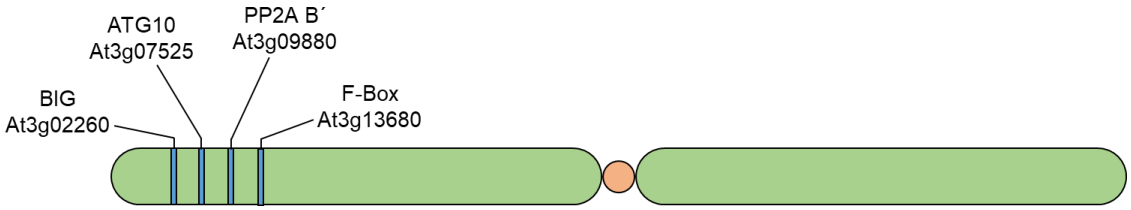

Figure 9 Candidate genes for possible Leu N-recognins in *Arabidopsis* of the putative complementation group PRT13. All four investigated genes are located on one arm of the chromosome 3.

The generation BC2F3 of the complementation group PRT13 consisted of 6 segregating plant lines and in total 33 plants were genotyped.

- PRT13-7-1 (8 plants)
- PRT13-37-1 (7 plants)
- PRT13-46-1 (6 plants)
- PRT13-102-5 (6 plants)
- PRT13-6-1-2 (3 plants)
- PRT13-29-7-1 (3 plants)

For BIG (At3g02260) as candidate gene, only the plant lines PRT13-102, -37 and -46 were genotyped by sequencing. As shown in Table 11, all investigated plants were WT for this gene. None of it had the mutation c.13493C>T (p.Ala4498Val).

ATG10 (At3g07525), genotyped by dCAPs with the restriction enzyme BspHI to investigate the presence of the SNPs at the positions 514 of the CDS (C>T), showed the strongest correlation between a blue GUS stain and a detected mutation (Figure 10). All plants defined

as homozygous carrier for the mutations had a positive GUS stain, demonstrating the stabilization of the L-GUS reporter construct. Plants genotyped as WT correlated with a negative GUS stain proving the degradation of the GUS enzyme linked to the Leu N-terminus. The same result applied to all heterozygous plants, except for one single plant named PRT13-7-1-17. It was genotyped as heterozygous but showed a blue colour in the GUS stain.

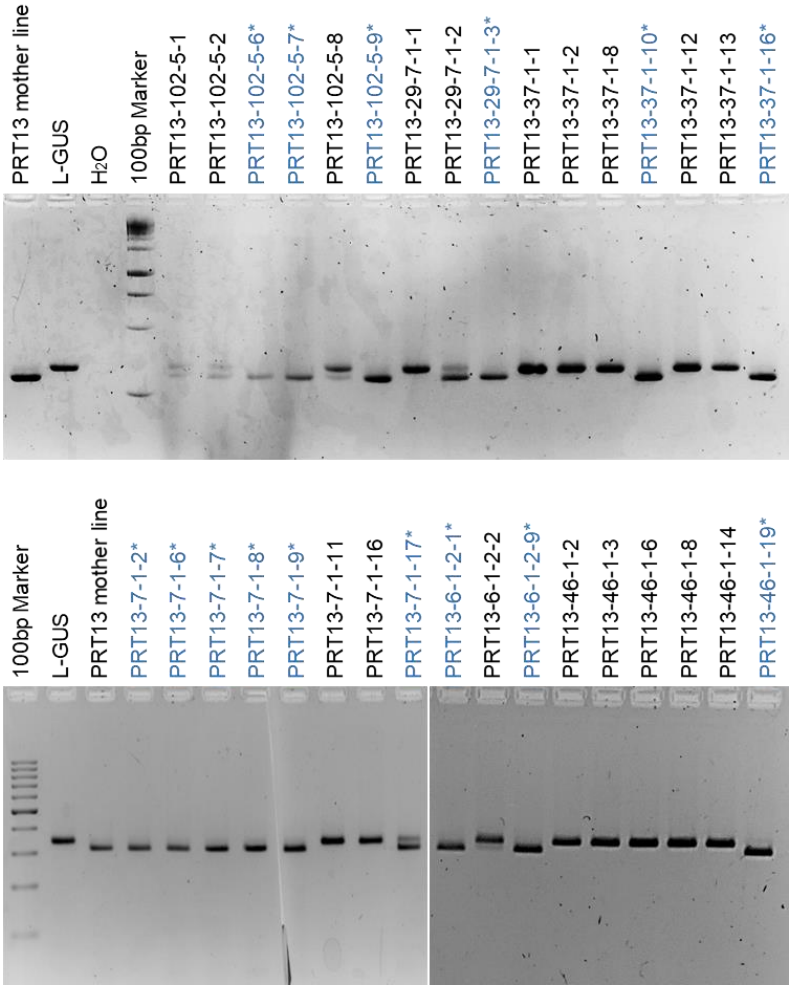

Figure 10 Genotyping of the candidate ATG10 of the putative complementation group PRT13 (BC2F3) for the mutation c.514C>T by dCAPs. The used restriction enzyme BspHI did not cleave the WT form of the gene resulting in the larger fragment. Samples with two bands were heterozygous for the mutation, the smaller band verified the presence of the SNPs. Samples written in blue and marked with* showed a positive GUS staining. A correlation between the blue phenotype and a homozygous genotype was detected in all samples except for PRT13-7-1-17. This plant was genotyped for a heterozygous phenotype and showed a blue colour in the GUS stain.

Another marker, the F-box protein (At3g13680) showed almost the same correlation between a homozygous mutation and a blue GUS stain as ATG10; except for plant line BC2F3-PRT13-37-1. All progenies of this line were genotyped as WT compared to the homozygosity in ATG10 and the blue GUS stain. Also, as for ATG10 the heterozygosity of the plant PRT13-7-1-17 prevented a 100% correlation between a stabilized L-GUS construct and a homozygous mutation, a heterozygous genotype and a blue GUS stain characterized this plant. The heterozygosity of this chromosomal region in plant PRT13-7-1-17 was verified by genotyping

the further candidate PP2A B' (At3g09880) located between ATG10 and the F-box protein by sequencing.

To detect a possible chromosomal crossing over event in the two progeny plants #10 and #16 of the plant line PRT13-37-1, PP2A B' was genotyped. As mentioned, this marker is located between the two candidates ATG10 and the F-box protein. The two investigated plants were homozygous carriers for the mutation in ATG10, while the F-box protein showed a WT genotype. PP2A B' was heterozygous in both plants.

Table 11 Overview of the characterized candidate genes for a Leu N-recognin of the complementation group PRT13 of the generation BC2F3.

					BIG	**ATG10**	**PP2A B´**	**F-Box**
					At3g02260	At3g07525	At3g09880	At3g13680
					c.13493C>T	c.514C>T	c.520G>A	c.1171A>G
					p.Ala4498Val	p.Pro172Ser	p.Glu174Lys	p.Arg391Gly
			plant	**GUS stain**	sequencing	BspHI (mut)	sequencing	sequencing
BC2F3	PRT13	6-1-2	**1**	blue	wt	homo mut		homo mut
BC2F3	PRT13	6-1-2	**9**	blue	wt	homo mut		homo mut
BC2F3	PRT13	6-1-2	**2**	white	wt	wt		wt
BC2F3	PRT13	29-7-1	**3**	blue		homo mut		homo mut
BC2F3	PRT13	29-7-1	**1**	white		wt		wt
BC2F3	PRT13	29-7-1	**2**	white		hetero		hetero
BC2F3	PRT13	7-1	**2**	blue	wt	homo mut		homo mut
BC2F3	PRT13	7-1	**6**	blue	wt	homo mut		homo mut
BC2F3	PRT13	7-1	**7**	blue	wt	homo mut		homo mut
BC2F3	PRT13	7-1	**8**	blue	wt	homo mut		homo mut
BC2F3	PRT13	7-1	**9**	blue	wt	homo mut		homo mut
BC2F3	PRT13	7-1	**17**	blue	wt	hetero	hetero	hetero
BC2F3	PRT13	7-1	**11**	white	wt	wt		wt
BC2F3	PRT13	7-1	**16**	white	wt	wt		wt
BC2F3	PRT13	46-1	**19**	blue	wt	homo mut		homo mut
BC2F3	PRT13	46-1	**2**	white	wt	wt		wt
BC2F3	PRT13	46-1	**3**	white	wt	wt		wt
BC2F3	PRT13	46-1	**6**	white	wt	wt		wt
BC2F3	PRT13	46-1	**8**	white	wt	wt		wt
BC2F3	PRT13	46-1	**14**	white	wt	wt		wt
BC2F3	PRT13	102-5-1	**6**	blue		homo mut		homo mut
BC2F3	PRT13	102-5-1	**7**	blue		homo mut		homo mut
BC2F3	PRT13	102-5-1	**9**	blue		homo mut		homo mut
BC2F3	PRT13	102-5-1	**1**	white		hetero		hetero
BC2F3	PRT13	102-5-1	**2**	white		hetero		hetero
BC2F3	PRT13	102-5-1	**8**	white		hetero		hetero
BC2F3	PRT13	37-1	**10**	blue		homo mut	hetero	wt
BC2F3	PRT13	37-1	**16**	blue		homo mut	hetero	wt
BC2F3	PRT13	37-1	**1**	white		wt		wt
BC2F3	PRT13	37-1	**2**	white		wt		wt
BC2F3	PRT13	37-1	**8**	white		wt		wt
BC2F3	PRT13	37-1	**12**	white		wt		wt
BC2F3	PRT13	37-1	**13**	white		wt		wt

Samples highlighted blue had a blue phenotype, samples highlighted white had a white phenotype in the GUS staining. The position of the mutation on DNA and on protein level were described and the genotyping method was annotated. The abbreviation wt stands for wildtype genotype, hetero for heterozygous and homo mut for homozygous mutant.

3.2 Putative candidates of Leu N-recognins in *A. thaliana*

The role of the two putative candidates for Leu N-recognins in *A. thaliana*, BIG (At3g02260) and cand16 (At3g12350), an F-box protein, was investigated in an ONPG assay (Figure 7) in *S. cerevisiae*. To summarize the principle of this method, the reporter enzyme βgal is coupled to different N-terminal amino acids. According to the N-end rule pathway, these polypeptides have different stabilities which are reflected in the yellow enzymatic product o-nitrophenol (ONP), photometrically detectable.

Further, two variants of the BIG gene, and as a control construct, a combination of the F-box of the yeast Ufo1 and the UBR domain of the plant PRT6, were tested.

As described earlier (chapter 1.2 The UPS in plants), different types of E3 ligases are known in *Arabidopsis*. The role of the here tested putative candidates was investigated as possible receptor site for ubiquitination targets as component of a Cullin ligase (Figure 11).

This type of ligases is built according to a modular principle consisting of different types of components. This leads to a huge variety and substrate specificity. The receptor site, an F-box protein, is linked via an adaptor to the scaffold protein Cullin, the assembly site of the protein complex. The specific E2 interacts at the Rbx1 subunit with the E3 ligase complex.

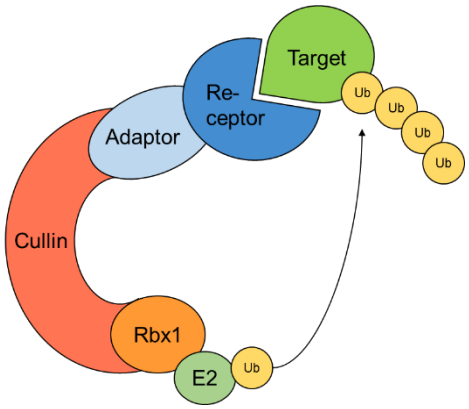

Figure 11 Cullin ligase. The function of the different candidates for Leu N-recognins in *Arabidopsis* were tested as possible components of a Cullin-RING ligase. The E2 interaction site, the RBX1, is linked to the C-terminal part of Cullin, that functions as a scaffold for the assembly of this Ub ligase type. At the N-terminus, the scaffold protein is linked to an adaptor such as Ask1 interacting with the receptor site for the ubiquitination target. Ub is directly transferred from the E2 to the target without being bound by the E3 ligase. This modular principle increases the number of possible ubiquitination targets.

3.2.1 BIG

As previously described in the chapter 3.1 Putative complementation group PRT13, the mutation in BIG caused by the EMS treatment did not correlate with a positive blue GUS

staining proving the stabilization of the L-GUS. This mutation was annotated at amino acid position 4498 (of 5098) and converted an Ala to a Val. Despite this result excluding BIG as a putative candidate for a Leu N-recognin mutated in line PRT13 of *Arabidopsis*, the outcome of a GUS stain performed for the plant line SALK_045560 showed a contrary result (Figure 12). This line has a T-DNA insertion in exon 5 of 14 of the BIG protein and was crossed with the reporter line expressing the L-GUS construct in the Col-0 background (Figure 5). The blue color reflected the stabilization of the L-GUS construct, the treatment with the autophagy inhibitor Concanamycin A (ConA) increased the blue staining, suggesting that BIG operates via UPS.

This results in the GUS stain with a T-DNA insertion strengthened the assumption that BIG plays a role in the Leu N-end rule pathway.

As a control, the instability of the L-GUS construct in the WT Col-0 expressing the reporter construct was demonstrated (Figure 12). The treatment with ConA led to a slight stabilization of L-GUS. The stain was performed by Nikola Winter who also kindly provided the picture.

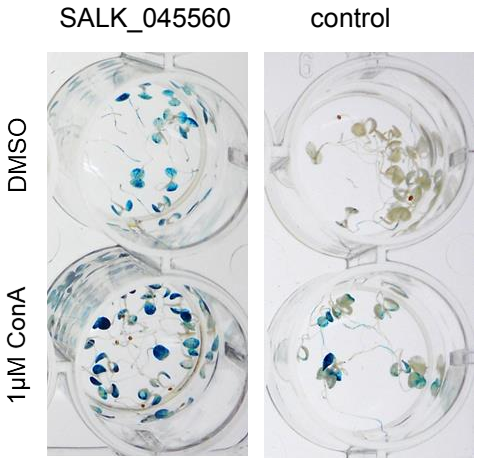

Figure 12 GUS stain of the plant line SALK_045560 (T-DNA insertion in exon 5 of BIG) and WT Col-0 expressing the L-GUS construct. The blue colour developed in seedlings proved the stabilisation of the L-GUS reporter construct. This effect was detected in the SALK line expressing the mutated BIG, a strengthening of the colour could be seen after the treatment with the autophagy inhibitor Concanamycin A (ConA). In the control line, the WT Col-0 transformed with the L-GUS construct, no stabilization of L-GUS in the untreated seedlings could be seen in contrast to the treated with a light development of a blue colour.

3.2.1.1 Cloning of BIG

The first part of the experiment consisted of cloning the complete CDS of BIG to allow its expression in bacteria and yeast. As raw material, the CDS divided in four fragments, generated from Klause Tanja during her bachelor's Thesis at the Leibniz Institute for Plant Biochemistry and the Martin-Luther-University of Halle-Wittenberg, was taken. Two different

strategies were pursued, one by Golden-Gate assembly and the other by In-Fusion® cloning, building the cDNA fragment by fragment.

The first approach using the Golden Gate assembly did not lead to the complete synthesis of the CDS in *E. coli* DH5α. Therefore, the method was changed to the Gibson assembly using the In-Fusion® Cloning Kit and building the CDS fragment by fragment.

An overview of the complete BIG CDS, the fragment border regions and the localization of the two putative CRDs and the ZZ-domain is given in Figure 13.

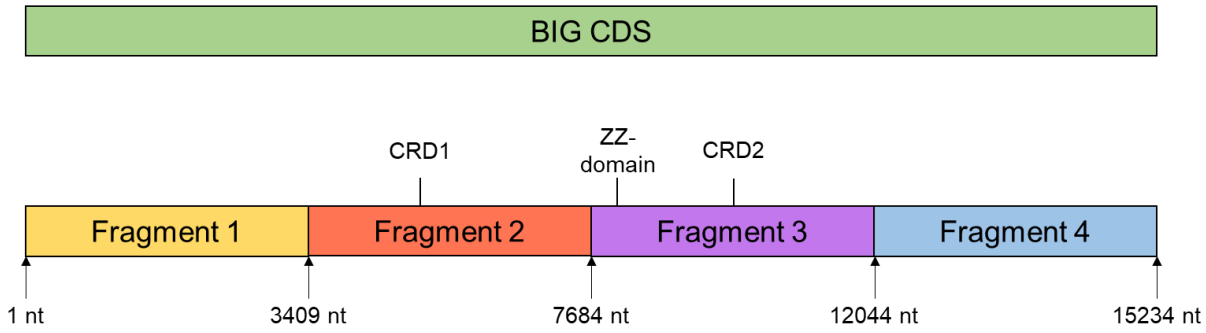

Figure 13 Overview of the BIG gene. The 15234 nt long CDS should be assembled from 4 fragments, each between 3.2 and 4.5 kb long. The two putative CRDs at the positions ~ 4680 and ~ 10320 nt, and the ZZ-domain at position ~7770 nt are shown.

The cloning was carried out in 5 steps (Figure 14). For each step, the starting vector and the restriction enzymes used for the linearization of the plasmid are shown on the left side, the insert with the corresponding primers for the amplification is shown on the right side. Detailed PCR conditions are listed in Table 12.

Due to a 400nt deletion in fragment 1, the 5th cloning step was necessary. The linearization of the vector with the restriction enzymes SmaI and PshAI led to the disruption of the KanR gene. To restore this selection marker, a KanR fragment was amplified from the undigested plasmid used in this cloning step. The missing 400nt fragment was synthesized from a cDNA template (kindly provided from Lilian Nehlin) in two steps, 1st amplifying a larger fragment covering the desired sequence, and 2nd, amplifying the insert for the cloning from the 1st fragment. By a 3-factor ligation, the KanR and the 400nt deletion fragments were joined to the linearized pACYC177 vector containing the supplemental sequence of the BIG CDS, restoring the KanR and replenishing the deletion. The final construct was transformed into the *E. coli* strain DH10β because of its higher transformation efficiency for large plasmids compared to DH5α, the strain used in the previous steps. (https://international.neb.com/products/c3019-neb-10-beta-competent-e-coli-high-efficiency#Product%20Information 28.05.2020).

1st step

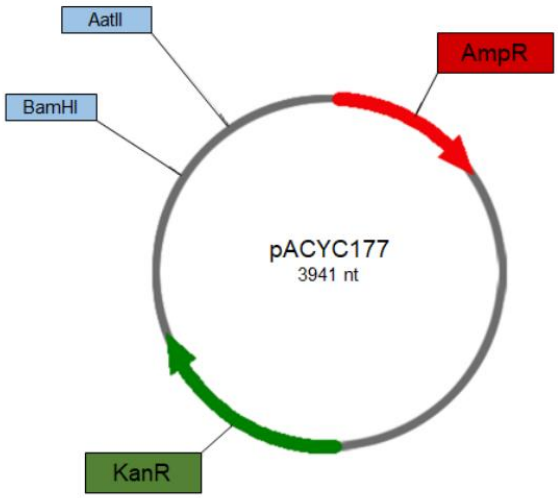

2-factor ligation and
transformation into *E. coli* DH5α

2nd step

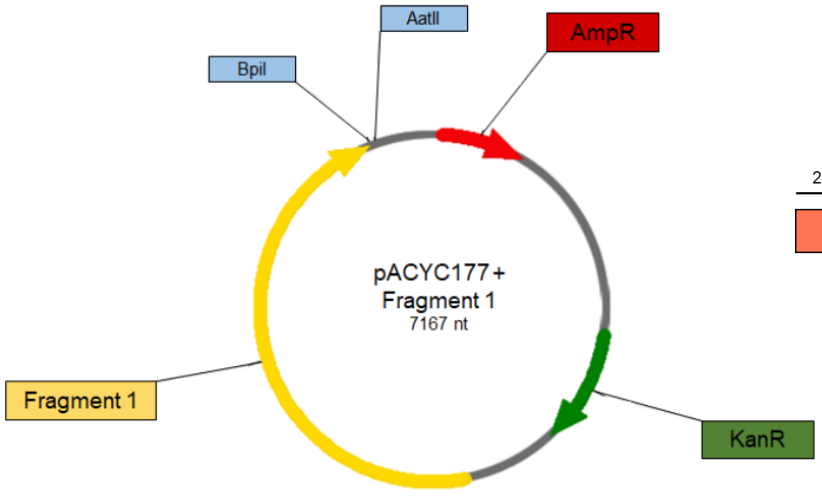

2-factor ligation and
transformation into *E. coli* DH5α

3rd step

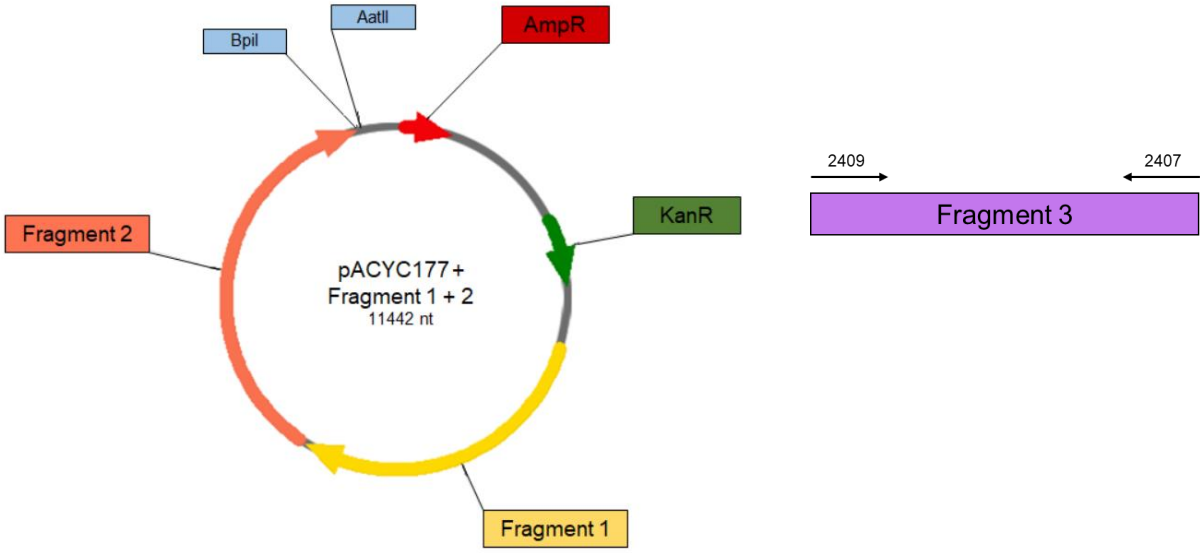

2-factor ligation and
transformation into *E. coli* DH5α

4th step

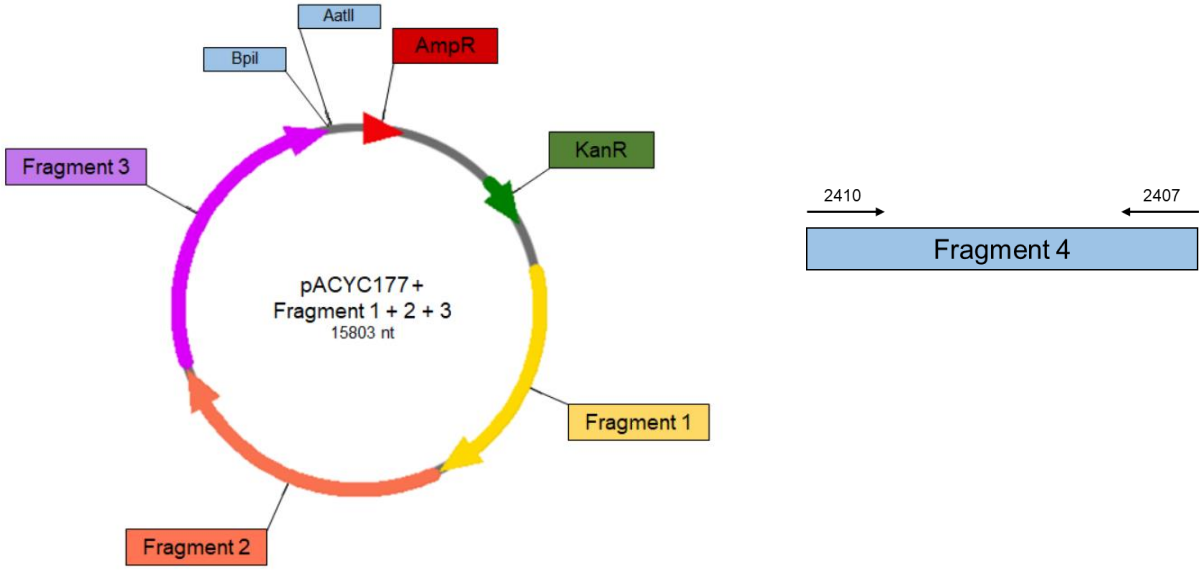

2-factor ligation and
transformation into *E. coli* DH5α

5th step

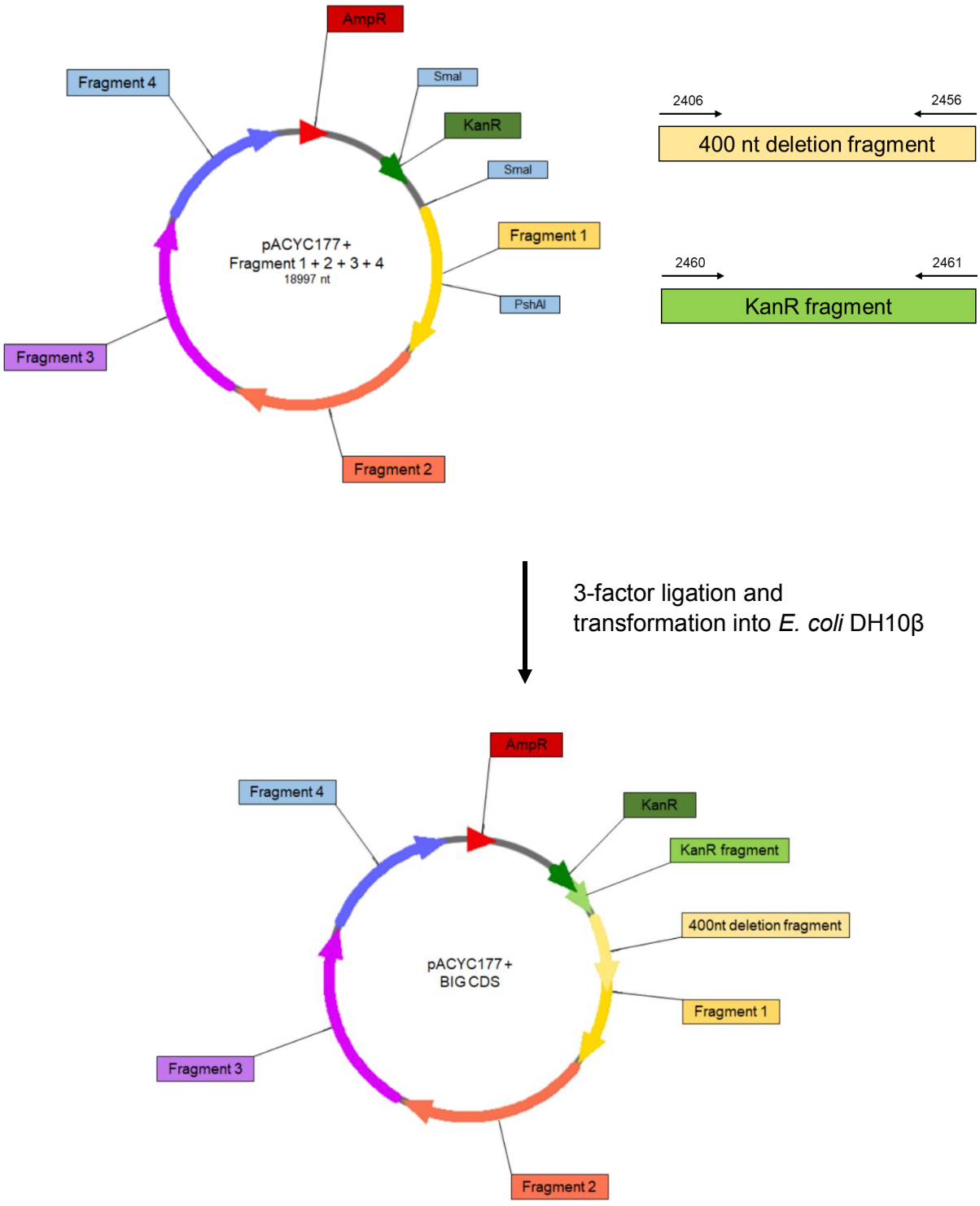

Figure 14 Cloning strategy of BIG. 5 cloning steps were carried to obtain the complete CDS of BIG in the pACYC177 vector. On the left side, the starting vector of each step and the restriction enzymes (light blue highlighted boxes) used for linearization are shown. On the right side, the amplification step of the inserts with the corresponding primer pair is shown (the exact PCR conditions are listed in Table 12 Overview **of constructs made during this Thesis.** The position of the two selection markers for Ampicillin (AmpR) and Kanamycin (KanR) are highlighted red and green. In the 5th step, the complete restriction digest with the two enzymes PshAI and SmaI led to the disruption of the KanR. In a 3-factor ligation, the 400nt deletion in fragment 1 and the lost KanR fragment were restored leading to the desired construct of the BIG CDS in the pACYC177 vector with a total size of 18997nt.

To allow the expression of the BIG protein in yeast, the CDS was transferred from the low copy vector pACYC177 to the ARS1-CEN4 yeast vector YCplac22 with a PGK promoter and terminator. Due to the huge size difference between insert (BIG, 15.2kb) and vector (YCplac22, 4.9kb), the insert was treated as vector and linearized by a restriction digest, and the vector was amplified by PCR to prepare the two fragments for the In-Fusion® cloning (detailed information are listed in Table 12). For the purification of the plasmid from *E. coli*, the colonies were scratched from plates as the selection with Amp in liquid culture was not productive enough. To exclude possible deletions or rearrangements, restriction digests were carried out before transforming the plasmid into the two yeast strain SUS13 and CB80.

3.2.1.2 ONPG assay in yeast (part 1)

In CB80, a wildtype *S. cerevisiae* strain, the influence of BIG on the stability of different N-termini was characterized compared to the vector YCplac22 without an insert. For none of the six different N-termini, a difference of the corresponding βgal activities between BIG and the empty vector could be detected (Figure 15). The stable amino-termini M, S and V in the cells comprising the vector without insert showed a slightly higher βgal activity than those comprising the BIG protein. As the WT strain expressed the only N-recognin in yeast, UBR1, the βgal enzymes linked to the primary unstable N-termini F, L and R had a short lifetime compared to the stable N-termini M, S and V.

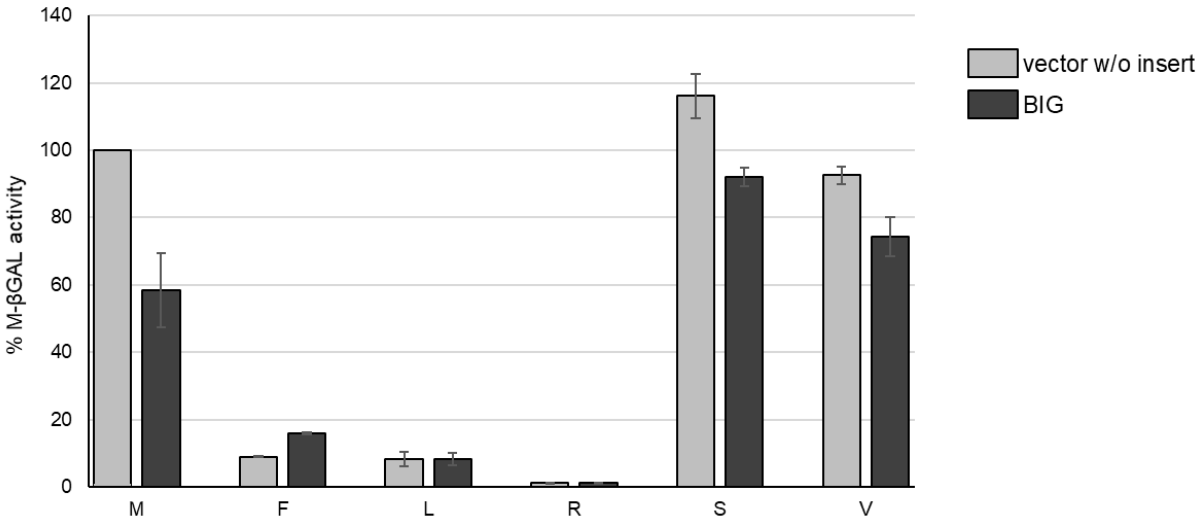

Figure 15 Relative metabolic stabilities of the reporter enzyme βgal in WT CB80 yeast cultures expressing the BIG protein compared to cultures comprising the empty YCplac22 vector. In the three stable N-termini M, S and V a slight increase of the enzymatic product in empty vector cells compared to BIG expressing cultures could be detected. The measured activity in cultures where the βgal was fused to the primary destabilizing residues F, L and R was as low as expected; no difference between the expression of BIG to the control group could be detected. The stabilities were calculated in relation to the activity measured in M N-terminus combined with an empty vector. Error bars represent the standard deviation calculated from three independent experiments.

To reveal the direct effect of the BIG protein as possible N-recognin on peptides with the primary destabilizing N-terminus L, the activity of the reporter enzyme was determined in the *ubr1*Δ yeast strain SUS13 compared to the vector YCplac22 without an insert. Lacking UBR1, the only N-recognin known in yeast, these cells were not able to degrade the primary destabilizing residues of the yeast N-end rule pathway.

No decrease in the L-βgal activity in the BIG expressing yeast cells compared to the vector without an insert could be measured (Figure 16) excluding BIG as N-recognin for L N-termini in this tested system. Also, the protein did not show an influence on the abundance of the βgal coupled to R although comprising an UBR domain comparable to that found in PRT6. The measured activities of the βgal with primary destabilized N-termini were at the same level as those of the stable N-termini M, S and V.

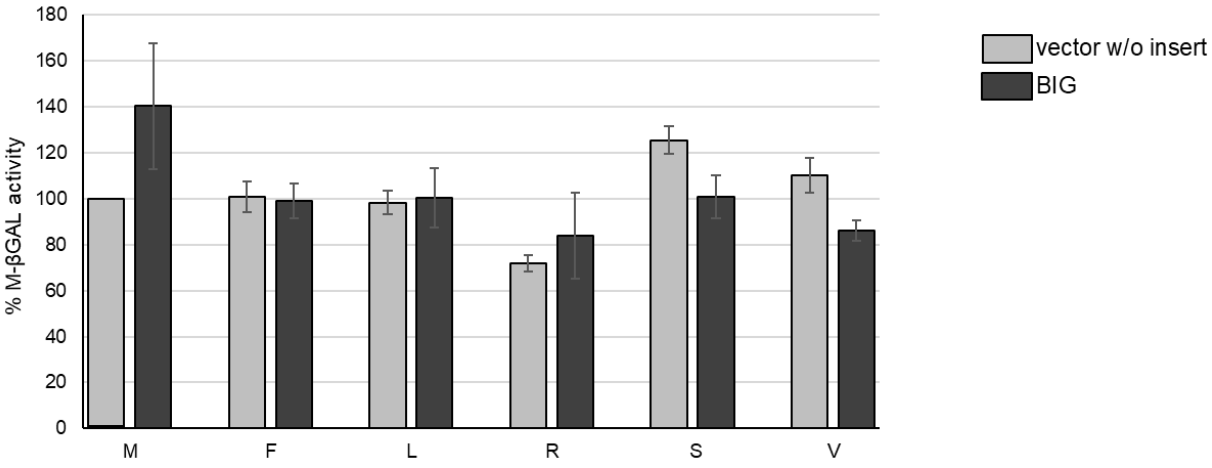

Figure 16 Relative metabolic stabilities of X-βgal constructs in yeast strain SUS13 (*ubr1*Δ) expressing the BIG protein. The enzymatic activity in BIG expressing cells was compared to cells of the corresponding N-terminus comprising the YCplac22 vector without an insert. In none of the investigated samples a significant difference between BIG expressing and control cells could be observed. The βgal activities for the different N-termini were shown relative to the M βgal expressing the vector without an insert, set to 100%.
Error bars represent the standard deviation calculated from four independent experiments.

According to Baker and Varshavsky (1991), the N-end rule pathway can be inhibited *in vivo.* By the addition of dipeptides or amino acid derivates to the medium, the substrate binding site on the N-recognin will be blocked. This prevents the degradation of the reporter enzyme X-βgal leading to an increase of enzymatic activity. To identify a possible L-binding site on BIG, the yeast cell cultures were treated with Leu-OMet which should lead to a stabilisation of L-βgal. In none of the tested N-termini an effect of Leu-OMet on the X- βgal activities compared to untreated cultures could be detected (Figure 17). The same results could be observed if Leu-OMet was dissolved in DMSO (data not shown here). Due to the induction of oxidative

stress and a possible toxicity, for further experiments the stock solution of Leu-OMet was dissolved in K-P-buffer instead of DMSO.

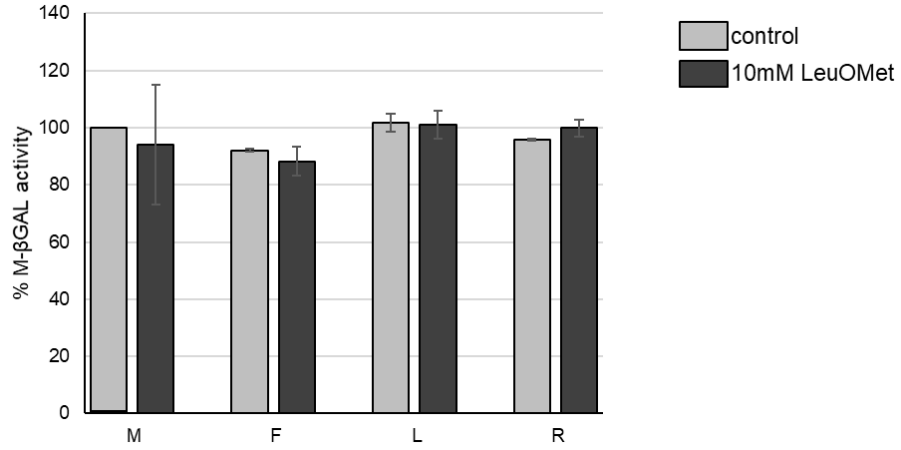

Figure 17 *In vivo* inhibition of the N-end rule pathway by the addition of Leu-O-methyl ester to detect a possible L-binding site on the putative candidate for a Leu N-recognin BIG. The experiment was conducted in the yeast strain SUS13 (*ubr1*Δ). No differences in the X- βgal activities between the individual N-termini, and within the treatment and control groups could be detected.
The enzymatic activities were calculated from two independent measurements, each conducted in duplicates.

Likewise, a partial inhibition of the Leu N-end rule pathway by LeuOMet, the enzymatic activity of X- βgal in treated WT CB80 yeast cultures was defined. As shown in Figure 18, the amino acid derivate did not lead to a difference in the activites between treated and control cultures of the corresponding N-termini.

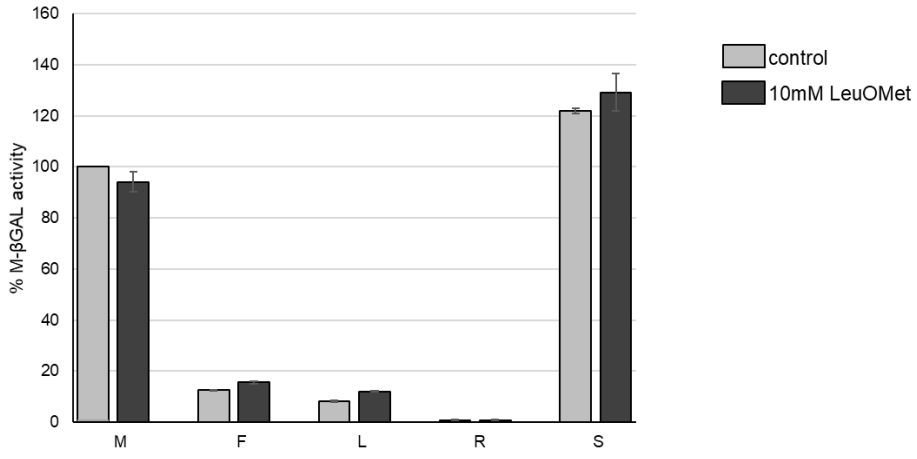

Figure 18 Relative metabolic stabilities of X- βgal constructs in CB80 yeast cells expressing the vector YCplac22 without an insert. The cells were treated with the amino acid derivate LeuOMet. In none of the investigated cultures a difference between treated and control cultures of the respective N-termini could be detected. The βgal activities for the different N-termini were shown relative to the untreated M-βgal, set to 100%.
The experiments were conducted in duplicates and the activities of the different X-βgal were calculated relative to the M-βgal, set to 100%.

3.2.2 Further candidates

In addition to BIG, five further fusion constructs were assembled by In-Fusion® Cloning to test their role in the N-end rule pathway using an ONPG assay. On overview of the fragments inserted into a linearized YCplac22 vector and the used primer pairs for their amplifications are shown in Figure 19 (detailed information in Table 12).

Four of these constructs were fused to a N-terminal F-box fragment of Ufo1, a F-box receptor protein found in the yeast *S. cerevisiae*. It acts as the substrate recognition component of a SCF E3 ubiquitin-protein ligase complex. The C-terminal fragments of two constructs consist of the two splicing variants of cand16 (At3g12350), a F-box protein of *Arabidopsis* and of the UBR domain of PRT6, the plant N-recognin for type I primary destabilizing residues comprising the basic amino acids Arg, Lys and His.

The other two constructs were fragments of the BIG protein. The 1259 amino acids long fragment of BIG covered the putative ZZ-domain. This variant was also tested in combination with the N-terminal F-box fragment of Ufo1.

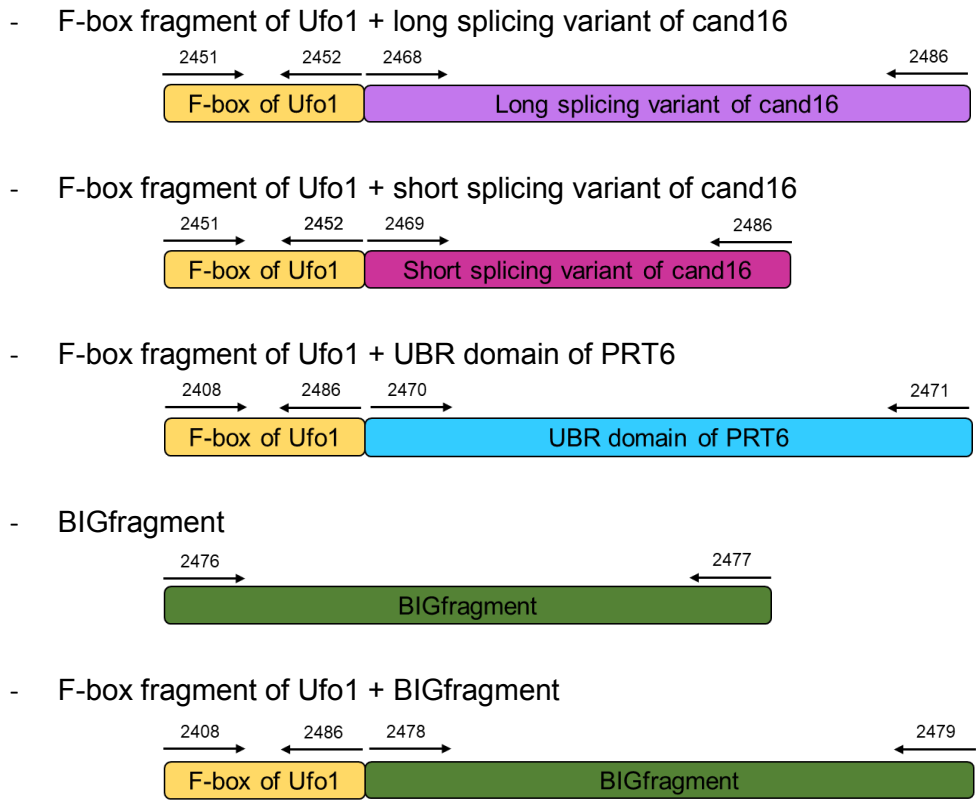

Figure 19 Cloning of further candidates for Leu N-recognins in *Arabidopsis*. The primer pairs used for the amplification of the inserts generating the 15 bp homologs for the In-Fusion® cloning are shown.

3.2.2.1 ONPG assay in yeast (part 2)

Two splicing variants of the F-box protein as putative candidate for Leu N-recognins, named short and long cand16, were tested. As for BIG, the used yeast strain SUS13 lacked an intact ORF of UBR1. This effect brought forward the direct influence of the investigated proteins on the stability of the reporter enzyme βgal coupled to different amino-termini.

As shown in Figure 20, the two cand16 splicing variants fused to an N-terminal Ufo1 fragment did not lead to a degradation of peptides with the primary destabilizing residues F, L and R compared to those with the stable M N-terminus. The stability of these fusion proteins consisting of the individual N-termini linked to the reporter enzyme βgal, was calculated relative to the stable M N-terminus set to 100%. As control for a working assay, PRT1, the N-recognin of the plant N-end rule pathway recognizing the aromatic amino-terminal residues F, Y and W, was expressed in this *ubr1*Δ strain. As published, PRT1 restores the degradation of F-βgal, leading to significantly lower measured enzymatic activity compared to the stable M-βgal (Stary et al., 2003).

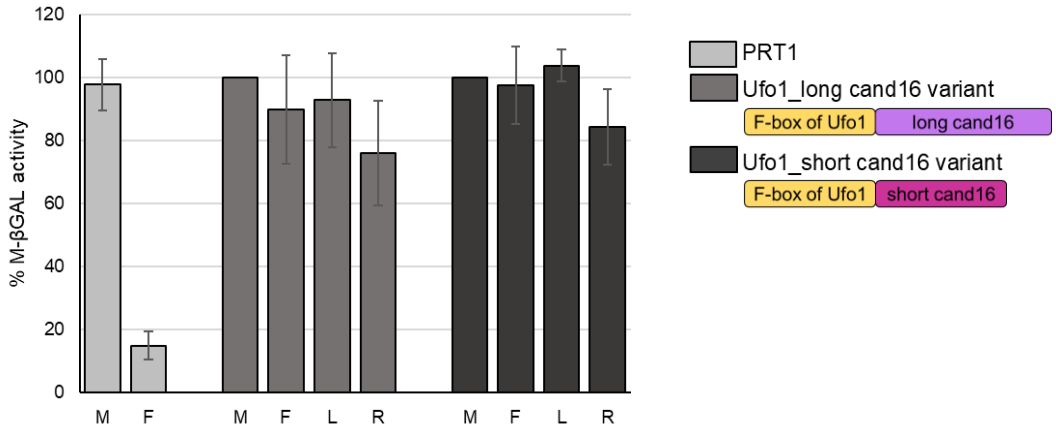

Figure 20 Relative metabolic stabilities of the βgal, linked to the N-termini M, F, L and R, in ONPG assays testing the role of the long and short splicing variants of cand16, N-terminally fused to the yeast Ufo1 F-box domain. The transgenes were expressed in an *ubr1*Δ yeast strain, SUS13. In none of the investigated cultures, a difference between the N-termini F, L and R compared to the stable M, set to 100%, could be detected. As controls, the activity of the two N-termini F and M was determined in the PRT1_ *ubr1*Δ background. SUS13 expressing the PRT1 N-recognin is able to degrade the reporter enzyme β-gal coupled to the F N-terminus compared to the stable M β-gal. All activities were calculated relative to the M β-gal activities of the candidates of each measurement.
The enzymatic activities were calculated from three independent measurements, each conducted in duplicates.

The here tested combination of the F-box of Ufo1 from yeast and the UBRdomain of PRT6 as a control construct was not sufficient to destabilize any of the F, L and R- βgal in the SUS13 *ubr1*Δ yeast strain compared to the stable M- βgal set to 100% (Figure 21).

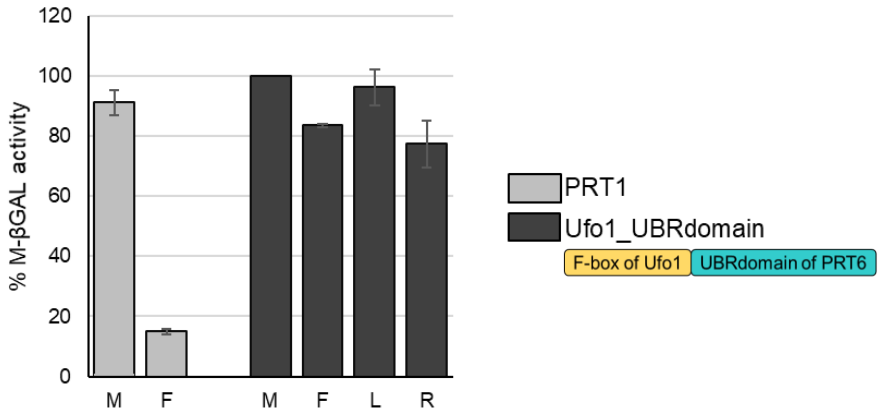

Figure 21 The yeast F-box domain of Ufo1 combined with the UBRdomain of PRT6 did not lead to the degradation of reporter enzyme with the amino-termini F, L and R compared to the stable residue M in the strain SUS13. The experiments were conducted in duplicates and the activities of the different X-βgal were calculated relative to the M-βgal, set to 100%.

As shown in Figure 22, the expression of a BIGfragment, covering the amino acid sequence 2160-3419 of BIG including the putative zinc finger domain at position ~2600, did not match the results of the ONPG assays performed with the complete BIG protein (Figure 16). The enzymatic activity of the M-βgal was much higher compared to F-, L and R- βgal. Due to these differences, further assays were carried out for direct comparison of the enzymatic activities in BIGfragment expressing yeast cells and cells transformed with a vector without an insert (Figure 23). An increased activity of βgal with an M N-terminus compared to F, L and R N-termini was also noted here, but no convincing difference of the corresponding cultures expressing the BIGfragment and those with an empty vector could be detected.

Further, the stabilization of the X- βgal with the N-termini M, F, L and R has been tested in combination with Ufo1_BIGfragment. In none of these investigated cultures, a significant reduction of a X-βgal activity compared to the stable M-βgal could be detected (Figure 22). As controls for a working assay, the activity of the M- and F-βgal in combination with PRT1, the plant N-recognin for the aromatic amino-termini, has been determined.

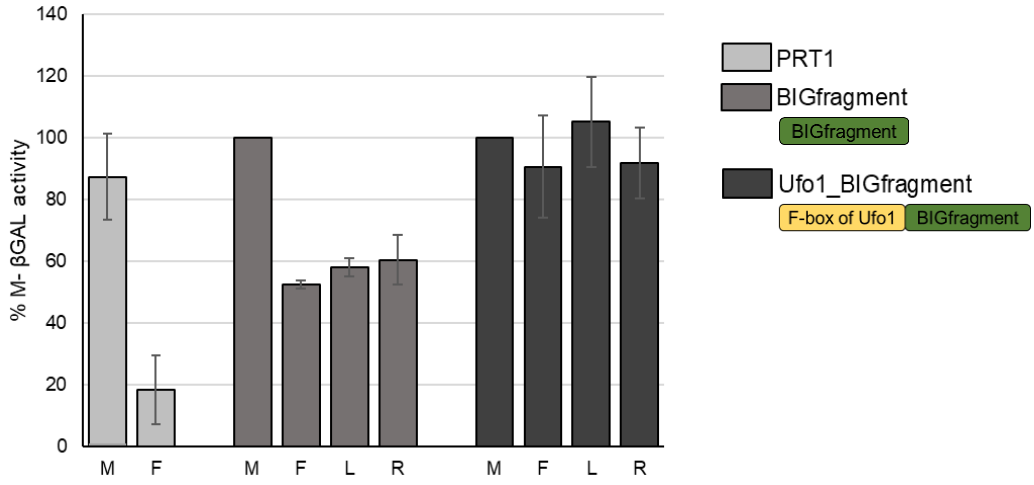

Figure 22 Relative metabolic stabilities of X-βgal constructs in the yeast strain SUS13 (*ubr1*Δ) in combination with two variants of BIG as candidate for a Leu N-recognin. A BIGfragment (amino acid position 2160-3419 of BIG) including the putative ZZ-domain at position ~2600 was tested. No differences between the βgal activities of the three N-termini F, L and R could be detected, but in comparison to the stable N-terminus M, the enzymatic activities in these three cultures were decreased.
The BIGfragment in combination with an N-terminal Ufo1 domain did not lead to a significant change of enzymatic activities measured in F, L and R compared to the M N-terminus, all four N-termini showed the same metabolic stability. As control for a working assay, PRT1 lowered the concentration of peptides with an aromatic amino-terminus as expected.
The values were calculated from two independent measurements conducted in duplicates and triplicates.

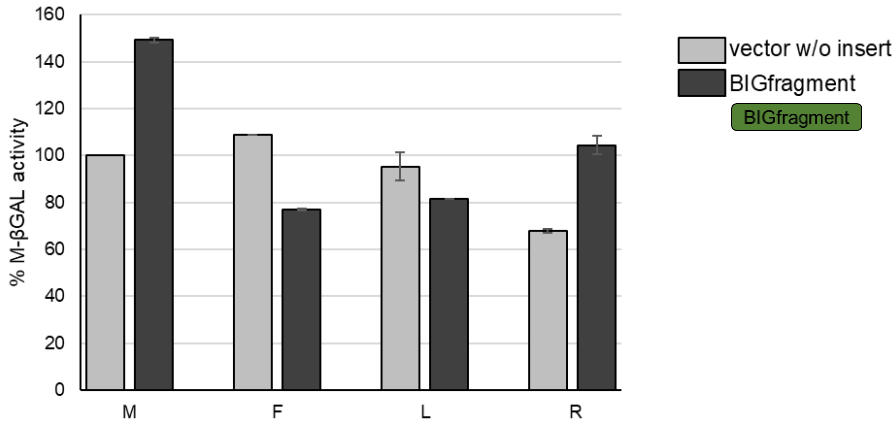

Figure 23 Relative metabolic stabilities of X-βgal constructs in yeast strain SUS13 (*ubr1*Δ) expressing the BIGfragment. The enzymatic activity in BIGfragment expressing cells was compared to those of the corresponding N-terminus comprising the YCplac22 vector without an insert. In none of the investigated samples a significant reduction of measured activity in BIGfragment expressing cells compared to empty vector cells could be detected. The βgal activities for the different N-termini were shown relative to the M-βgal expressing vector without an insert, set to 100%.
Error bars represent the standard deviation calculated from two independent experiments.

Taken together, none of the investigated putative candidates, the F-box protein cand16 with its two splicing variants, and BIG and its two variants, showed a possible role as a Leu N-recognin in the tested system. Also, no influence of BIG on the stability of a protein with R as N-terminus could be detected.

3.3 Development of a new yeast strain with UBR1 deletion

The aim of this gene editing was the development of a second yeast strain besides SUS13 lacking an intact UBR1 ORF. As starting culture, the WT strain CB80 was taken to achieve better experimental conditions. Further assays can then be performed in two isogenic yeast strains differing exclusively in the functionality of UBR1.

Colonies grown on G418 containing plates positively selected for the insertion of the KanMX disruption cassette were tested in colony-PCRs for its presence. Seven different colonies were investigated (Figure 25) amplifying the four possible border regions; the upper and lower border regions if i) cells still comprise an ORF for UBR1 or ii) the KanMX disruption cassette disrupting the ORF (Figure 24).

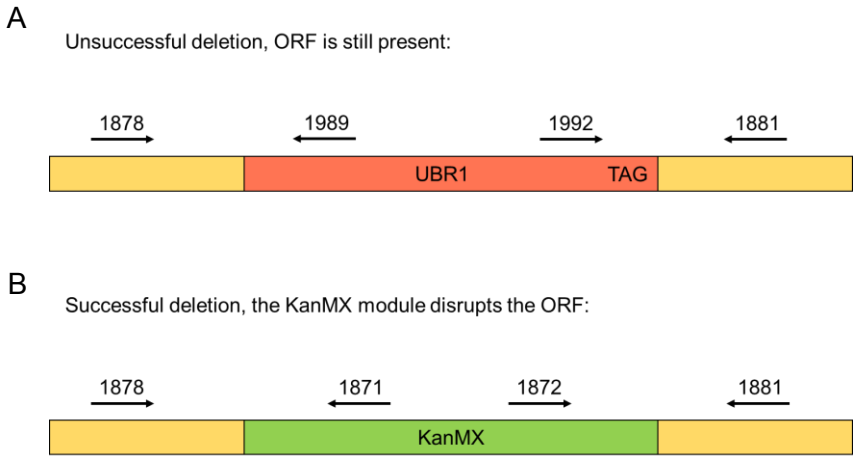

Figure 24 UBR1 gene editing. A) If the deletion of the UBR1 ORF is not successful, the WT form of the gene is present. This can be proved by the combination of the primer pairs 1878 + 1989 and 1992 + 1881. B) If the deletion of the UBR1 gene is successful, the ORF is disrupted by the insertion of a kanamycin resistance module (KanMX cassette). Different reactions were tried. The homologous recombination was mediated either with a CRISPR construct or without. The successful deletion can be verified by the amplification of the border regions with the primer pairs 1878 + 1871 and 1872 + 1881.

Colony #4 had been the only one with positive PCR results for the amplification of the border region fragments of *ubr1*Δ. In this colony, also faint bands for the detection of the WT UBR1 gene were detectable.

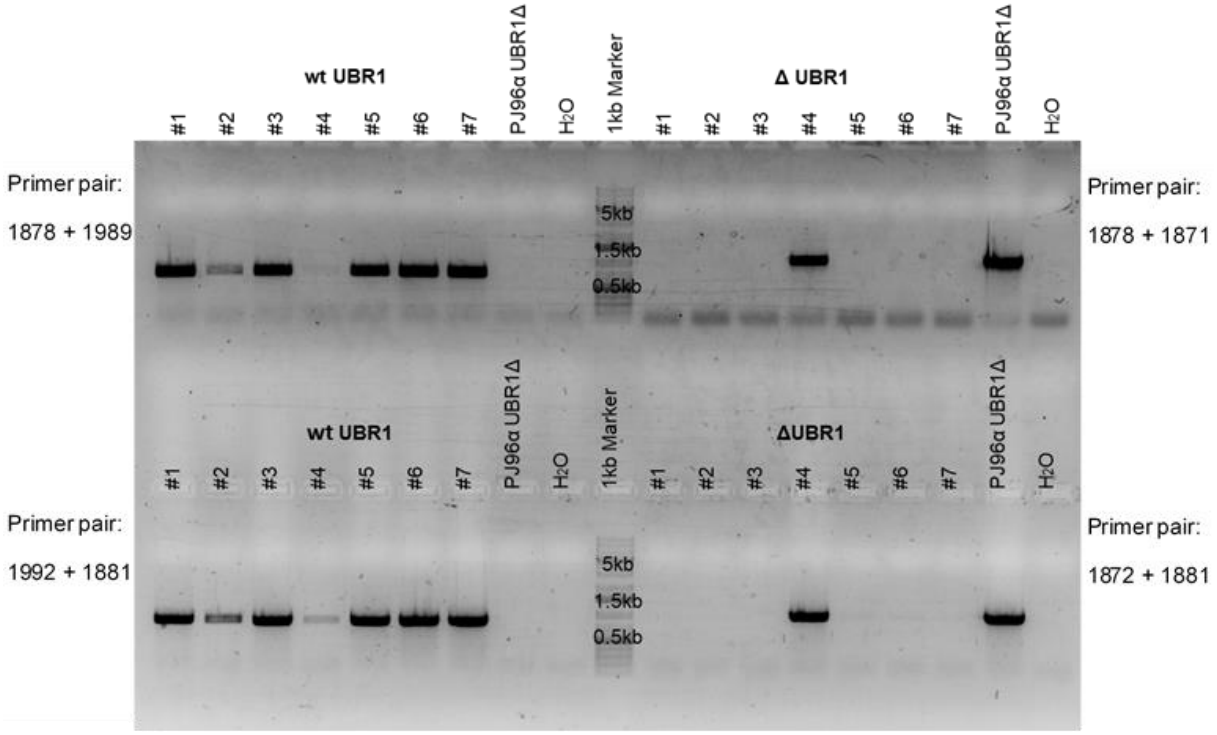

Figure 25 Genotyping of possible CB80 yeast colonies lacking an ORF for UBR1 aimed for the development of a novel yeast strain. The upper lanes detected the upper border regions of the UBR1 locus, either for a correct ORF of UBR1 or for the insertion of the KanMX cassette (ΔUBR1), the lower bands present the genotype of the lower border region. As control, the ΔUBR1 strain PJ96α was used.
Colony #4 was the only positive tested colony for an insertion of the KanMX cassette by homologous recombination disrupting the ORF of UBR1. No other colony showed the expected bands. All investigated colonies show a band for the upper and the lower border region in the detection of the WT form of the gene; also, colony #4.

3.4 Development of novel reporter constructs (tFT constructs)

The first attempt of developing tFTs in *Arabidopsis* resulted in three different combinations of fluorophores, mScarlet-I + mNeonGreen, YFP + mCherry and mCherry + sfGFP. They were linked to a ubiquitin fusion protein and translated as a single entity. In the context of PTM, DUBs cleaved it and the three different amino-termini M, L and R were exposed (Figure 26). In total, 9 different constructs were established. Already in previous experiments, these constructs were transformed into the two plants line S7 and 6-1-1.

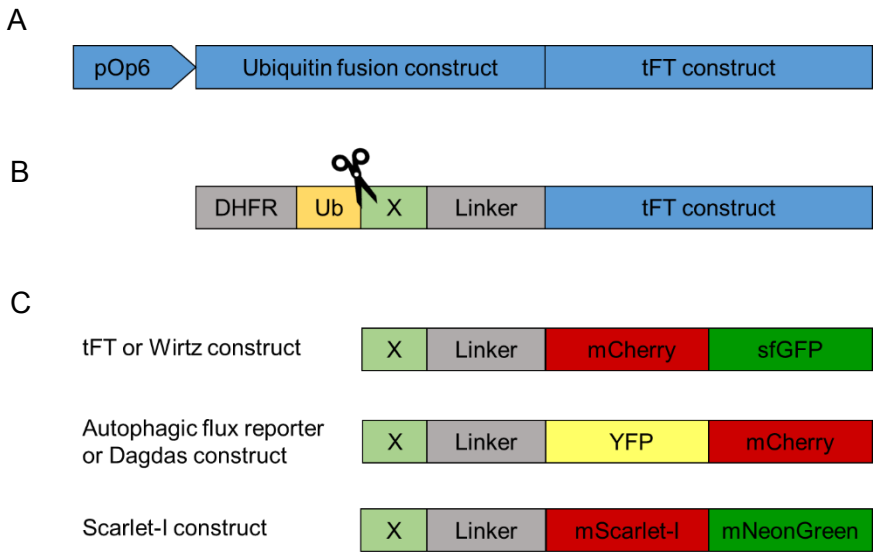

Figure 26 Novel reporter constructs of the first attempt of developing tFTs. A) In general, the constructs consist of two parts, the ubiquitin fusion part and the tFT part, the combination of the two fluorophores. They were under the pOp6 promoter on the pV-Top vector. B) The ubiquitin fusion part contains the ORF for a DHFR, Ub and X, the triplett coding for the different amino acids at the N-terminus, and connects via a linker to the fluorophores. During a PTM event, DUBs cleave after Ub setting free the different N-termini. C) Three different combinations of fluorophore pairs were used. The tFT or Wirtz construct contained the two fluorophores mCherry and sfGFP, the Autophagic flux reporter received from Yasin Dagdas YFP and mCherry. The combination of mScarlet-I and mNeonGreen, named Scarlet-I construct, was developed in the Bachmair lab.

As the used vector pV-Top is part of the two component system for transgene activation (Moore et al., 2006), both plant lines contain the ORF for the synthetic transcription factor LhGR2 under different promoters inducible by Dexamethasone (Figure 27). In this work, these plants were investigated for the expression of the transgenes.

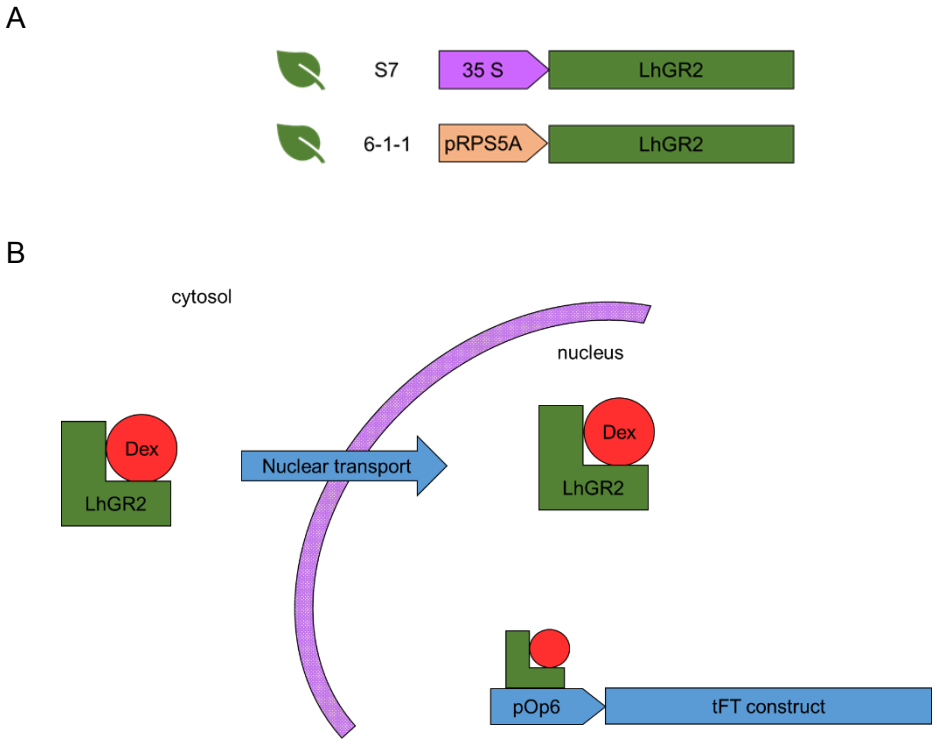

Figure 27 Two component system for transgene activation in *Arabidopsis*. A) Two activator plant lines were used during this Thesis expressing the artificial transcription factor LhGR2. In line S7, LhGR2 is under the CaMV 35S promoter (35S) while in line 6-1-1 under the ribosomal protein promoter pRPS5A. B) The chemical inducer Dexamethasone enables the nuclear transport of the transcription factor LhGR2. It binds to the promoter pOp6 triggering the transcription of the tFT construct, transformed into the activator plant line using the floral dip method.

By fluorescence microscopic analysis, in none of the investigated 8 days old seedlings a signal after the induction of the transgenes could be detected, neither in plants grown on plates nor in plants grown in liquid MS medium. Only plants with tFT constructs fused to the M N-terminus were used for the screenings because of their known stability in the plant N-end rule pathway compared to the fast degradation of peptides with the primary destabilizing residues R and L. As control for a working Dexamethasone induction, plant line RV-86-5 was chosen expressing a lethal Ub variant with the substitution of a Lys to an Arg at the protein position 48 (ubK48R). This prevents the formation of Ub chains (Schlögelhofer et al., 2006).

As the transgenes on the pV-Top vector were under a bidirectional promoter also encoding the reporter enzyme GUS, an *in vivo* GUS stain was performed to verify the integrity of the promoter. In plant line S7, no development of a blue colour was observable. On the other hand, a strong formation of a blue colour in the plant line 6-1-1 was noticed, but due to an internal GUS in this plant line, the origin of the enzymatic activity could not be determined (Figure 28).

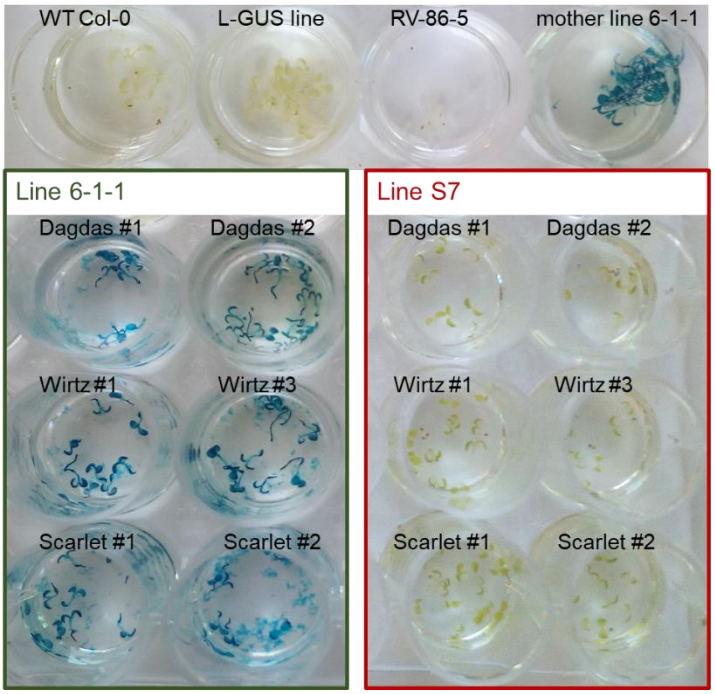

Figure 28 GUS stain of the T2 generation of tFT constructs developed in the first attempt. Transformed plants from the line 6-1-1, comprising an internal GUS gene, showed an equal development of the blue colour proving the presence of GUS. In the WT Col-0 and in pER L-GUS, no development of a blue colour was detectable. In the mother line of the transformed plants a blue colour developed. Plant line S7 without a chromosomal GUS did not show a blue colour formation in the *in vivo* GUS staining. As control for the working of the Dexamethasone mediated induction of the transgenes, plant line RV-86-5 did not survive the as expected because to the ubK48R transgene. The medium, in which Col-0 and mother line 6-1-1 were grown, lacked Hygromycin, the selection marker for the transgenes.

In the next step, a PCR-based genotyping of the seedlings verifying the presence of both transgenes of the two component system for gene induction, the artificial transcription factor LhGRII and the pV-Top vector encoding the fluorescence genes, was performed. As shown in Figure 29, although the plants were negative for the detection of the tFT constructs by fluorescence microscopic analysis and in the GUS stain, they contained both transgenes.

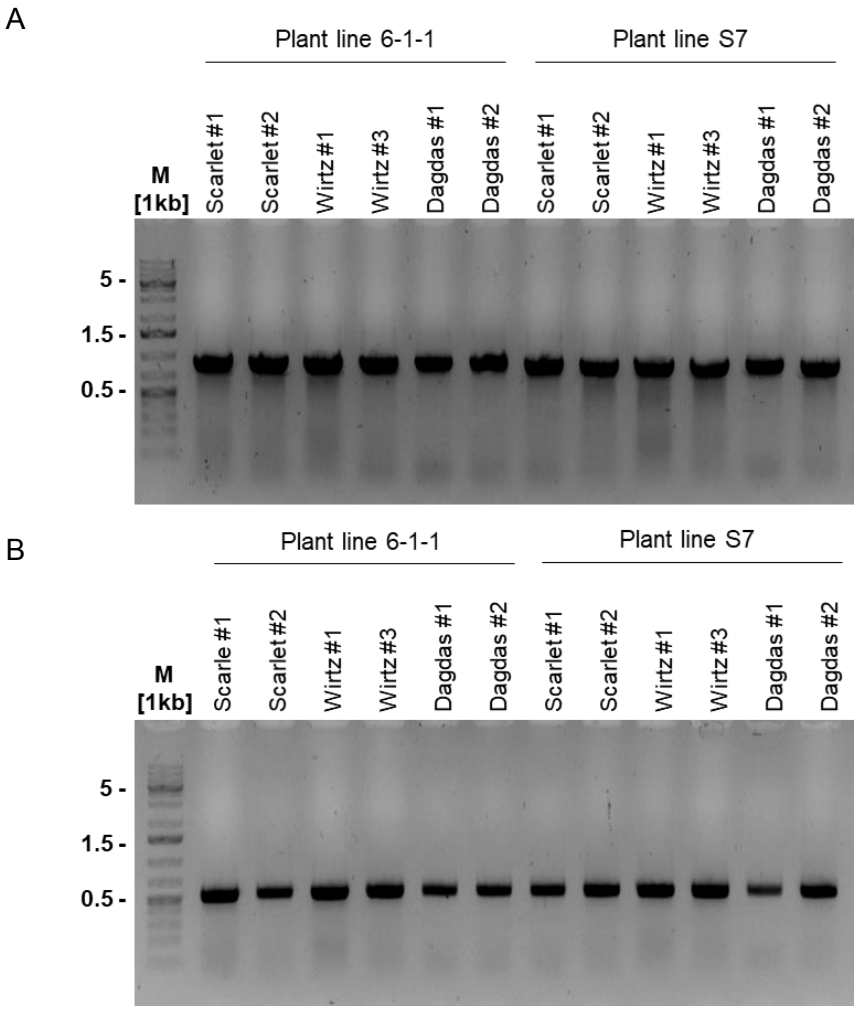

Figure 29 PCR-based genotyping for the presence of the transgenes of the two component system for gene induction in *Arabidopsis* seedlings. Only tFT constructs with an N-terminal Met were investigated. A) The amplified fragment of 1kb corresponded to the desired band for the detection of the artificial transcription factor LhGRII. B) Verification of the presence of the pV-Top transgene by amplifying the region from the GUS gene at the pV-TOP vector to the DHFR as part of the ubiquitin fusion construct. The size of the appearing band matched the expected band of around 0.5kb. In all investigated samples, the two transgenes were present.

After the verification of the presence of the transgenes on DNA level, a Western blot was performed to detect the expression of tFT constructs on protein level (Figure 31). The success of the protein extraction from 9 day old *Arabidopsis* seedlings was controlled by a Ponceau S stain (Figure 30). Only constructs with the stable N-terminus M in the plant line 6-1-1 were investigated because of the negative results in the GUS stain in plants from line S7. In none of the samples the expected band for the detection of the HA-tag appeared. Also, the seedlings treated with the proteasome inhibitor Bortezomib, added to the media the evening before the plant sample harvesting in the morning, did not show the presence of the desired proteins.

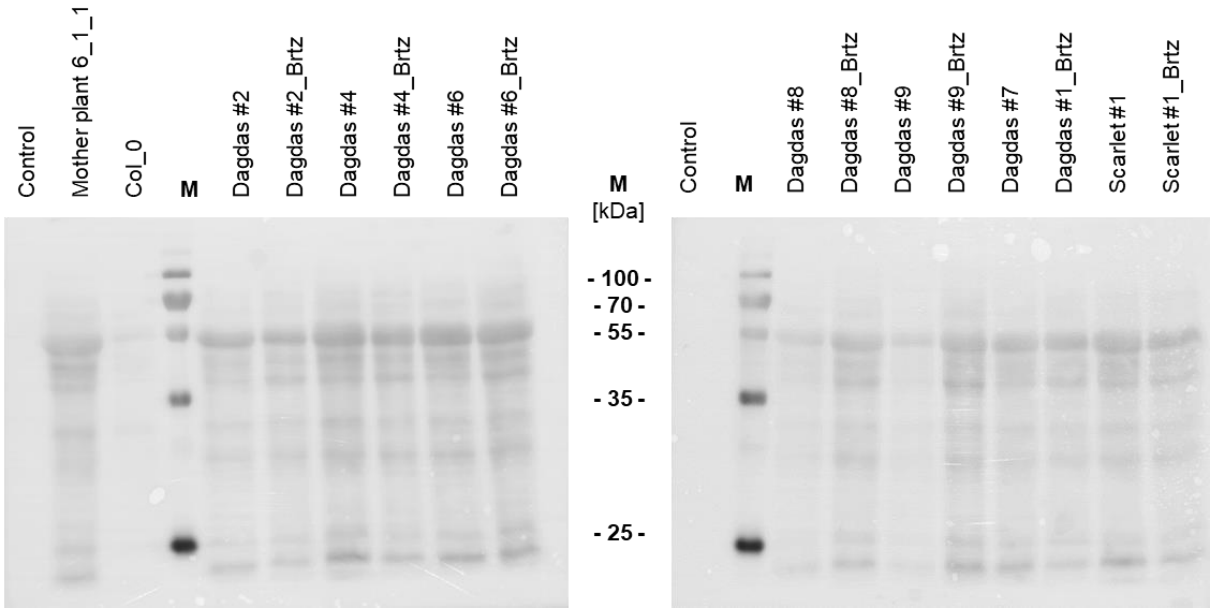

Figure 30 Ponceau S stain. The protein extraction of *Arabidopsis* seedling and the blotting from the resolving gel to the PVDF membrane worked.

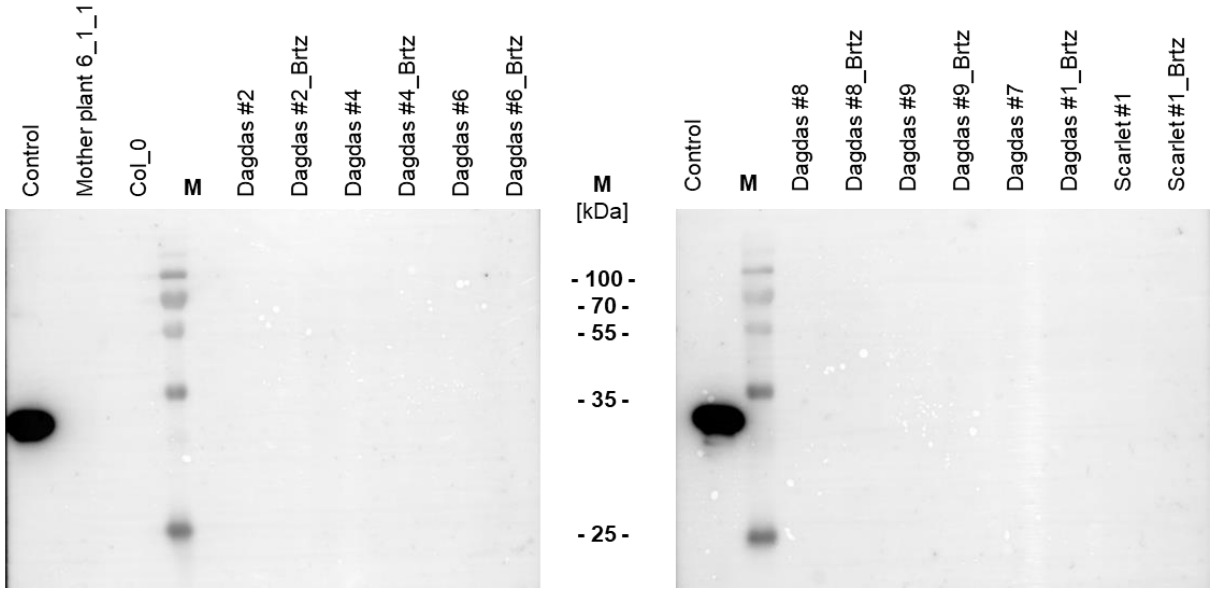

Figure 31 Western blot for the detection of the tFT constructs in isolated proteins from Dexamethasone-induced *Arabidopsis* seedlings. Extracts from different plants were separated on an SDS-PAGE and subsequently blotted on a PVDF membrane. As first detection step, an anti-HA antibody was used followed by an HRP coupled secondary antibody. In none of the investigated M-Dagdas and M-Scarlet samples, a translational product could be detected. Brtz refers to seedlings treated with the proteasome inhibitor Bortezomib. Col-0 and the mother plant 6-1-1 served as negative control for the transgene. A protein extract from *E. coli* expressing an HA-tagged protein was used as positive control. The expected protein should show up ~34kDa.

In the second attempt, tFT constructs with the combination of the two fluorophores mScarlet-mNeonGreen, fused to the three N-termini R, M and L, should be developed in the different vectors pNIGEL07, pBIBpOpTec-c1 and pBIN_AR_Sat5_tFT. This generation of the constructs via the Gibson cloning strategy was performed using the In-Fusion® HD Cloning Kit developed from Takara (France). The constructs in the pNIGEL07 vector were meant to be transformed into *Arabidopsis* WT Col-0, those in the pBIB vector into the activator plant line 6-1-1, while clones in the pBIN_AR vector should be sent to the Wirtz lab at the Ruprechts-Karls University of Heidelberg. After seed harvesting, transformed plants can be selected on media containing the specific antibiotic.

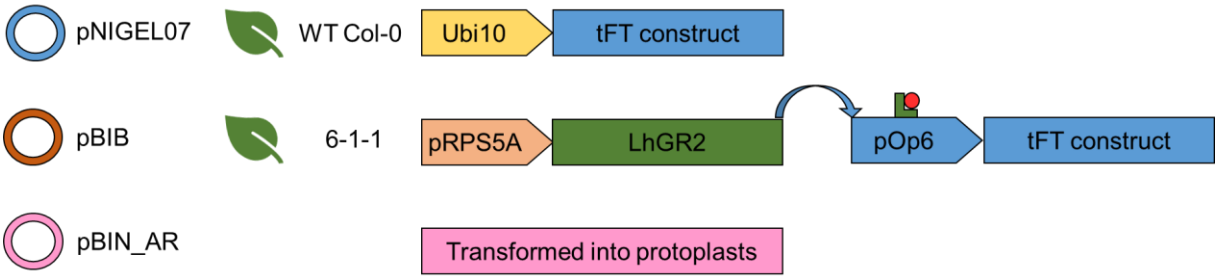

Figure 32 Novel reporter constructs of the second attempt of developing tFTs. Three different vectors were used, pBIB and pBIN_AR as part of the two-component system, and pNIGEL07 with the Ubi10 promoter. Constructs in this latter vector were transformed into the WT Col-0 Arabidopsis while constructs in the pBIB vector into plant line 6-1-1. During this Thesis, tFT constructs in the pBIN_AR were prepared to be sent to the Wirtz lab at the Ruprechts-Karl University of Heidelberg for protoplast transformation.

Constructs in the pBIB vector, together with the synthetic transcription factor LHGRII forming the two component system for transgene activation, were built in an In-Fusion cloning step in *E. coli* DH5α. The correctness of the clones was verified by restriction digests and sequencing. After the propagation of the clones in *Agrobacterium*, flowering plants were transformed using the floral dip method. In the time frame of this practical work, the selection of resistant plants on Hygromycin confirming a successful transformation could not be performed.

The propagation of the correct *Agrobacterium* colonies containing the constructs in the pNIGEL07 vector included difficulties, particularly in the selection of positive transformants on the resistance marker ampicillin. The transformation rate of plasmids, isolated from *E. coli* and transformed into *Agrobacterium*, was much higher compared to pBIB constructs and previous performed transformations. Also, it was not possible to back-transform the purified plasmid from an *Agrobacterium* colony into *E. coli*, suggesting problems in the selection of the correct colony of *Agrobacterium* on Ampicillin plates. Subsequently, selection of the *Agrobacterium* strain GV3101 carrying the helper plasmid pSoup on LB plates including Ampicillin confirmed

the resistance of the strain against this selection marker explaining the high transformation rate and the not-possible back-transformation into *E. coli*. Therefore, the floral dip was carried out using a mixture of different *Agrobacterium* colonies anticipating that one colony contained the correct constructs. Bacteria with a wrong or rearranged plasmid should not be able to transform plant cells efficiently. Due to time issues, the positive *Arabidopsis* transformants with the desired protein constructs could not be selected by analysing their resistance on Basta® containing MS plates.

The cloning of the constructs in the pBIN_AR vector was not as successful, only the construct with Arg as N-terminus could be generated. Its integrity was verified by restriction digests and sequencing. Subsequent sequencing of the vector performed by Nikola Winter showed, that the sequence of the plasmid received from the Wirtz lab did not match the actual sequence of the plasmid. The designed homologous region of the primers was not present in the vector. The cloning of the R construct was only possible due to a rearrangement in the plasmid.

Summarizing, the different detection methods for the presence of the tFT constructs in the pV-Top vector showed negative results for a protein product although the presence of the transgenes was verified by PCR. From the second attempt, seven of the nine constructs were generated in *E. coli*, three of them could be transformed successfully into *Agrobacterium.* These three correct clones in the pBIB vector were transformed in the plant line 6-1-1, a mixture of different colonies containing the transgenes in the pNIGEL07 vector were transformed in the WT Col-0.

4 Discussion

As part of the UPS degradation system, the N-end rule pathway connects the half-life of a protein to its amino-terminus. This leads to the categorization of the N-terminal amino acids into stable N-termini and primary, secondary and tertiary destabilizing N-termini. This degradation pathway is conserved in eukaryotes. It is essential for the control of protein stability, crucial for regulatory proteins such as enzymes and hormones in plants.

The ubiquitin signalling cascade ends with a E3 ligase called N-recognin. In plants, so far, two N-recognins are known, PRT 1 and 6. PRT1 mediates the destabilization and degradation of proteins withbulky aromatic amino termini of the type II primary destabilizing residues through its RING domain, while PRT6 leads to the degradation of basic N-terminal residues by interaction with its UBR box. Ile and Leu belong to the class of hydrophobic primary destabilizing amino acids, and their N-recognins are still unknown.

During this thesis, the role of different candidates for a Leu N-recognin was investigated, as well as the development of tFT constructs for the spatiotemporal resolution of this protein degradation pathway.

4.1 Putative complementation group PRT13

The treatment of transgenic *Arabidopsis* seedlings with the mutagenic compound EMS caused a variety of different mutations in the genome. Possible candidates for a Leu N-recognin were identified due to the stabilisation of the contained L-GUS reporter construct.

This forward genetic approach led to the clustering of candidate genes into complementation groups named PROTEOLYSIS (PRT). In this work, candidates as part of PRT13 have been investigated for a possible role as Leu N-recognin.

The E2 like enzyme ATG10 showed the strongest correlation between a homozygous mutated genotype and a blue GUS stain verifying, the stabilisation of the Leu N-terminus (Table 11).

BIG, also part of this putative complementation group, did not show a correlation between a point mutation and the L-GUS stabilization. A more detailed discussion can be found in the chapter 4.2.1 BIG.

4.2 Putative candidates of Leu N-recognins in *A. thaliana*

As method of choice to investigate the role of candidates as possible Leu N-recognin, ONPG assays after heterologous expression in yeast were performed to check their influence of the stability on the reporter enzyme βgal coupled to different N-termini.

These ONPG assays were performed in comparison to two control constructs. For a working assay, the enzymatic activity of the βgal linked to an M and an F N-terminus, was determined in yeast cells expressing PRT1. As N-recognin for the three aromatic amino acids F, W and Y belonging to the primary destabilizing residues of type II, the F βgal was destabilized and degraded as expected.

The second control construct was a fusion between the yeast F-box domain of Ufo1 and the UBR domain of the plant N-recognin PRT6. This fusion protein did not show any decrease of a βgal activity of the different tested N-termini compared to the stable M N-terminus. The reasons for this were not investigated. Possible explanations for these observations could be sterical hindrances of the two subunits, or that the two subunits could not fold properly to a functional unit.

Ufo1 is a substrate recognition component of a SCF complex mediating the degradation of the HO endonuclease involved in the DNA damage response pathway (Kaplun et al., 2000, Jelinsky et al., 2000). Only the F-box fragment of this receptor protein was taken in these experiments. Maybe the interaction site with the adaptor Skp1 enabling the interaction with the scaffold protein Cul1 was prevented by fusion to the UBR domain.

PRT6 was identified as an N-recognin due to its sequence similarity to the yeast UBR1, both proteins contain a UBR box, a zinc-finger like domain with conserved Cys and His residues. This substrate recognition domain has also been identified in the mammalian ubiquitin ligases UBR1 and 2, a protein pull-down led to the characterization of UBR4, the mammalian homolog of BIG in plants and PUSHOVER in Drosophila.

Tasaki et al. (2009) work on substrate recognition domains of the N-end rule pathway led to the characterization of the UBR domain of this UBR4 as a 72 amino acids long region, the binding site of the primary destabilizing residues of type I (Arg, Lys, His). They tested different fragment lengths and discovered, that this region is able to fold independently/autonomously and is sufficient for its activity. The structural integrity is retained and allows the binding of the substrates. The here tested UBR domain of PRT6 covered approximately 185 amino acids. The same region of the PRT6 fused to an Avi-tag was used successfully in biotinylation assays (performed by Nikola Winter) for the identification of interaction partners as control construct.

4.2.1 BIG

This protein is often discussed as possible Leu N-recognin because of its predicted domains. It contains a UBR domain homologous to that found in the yeast N-recognin UBR1 and in the PRT6 of *Arabidopsis* (Graciet et Wellmer, 2010). Furthermore, a ZZ-domain was identified as protein-protein interaction site discussed as possible binding site of a E2.

As mentioned above, an EMS-induced point mutation in BIG (At3g02260) as part of PRT13 did not co-segregate with the stabilised L-GUS reporter construct. A possible reason for the negative result for BIG as N-recognin in the GUS stain could be the site of the mutation at amino acid position 4498 of 5098. This non-synonymous mutation converted an Ala to a Val, both highly hydrophobic residues most of the time found on protein surfaces and rarely involved in catalytic reactions (Holliday et al., 2009).

On the other hand, the investigated SALK line with a T-DNA insertion in exon 5 of 14 in BIG showed a stabilisation of the L-GUS reporter construct, which contradicts the result of the PRT13 genotyping. Therefore, the CDS of this huge protein was cloned in a five-step cloning process to allow its expression in yeast and to simplify the experimental conditions. BIG did not show any activity as E3 ligase in the two transformed yeast strains, neither in the strain SUS13 lacking a functional UBR1 nor in the WT strain CB80. The protein probably is not a fully functional N-recognin itself but may act as a substrate recognition unit of a E3 complex. Due to the higher complexity of *Arabidopsis* and no known homolog in yeast, maybe an essential protein for the assembly of this protein complex is missing in yeast and prevented the activity of the BIG protein. It is to be determined whether BIG itself acts as N-recognin or whether it influences the abundance and activity of regulator proteins of the Ub mediated degradation of polypeptides with a Leu N-terminus. Another possibility for no degradation of the reporter enzyme βgal could be the essential interaction of two Leu N-recognins in plants. Due to the transformation of only one plant protein into yeast where no homolog exists, the reaction or binding partners of BIG may be missing.

To shift the experimental reactions to more *in vivo* like conditions, the expression of E2s from *Arabidopsis* in yeast, additionally to BIG and the X-βgal enzyme, could be tried. As most promising candidates, the four E2s PFU1 (At3g15355), PFU2 (At2g16920), PFU3 (At1g53025) and PHO2 (At2g33770) were identified by Karolin Eifler (2010). Additionally, the adaptor proteins ASK (*Arabidopsis* SKP-LIKE) forming the link between the F-box receptor subunits and the Cullin scaffold subunits from *Arabidopsis* could be restored in yeast. So far, only one of these subunits has been identified in yeast, the SKP1 gene, whereas in *Arabidopsis* 21 ASK genes are known (Farrás et al., 2001).

According to Baker and Varshavsky (1991), the degradation of polypeptides through the N-end rule pathway could be inhibited by the addition of dipeptides or amino acid derivates to the

media, in which the yeast cells are growing. These substances block the binding site of the substrate inhibiting their degradation. This approach was also tested to identify a possible binding site of a peptide with a Leu N-terminus at the BIG protein with the addition of a Leu-OMet ester. No effect of an increase or decrease of the Leu βgal activity could by detected, neither in the WT strain CB80 nor in the SUS13 strain expressing the BIG protein. This result suggests that this amino acid derivate did not have an effect in these yeast strains. Otherwise, a stabilization of the reporter enzyme should be visible in the WT strain transformed with an empty YCplac22 vector blocking the binding site on UBR1, the only N-recognin known in yeast. It is possible that, in these cells, the ester was transported more efficiently into the vacuole and thus inactivated than in yeast strains in which it showed an effect. Furthermore, a higher activity of hydrolases may have cleaved off the Met which would lead to the instability of Leu. Further experiments would be necessary to determine the inefficiency of the amino acid derivative in the WT CB80

One of the predicted domains in BIG was a UBR domain, homologous to that found in PRT6. Because of the binding affinity to amino acids of type I primary destabilizing residues it was suggested, that BIG could have an Arg binding site. This may lead to the degradation of peptides with this N-terminus or to a stabilization protecting them from degradation.

In CB80, the WT *S. cerevisiae* strain, no significant increase of R-βgal in BIG expressing cultures compared to cultures expressing an empty YCplac22 vector could be detected. This does not reinforce the hypothesis of a possible Arg binding site, neither for degradation nor for stabilization of these peptides. Further studies could be accomplished by the addition of the dipeptide Arg-Ala to block the Arg binding sites. If a binding site on the protein is present and accessible, and the cells are able to uptake the dipeptide, the activity of R-βgal should increase in BIG expressing cells compared to the control group.

Due to the high standard deviations in the ONPG assays testing the candidate BIG in yeast, the experimental conditions have to be improved for further studies. A major point is the adaption of the growth conditions of the yeast cells expressing the BIG protein. Compared to cells expressing an empty YCplac22 vector or another construct, they had a notably slower replication time.

Although no clear function of BIG acting as N-recognin for Leu N-termini could be identified during this thesis, neither in the genotyping of PRT13 nor in the ONPG interaction assays, it is possible that the experimental conditions did prevent its activity. To ensure isogenic conditions in further experiments, the newly developed ΔUBR1 CB80 yeast strain can be used. So, the

WT and the ΔUBR1 strain differ exclusively in the functionality of the only known N-recognin in yeast.

4.2.2 Further candidates

The role of the F-box protein cand16 was investigated in combination with the N-terminal F-box domain of Ufo1. This latter domain was the same as tested in combination with the UBR domain of PRT6. To complement this fusion protein, two splicing variants of cand16 were ligated to the yeast F-box fragment as C-terminal domain. As with the candidates tested so far, no differences in the tested X-βgal activities compared to the stable M βgal activity could be determined. The same problems as mentioned for the Ufo1-UBRdomain construct or respectively BIG due to missing interaction partners could have prevented an activity of the cand16 as putative Leu N-recognin.

A fragment of BIG, including the putative ZZ-domain, was tested in two variants; on the one hand as an independent unit, on the other hand in combination with the F-box domain of Ufo1. If the fusion protein showed any activity, it would have functioned as E3 ligase. It could be integrated into a SCF complex in which the F-Box domain of Ufo1 would act as a docking site for the degradation target. The ZZ-domain of the BIG fragment could be a E2 interaction site.

Taken together, according to the results of the ONPG assays, none of the investigated putative candidates showed any activity as a N-recognin for Leu N-termini in the tested system.

4.3 The development of tandem fluorescent timers

Tandem fluorescent timers were developed as a tool for the pH dependent cellular localization of a peptide tagged with two fluorescent proteins. Simultaneously, due to the differing folding kinetics of the two proteins, the relative lifespan of the tagged peptide can be determined. Zhang et al. (2019) were the first scientists, who brought the well-established application from yeast into *Arabidopsis*. As reporter markers they have chosen the combination sfGFP-mCherry.

Since they successfully established this relative protein lifetime measurement, one aim of the Thesis was the development of further tFT constructs consisting of the fluorophore combinations mCherry-sfGFP, YFP-mCherry and mScarlet-I-mNeonGreen for the spatiotemporal investigation of the N-end rule pathway of the three N-termini Arg, Leu and Met. As target vector for the cloning process, the binary vector pV-TOP was chosen as part of

the two component system for transgene activation in plants. The construct was under a bidirectional promoter regulating also the expression of the reporter enzyme GUS. As no protein product was detectable in seedlings after transgene activation of the tFt constructs with Dexamethasone, neither by microscopic analysis, nor in an immunodetection by Western blot, nor in a GUS stain, it can be assumed, that the promoter was not able to activate the transcription of the genes. The added proteasome inhibitor Bortezomib blocks the degradation through the proteasome leading to the accumulation of ubiquitin protein aggregates (Adams and Kauffman, 2004). This treatment would have led to a further stabilization of the tFT constructs coupled to different N-termini to facilitate their detection. As the different detection methods did not verify a successful transcription or translation of the tFT constructs although both transgenes, the artificial transcription factor LhGR2 and the tFT constructs, were present, this approach was given up.

A second attempt was started in which the three different combinations of fluorescent proteins were given up for the benefit of three vectors differing in their promoters. Only the combination of mScarlet-I and mNeonGreen should be investigated.

Only the transformation of this tFT construct in the binary vector pBIB was successful. The propagation of *Agrobacterium tumefaciens colonies* containing the constructs in the pNIGEL07 vector was not possible due to selection problems. The chosen strain GV3101 was Amp resistant, and the selection marker for the plasmid was Amp. It was also not possible to select positive clones on a high concentration of the more stable Carbenicillin. The resistance against both antibiotics is given by β-lactamase (Sambrook et al., 2001).

As the time frame of this Thesis was not sufficient to investigate the efficient transformation of the tFT constructs in the pBIB vector into *Arabidopsis*, the Master student Katrin Rose continued with this project. She kindly provided a microscopic picture of *Arabidopsis* roots of plant line 6-1-1, expressing the tFT constructs consisting of mScarlet-I and mNeonGreen in under the pRPS5A promoter (Figure 33). The seedlings were treated with the proteasome inhibitor Bortezomib a few hours before taking the picture. A signal for mScarlet-I is detectable in the whole cell except for the nucleus, while the signal for mNeonGreen is missing in the vacuole, but present in the nucleus. This result will not be discussed further in this Thesis and serves to illustrate the principle of a tFT construct. It proves, that the transformation of *Arabidopsis* plants with the pBIB vector and its induction with Dexamethasone worked.

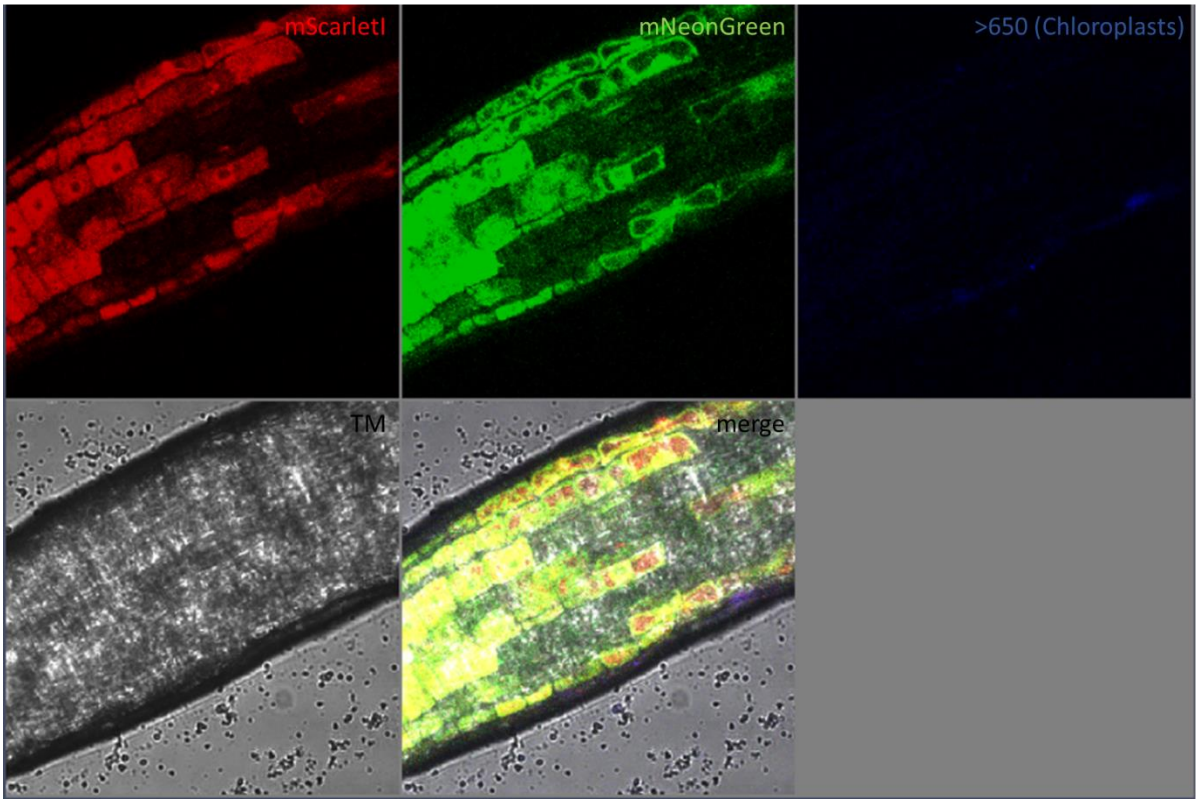

Figure 33 Microscopic analysis of the tFT construct (mScarlet-I – mNeonGreen) in the pBIB vector with an N-terminal Met. The *Arabidopsis* seedlings were treated with Bortezomib few hours before taking the picture. The mScarlet-I signal was present in the whole cell, except for the nucleus. A signal for mNeonGreen could be detected in all parts of the cells with exception of the vacuole.

5 Conclusion and outlook

This Thesis has not directly contributed to the identification of a Leu N-recognin of *Arabidopsis*, but it did lay some foundations for further experiments.

The cloning of the CDS of BIG as putative candidate for a Leu N-recognin of *Arabidopsis* was successful, allowing its expression in bacteria and yeast. This will facilitate the experimental conditions for further studies and investigations such as the resolving of its 3D structure. Moreover, several constructs of additional putative candidates were cloned. To allow isogenic conditions in prospective experiments in yeast, the WT strain CB80 was mutated to develop a new strain, besides SUS13, with a UBR1 deletion. So, the direct effect of a putative candidate on the stability of polypeptides with a Leu N-terminus can be studied in two yeast strains that differ exclusively in the functionality of UBR1.

With Atg10 as putative candidate of the complementation group PRT13 showing the best correlation of a mutation and the stabilization of the L-GUS reporter construct, the interrelation between the UPS and the autophagy pathway could be demonstrated.

The development of tFT constructs could not be completed. The first attempt did not lead to a transgene expression, maybe due to a non-functional vector. For the second attempt, plants were transformed, but those could not be investigated due to the timeframe of the practical part of this Thesis. Further studies might shed light on the cellular localization of this protein degradation pathway.

6 Literature

Adams J, Kauffman M. (2004) Development of the ProteasomeInhibitor Velcade™ (Bortezomib), Cancer Investigation, 22:2, 304-311, doi: 10.1081/CNV-120030218.

Bachmair A, Finley D, Varshavsky A. (1986). In vivo half-life of a protein is a function of its amino-terminal residue. Science. 1986 Oct 10;234(4773):179-86. doi: 10.1126/science.3018930

Baker RT, Varshavsky A. (1991). Inhibition of the N-end rule pathway in living cells. Proc Natl Acad Sci U S A. 1991 Feb 15; 88(4): 1090–1094. doi: 10.1073/pnas.88.4.1090

Bindels DS, Haarbosch L, van Weeren L, Postma M, Wiese KE, Mastop M, Aumonier S, Gotthard G, Royant A, Hink MA, Gadella TW Jr. (2017). mScarlet: a bright monomeric red fluorescent protein for cellular imaging. Nat Methods. 2017 Jan;14(1):53-56. doi: 10.1038/nmeth.4074.

Blakeslee JJ, Wendy A Peer WA, Murphy AS. (2005). Auxin Transport. Curr Opin Plant Biol. 2005 Oct;8(5):494-500. doi: 10.1016/j.pbi.2005.07.014.

Burroughs AM, Balaji S, Iyer LM, Aravind L. (2007). Small but versatile: the extraordinary functional and structural diversity of the β-grasp fold. Biol Direct 2, 18 (2007). doi:10.1186/1745-6150-2-18.

Callis, J. (2014). The Ubiquitin Machinery of the Ubiquitin System. Arabidopsis Book. 2014; 12: e0174. doi:10.1199/tab.0174.

Chan KM, Liu YT, Ma CH, Jayaram M, Sau S. (2013). The 2 micron plasmid of Saccharomyces cerevisiae: a miniaturized selfish genome with optimized functional competence. Plasmid. 2013 Jul;70(1):2-17. doi: 10.1016/j.plasmid.2013.03.001.

Clague MJ, Heride C, Urbé S. (2015). The demographics of the ubiquitin system. Trends in Cell Biology. Trends Cell Biol. 2015 Jul;25(7):417-26. doi:10.1016/j.tcb.2015.03.002.

Clough SJ, Bent AF. (1998). Floral dip: a simplified method for Agrobacterium-mediated transformation of Arabidopsis thaliana. Plant J. 1998 Dec;16(6):735-43. doi: 10.1046/j.1365-313x.1998.00343.x.

Desgagné-Penix I, Eakanunkul S, Coles JP, Phillips AL, Hedden P, Sponsel VM. (2005). The auxin transport inhibitor response 3 (tir3) allele of BIG and auxin transport inhibitors affect the gibberellin status of Arabidopsis. The Plant Journal (2005) 41, 231-242. doi: 10.1111/j.1365-313X.2004.02287.x.

Dikic I. (2017). Proteasomal and Autophagic Degradation Systems. Annu. Rev. Biochem. 2017. 86:31.1-31.32. doi:10.1146/annurev-biochem-061516-044908.

Dissmeyer N, Rivas S, Graciet E. (2017). Life and death of proteins after protease cleavage: protein degaration by the N-end rule pathway. New Phytologist (2018) 218: 929-935. doi:10.1111/nph.14619.

Downes BP and Vierstra RD. (2005). Post-translational regulation in plants employing a diverse set of polypeptide tags. Biochem.Soc.Trans. 33,393–399. doi: 10.1042/BST0330393

Eifler, Karolin. (2010). The PHO2 family of ubiquitin conjugating enzymes in Arabidopsis thaliana and its contribution to plant programmed cell death. Doctoral thesis, University of Cologne, 2010.

Engler C and Marillonnet S. (2014). Golden Gate cloning. Methods Mol Biol. 2014;1116:119-31. doi: 10.1007/978-1-62703-764-8_9.

Erpapazoglou Z, Walker O, Haguenauer-Tsapis. (2014). Versatile Roles of K63-Linked Ubiquitin Chains in Trafficking. Cells 2014, 3, 1027-1088; doi:10.3390/cells3041027

Farrás, R., Ferrando, A., Jasik, J., Kleinow, T., Okresz, L., Tiburcio, A., Salchert, K., Del Pozo, C., Schell, J. and Koncz, C. (2001) SKP1-SnRK protein kinase interactions mediate proteasomal binding of a plant SCF ubiquitin ligase. EMBO J. 20, 2742–2756. doi: 10.1093/emboj/20.11.2742.

Feng J, Shen WH. (2014). Dynamic regulation and function of histone monoubiquitination in plants. Front Plant Sci. 2014 Mar 13;5:83. doi:10.3389/fpls.2014.00083.

Garzon M, Eifler K, Faust A, Scheel H, Hofmann K, Koncz C, Yephremov A, Bachmair A (2007). PRT6/At5g02310 encodes an Arabidopsis ubiquitin ligase of the N-end rule pathway with arginine specificity and is not the CER3 locus. FEBS Lett. 581, 3189-3196. doi: 10.1016/j.febslet.2007.06.005.

Generoso WC, Gottardi M, Oreb M, Boles E. (2016). Simplified CRISPR-Cas genome editing for Saccharomyces cerevisiae. J Microbiol Methods. 2016 Aug;127:203-5. doi: 10.1016/j.mimet.2016.06.020.

Gietz RD, Sugino A. (1988). New yeast-Escherichia coli shuttle vectors constructed with in vitro mutagenized yeast genes lacking six-base pair restriction sites. Gene. 1988 Dec 30;74(2):527-34. doi: 10.1016/0378-1119(88)90185-0

Gil P, Dewey E, Friml J, Zhao Y, Snowden KC, Putterill J, Palme K, Estelle M, Chory J. (2001). BIG: a calossin-like protein required for polar auxin transport in Arabidopsis. Genes and development 15:1985-1997. doi: 10.1101/gad.905201.

Graciet E and Wellmer F. (2010). The plant N-end rule pathway: structure and functions. Trends Plant Sci. 2010 Aug;15(8):447-53. doi: 10.1016/j.tplants.2010.04.011.

Graciet E, Mesiti F, Wellmer F. (2010). Structure and evolutionary conservation of the plant N-end rule pathway. Plant J. 2010 Mar;61(5):741-51. doi: 10.1111/j.1365-313X.2009.04099.x.

Guo X, Lu W, Ma Y, Qin Q, Hou S, (2013). The BIG gene is required for auxin-mediated organ growth in Arabidopsis. Planta (2013) 237:1135-1147 doi: 10.1007/s00425-012-1834-4

Hatfield PM, Gosink MM, Carpenter TB, Vierstra RD. (1997). The ubiquitin-activating enzyme (E1) gene family in *Arabidopsis thaliana*. The Plant Journal (1997) 11(2), 213-226. doi: 10.1046/j.1365-313x.1997.11020213.x.

He J, Zhang RX, Peng K, Tagliavia C, Li S, Xue S, Liu A, Hu H, Zhang J, Hubbard KE, Held K, McAinsh MR, Gray JE, Kudla J, Schroeder JI, Liang YK, Hetherington AM. (2018). The BIG protein distinguishes the process of CO_2 -induced stomatal closure from the inhibition of stomatal opening by CO_2. New Phytol. 2018 Apr;218(1):232-241. doi: 10.1111/nph.14957.

Hearn TJ, Marti Ruiz MC, Abdul-Awal SM, Wimalasekera R, Stanton CR, Haydon MJ, Theodoulou FL, Hannah MA, Webb AAR. (2018). BIG Regulates Dynamic Adjustment of Circadian Period in Arabidopsis thaliana. Plant Physiol. 2018 Sep;178(1):358-371. doi: 10.1104/pp.18.00571.

Hershko A, Ciechanover A. (1998). The ubiquitin system. Annu Rev Biovhem 1998; 67: 425-479. doi: 10.1146/annurev.biochem.67.1.425.

Hu RG, Sheng J, Qi X, Xu Z, Takahashi TT, Varshavsky A. (2005). The N-end rule pathway as nitric oxide sensor controlling the levels of multiple regulators. Nature 437, 981-986. doi: 10.1038/nature04027.

Ignacio Marín. (2010). Diversification and Specialization of Plant RBR Ubiquitin Ligases. PLoS One. 2010 Jul 14;5(7):e11579. doi: 10.1371/journal.pone.0011579.

Irwin, CR.; Farmer, A.; Willer, DO.; Evans, DH. (2012). In-Fusion® cloning with vaccinia virus DNA polymerase. Methods Mol Biol. 2012;890:23-35. doi: 10.1007/978-1-61779-876-4_2.

Isono E, Nagel MK. (2014). Deubiquitylating enzymes and their emerging role in plant biology. Front Plant Sci. 2014; 5: 56. doi:10.3389/fpls.2014.00056.

Jelinsky SA, Estep P, Church GM, Samson LD. (2000). Regulatory networks revealed by transcriptional profiling of damaged Saccharomyces cerevisiae cells: Rpn4 links base excision repair with proteasomes. Mol Cell Biol. 2000 Nov; 20(21):8157-67. doi: 10.1128/mcb.20.21.8157-8167.2000.

Kanyuka K, Praekelt U, Franklin KA, Billingham OE, Hooley R, Whitealm GC, Halliday KJ. (2003). Mutations in the huge Arabidopsis gene BIG affect a range of hormone and light responses. The Plant Journal (2003) 35, 57-70 doi: 10.1045/j.1365-313X.2003.01779.x

Kaplun L, Ivantsiv Y, Kornitzer D, Raveh D. (2000). Functions of the DNA Damage Response Pathway Target Ho Endonuclease of Yeast for Degradation via the ubiquitin-26S Proteasome System. Proc Natl Acad Sci USA. 2000 Aug 29;97(18):10077-82. doi: 10.1073/pnas.97.18.10077.

Kim SH, Kwon C, Lee JH, Chung T. (2012). Genes for Plant Autophagy: Functions and Interactions. Mol. Cells 34, 413-423. doi:10.1007/s10059-012-0098y.

Kraft E, Stone SL, Ma L, Su N, Gao Y, Lau OS, Deng XW, Callis J. (2005). Genome Analysis and Functional Characterization of the E2 and RING-Type E3 Ligase Ubiquitin Enzymes of Arabidopsis. Plant Physiol. 2005 Dec; 139(4): 1597–1611. doi: 10.1104/pp.105.067983.

Labus K. (2018). Effective detection of biocatalysts with specified activity by using a hydrogel-based colourimetric assay - β-galactosidase case study. PLoS One. 2018 Oct 11;13(10):e0205532. doi: 10.1371/journal.pone.0205532.

Li H, Altschmied L, Chory J. (1993). Arabidopsis mutants define downstream branches in the phototransduction pathway. Genes Dev. 1994 Feb 1;8(3):339-49. doi: 10.1101/gad.8.3.339.

López-Bucio J, Hernández-Abreu E, Sánchez-Calderón L, Pérez-Torres A, Rampey RA, Bartel B, Herrera-Estrella L. (2005). An Auxin Transport Independent Pathway Is Involved in Phosphate Stress-Induced Root Architectural Alterations in Arabidopsis. Identification of BIG as a Mediator of Auxin in Pericycle Cell Activation. Plant Physiol. 2005 Feb;137(2):681-91.. doi: 10.1104/pp.104.049577.

Merzylak EM, Goedhart J, Shcherbo D, Bulina ME, Shcheglov A, Fradkov AF, Gaintzeva A, Lukyanov KA, Lukyanov S, Gadella TWJ, Chudakov DM. (2007). Bright monomeric red fluorescent protein with an extended fluorescence lifetime. Nat Methods. 2007 Jul;4(7):555-7. doi: 10.1038/nmeth1062. doi: 10.1038/nmeth106.

Moore I, Samalova M, Kurup S. (2006). Transactivated and chemically inducible gene expression in plants. The Plant Journal (2006) 45, 651–683. doi: 10.1111/j.1365-313X.2006.02660.x.

Muday GK, Murphy AS. (2002). An emerging model of auxin transport regulation. Plant Cell. 2002 Feb;14(2):293-9. doi: 10.1105/tpc.140230.

Neff MM, Neff JD, Chory J, Pepper AE. (1998). dCAPS, a simple technique for the genetic analysis of single nucleotide polymorphisms: experimental applications in Arabidopsis thaliana genetics. Plant J. 1998 May;14(3):387-92. doi: 10.1046/j.1365-313x.1998.00124.x.

Ohi MD, Vander Kooi CW, Rosenberg JA, Chazin WJ, Gould KL. (2003). Structural insights into the U-box, a domain associated with multi-ubiquitination. Nat Struct Biol. 2003 Apr;10(4):250-5. doi: 10.1038/nsb906.

Pédelacq JD, Cabantous S, Tran T, Terwilliger TC, Waldo GS. (2006). Engineering and characterization of a superfolder green fluorescent protein. Nat Biotechnol. 2006 Jan;24(1):79-88. doi: 10.1038/nbt1172.

Petrášek J, Friml J. (2009). Auxin transport routes in plant development. Development 136, 2675-2688 (2009) doi:10.1242/dev.030353.

Pickart CM and Eddins MJ. (2004). Ubiquitin: structures, functions and mechanisms. Biochimica et Biophysica Acta 1695 (2004) 55–72. doi:10.1016/j.bbamcr.2004.09.019.

Potuschak T, Stary S, Schlögelhofer P, Becker F, Nejinskaia V, Bachmair, A. (1998). PRT1 of Arabidopsis thaliana encodes a component of the plant N-end rule pathway. Proc. Natl. Acad. Sci. USA 95, 7904-7908. doi: 10.1073/pnas.95.14.7904.

Richards S, Hillman T, Stern M. (1996). Mutations in the Drosophila pushover gene confer increased neuronal excitability and spontaneous synaptic vesicle fusion. Genetics 142: 1215-1223 (1996).

Roberts TM, Rudolf F, Meyer A, Pellaux R, Whitehead E, Panke S, Held M. (2016). Identification and Characterization of a pH-stable GFP. Sci Rep. 2016; 6: 28166. doi: 10.1038/srep28166.

Romero-Barrios N, Vert G. (2017). Proteasome-independent functions of lysine-63 polyubiquitination in plants. New Phytologist (2018) 217: 995–1011; doi:10.1111/nph.14915.

Ruegger M, Dewey E, Hobbie L, Brown D, Bernasconi P, Turner J, Muday G, Estelle M. (1997). Reduced Naphthyphthalamic Acid Binding in the tir3 Mutant of Arabidopsis Is Associated with a Reduction in Polar Auxin Transport and Diverse Morphological Defects. The Plant Cell 9, 745-757. doi: 10.1105/tpc.9.5.745.

Sambrook, J, Fritsch, EF, Maniatis T. (2001). Molecular Cloning: A Laboratory Manual, 3rd ed., Cold Spring Harbor Laboratory Press, Cold Spring Harbor, NY.

Schlögelhofer P, Garzon M, Kerzendorfer V, Nizhynska V, Bachmair A. (2006). Expression of the ubiquitin variant ubR48 decreases proteolytic activity in Arabidopsis and induces cell death. Planta 2006 Mar;223(4):684-97. doi: 10.1007/s00425-005-0121-z.

Sekelsky JJ, McKim KS, Messina L, French RL, Hurley WD, Arbel T, Chin GM, Deneen B, Force SJ, Hari KL, Jang JK, Laurencon AD, Madden LD, Matthies HJ, Milliken DB, Page SL, Ring AD, Wayson SM, Zimmerman CC, Hawley RS. (1999). Identification of novel Drosophila meiotic genes recovered in a P-element screen. Genetics. 1999 Jun;152(2):529-42.

Shaid S, Brandts CH, Serve H, Dikic I. (2013). Ubiquitination and selective autophagy. Cell Death and Differentiation (2013) 20, 21-30. doi:10.1038/cdd.2012.72.

Shaner NC, Campbell RE, Steinbach PA, Giepmans BN, Palmer AE, Tsien RY. (2004). Improved monomeric red, orange and yellow fluorescent proteins derived from Discosoma sp. red fluorescent protein. Nat Biotechnol. 2004 Dec;22(12):1567-72. doi:10.1038/nbt1037.

Shu K and Yang W. (2017). E3 Ubiquitin Ligases: Ubiquitous Actors in Plant Development and Abiotic Stress Responses. Plant Cell Physiol. 58(9): 1461-1476. doi:10.1093/pcp/pcx071.

Stary S, Yin, X, Potuschak T, Schlögelhofer P, Nizhynska V, Bachmair A. (2003). PRT1 of Arabidopsis Is a Ubiquitin Protein Ligase of the Plant N-End Rule Pathway with Specificity for Aromatic Amino-Terminal Residues. Plant Physiol. 2003 Nov;133(3):1360-6.doi: 10.1104/pp.103.029272.

Tasaki T, Mulder LCF, Iwamatsu A, Lee MJ, Davydov IV, Varshavsky A, Muesing M, Kwon, YT. (2005) A Family of Mammalian E3 Ubiquitin Ligases That Contain the UBR Box Motif and Recognize N-Degrons. Molecular and Cellular Biology 7120-7136. doi:10.1128/MCB.25.16.7120-7136.2005

Tasaki T, Zakrzewska A, Dudgeon DD, Jiang Y, Lazo JS, Kwon YT. (2009). The substrate recognition domains of the N-end rule pathway. J Biol Chem. 2009 Jan 16;284(3):1884-95. doi: 10.1074/jbc.M803641200.

van Doorn WG and Papini A. (2013) Ultrastructure of autophagy in plant cells. Autophagy, 9:12, 1922-1936, doi:10.4161/auto.26275.

Vierstra RD. (2009). The Ubiquitin-26S Proteasome System at the Nexus of Plant Biology. Nat Rev Mol Cell Biol. 2009 Jun;10(6):385-97. doi: 10.1038/nrm2688.

Waadt R, Manalansan B, Rauniyar N, Munemasa S, Booker MA, Brandt B, Waadt C, Nusinow DA, Kay SA, Kunz HH, Schumacher K, DeLong A, Yates JR 3rd, Schroeder JI. (2015). Identification of open stomata1-interacting proteins reveals interactions with sucrose non-fermenting1-related protein kinase2 and with type 2A protein phosphatases that function in abscisic acid response. Plant Physiol. 2015 Sep;169(1):760-79. doi: 10.1104/pp.15.00575.

Wachter RM, Elsliger MA, Kallio K, Hanson GT, Remington SJ. (1998). Structural basis of spectral shifts in the yellow-emission variants of green fluorescent protein. Structure. 1998 Oct 15;6(10):1267-77. doi: 10.1016/s0969-2126(98)00127-0.

Walden H, Rittinger K. (2018). RBR ligase-mediated ubiquitin transfer: a tale with many twists and turns. Nat Struct Mol Biol. 2018 Jun;25(6):440-445. doi: 10.1038/s41594-018-0063-3.

Walsh CK, Sadanandom A. (2014). Ubiquitin chain topology in plant cell signalling: a new facet to an evergreen story. Front. Plant Sci. 2014 Apr 1;5:122. doi: 10.3389/fpls.2014.00122.

Wang H, Schippers JHM. (2019). The role and regulation of autophagy and the proteasome during aging and senescence in plants. Genes 2019, 10, 267; doi:10.3390/genes10040267.

Wang R, Liu M, Yuan M, Oses-Prieto JA, Cai X, Sun Y, Burlingame AL, Wang ZY, Tang W. (2016). The Brassinosteroid-Activated BRI1 receptor kinase is switched off by dephosphorylation mediated by cytoplasm-localized PP2A B'Subunits. Mol Plant. 2016 Jan 4;9(1):148-157. doi: 10.1016/j.molp.2015.10.007.

Yamaguchi N, Komeda Y. (2013). The role of CORYMBOSA1/BIG and auxin in the growth of Arabidopsis pedicel and internode. Plant Sci. 2013 Aug;209:64-74. doi: 10.1016/j.plantsci.2013.04.009.

Yamaguchi N, Suzuki M, Fukaki H, Morita-Terao M, Tasaka M, Komeda Y. (2007). CRM1/BIG-Mediated Auxin Action Regulates Arabidopsis Inflorescence Development. Plant Cell Physiol. 2007 Sep;48(9):1275-90. doi: 10.1093/pcp/pcm094.

Ye Y and Rape M. (2009). Building ubiquitin chain: E2 enzymes at work. Nat Rev Mol Cell Biol. 2009 November; 10(11): 755–764. doi:10.1038/nrm2780.

Yoshida S, Ito M, Callis J, Nishida I, Watanabe A. (2002). A delayed leaf senescence mutant is defective in arginyl-tRNA:protein arginyltransferase, a component of the N-end rule pathway in Arabidopsis. Plant J. 32,129-137. doi:10.1046/j.1365-313x.2002.01407.x

Yuan G, Ahootapeh BH, Komaki S, Schnittger A, Lillo C, De Storme N, Geelen D. (2018). Protein Phosphatase 2A B'α and β maintain centromeric sister chromatid cohesion during meiosis in Arabidopsis. Plant Physiol. 2018 Sep;178(1):317-328. doi: 10.1104/pp.18.00281.

Zhang H, Linster E, Gannon L, Leemhuis W, Rundle CA, Theodoulou FL, Wirtz M. (2019). Tandem Fluorescent Protein Timers for noninvasive relative protein lifetime measurements in plants. Plant Physiology 2019, 180:718-731. Plant Physiol. 2019 Jun;180(2):718-731. doi: 10.1104/pp.19.00051.

Zhang RX, Ge S, He J, Li S, Hao Y, Du Y, Liu Z, Cheng R, Feng YQ, Xiong L, Li C, Hetherington AM, Liang YK. (2018). BIG regulates stomatal immunity and jasmonate production in Arabidopsis. New Phytol. 2019 Apr;222(1):335-348. doi: 10.1111/nph.15568

Zhang RX, Li S, He J, Liang YK. (2019). BIG regulates sugar response and C/N balance in Arabidopsis. Plant Signal Behav. 2019;14(11):1669418. doi: 10.1080/15592324.2019.1669418.

7 Appendix

7.1 Primer list

Primer	5' -> 3' sequence
1722-lacIseq2	GTA TTG GGC GCC AGG GTG GTT
1871-KanMXup1	TCG CGG CCT CGA AAC GTG AGT CTT
1872-KanMXdn1	CAG TTT CAT TTG ATG CTC GAT GAG TT
1878-UBR1Bsi113	CCG CGA ACC GTA CGA GGA AAC CAA ATT GTA AGC
1881-UBR1Spe6790	GCC GAC CTC CAC TAG TGC ATT GAC TTC CCC GCG TTT
1919-UBR113Bsi	GAA CGC GGC CGC CAG CTG AAG CTT CGT ACG AGG AAA CCA AAT TGT AAG CAT
1935-UBR6790Spe	GAG ACC GGC AGA TCC GCG GCC GCA TAG GCC ACG GCA TTG ACT TCC CCG CGT
1989-UBR1_840-820	GCT CTG CTC ATG TCA GCC CTT
1992-UBR1_5942-5964	CTC CAT TTG ACA CAG CCT CCT TC
2073-prt13BspH	TCC TCA GTC CCA CAG GGA TGT AGC TTG AAT CAT G
2074-prt13dn1	TTC GCG GAT ACT GCA GCG GTA TGT
2076-yUBR_Fw1	CCC TAT TTT AGG TAT ACG AGG TTT TAG AGC TAG AAA TAG CAA GTT AAA ATA AGG
2077-yUBR_Rv1	CTC GTA TAC CTA AAA TAG GGG ATC ATT TAT CTT TCA CTG CGG AG
2185-13_3g0988dn1	TAA GAG GCA AAC GTT GTT GGA GCT
2186-13_3g0988up1	ATC CCA CTG TGT CTC TCT GTC TC
2187-13_3g1368dn1	CTT CAA ATC TGT CAA CAT GGG AGT T
2188-13_3g1368up1	CTA TTT CCA TAT GGA CTC CTA CAT C
219A URA3tdn	GCT CTA GAA GCT TGT AAA TGC ATG TAT ACT AAA
2293Xfragdn1	AGC TAG CTT ATC GAT ACC GTC GAC AAT TAC TAT TTA CAA TTA CAAT
2294-Xfragup1	TCC TCG CCC TTG CTC ACC ATG GTA CCA GCG TAA TCT GGA AC
2295-Xfragup2	CTT CAC CCT TGC TCA CCA TGG TAC CAG CGT AAT CTG GAAC TGG TAC CAG CGT AAT CTG GAAC
2296-Dagdasdn1	ATG GTG AGC AAG GGC GAG GAG CTG TT
2297-Dagdasup1	CCG GGC CCC CCC TCG AGG TCG ACT ACT TGT ACA GCT CGT CCA TGC CGC C
2298-Wirtzdn1	ATG GTG AGC AAG GGC GAG GA
2299-Wirtzup1	CCG GGC CCC CCC TCG AGG TCG ACT TAC TTA TAA AGC TCG TCC AT
2300-ScarletNeon1(dn1)	ATG GTG AGC AAG GGT GAA GCC GT
2301-ScarletNeon1(up1)	CCG GGC CCC CCC TCG AGG TCG ACT ACT TGT ACA ACT CAT CCA TTC CCA T
2406-BIG1-177dn	GAA CGC CGG AGG ATC CCG GGA TAA TGG CAG ATG ACT TGG C
2407-BIG1234-177up	GAA AAG TGC CAC CTG ACG TCG TAT CAC GAG GCC CTT TC
2408-BIG2-177dn	CCC ACT AGT CTC CAA ACT TCT AGT GCG ATT C
2409-BIG3-177dn	TTG ACA ACA GAT GAT TTG GTT GAC AAT GTT AC
2410-BIG4-177dn	ATC TCT AGA AAG GAG CCT TCA GAT TGA CAT TTC
2451-PGK-Fbxdn1	CCA AAA GAT CCC ATA TGG AGC GGC CTG GCT TGG T
2452-PGK-Fbxlup1	ATG GGA GAT CCC ATA AGC GCT TGT CCT TTC AAT ATA CTC TAC AC
2453-PGK-Fbxsup2	ATG GGA GAT CCC ATA AGC GCT AGT CGT GTG AAC TCT AGA CTT
2456-BIGcDNAPshup2	ATA TCA ATG TGA CCA GTG TCA AGC TTT TTA C

2460-CYCSma2226up	ACC ACT GCG ATC CCC GGG AAA ACA GCA TTC CAG GT
2461-CYCBam3320dn	GAT CCT CCG GCG TTC AGC CTG T
2462-BIG_YCpstart	ATC TGC CAT TAT CCC TAT GGG ATC TTT TGG TTT TAT
2463-BIG_YCpend	CCT CGT GAT ACG ACG TC T ATG GGA TCT CCC ATG TC
2467-UFO1c16dn	GTT CAC ACG ACT AGC ATG GCT ACA TTT GCA CTT CC
2468-UFO1c16lup	GGA GAT CCC ATA AGC TCA CAT ACA AGC TTC TAC CT
2469-UFO1c16sup	GGA GAT CCC ATA AGC TCA AAC ATT ATC AAT GAA AAC
2470-UFO1UBRdn	ATT GAA AGG ACA AGC ATG GAG ACC AAC TCT TCT C
2471-UFO1UBRup	GGA GAT CCC ATA AGC TCA ACC TTT ATG ATT TGA ACA GAA AC
2476-BIGfrNdedn	CCA AAA GAT CCC ATA TGA CAG CAG ATG TGA GAC TTG GT
2477-BIGfrNdeup	ATG GGA GAT CCC ATA TCA AGC AGT AAT AGG AAT AGG AAA T
2478-BIGfrUFO1dn	ATT GAA AGG ACA AGC ACA GCA GAT GTG AGA CTT GGT
2479-BIGfrUFO1up	GGA GAT CCC ATA AGC TCA AGC AGT AAT AGG AAT AGG AAA T
2486-UFO1lc16dn	AAT GAA AGG ACA AGC ATG GCT ACA TTT GCA CTT CC
2488 Telserdn1	CGA ACG ATA GCT CGA GAA TGG TTC GAC CAT TGA ACT
2489 Telserup1	CGG GCA TAT GCT CGA CTA CTT GTA CAA CTC ATC CAT
2490 Telserdn2	CAC GGG GGA CGG TAC CAT GGT TCG ACC ATT GAA CT
2491 Telserup2	CGA CTC TAG AGG ATC TAC TTG TAC AAC TCA TCC AT
2492 Telserdn3	TGA TTA ACA GCC ATG GTT CGA CCA TTG AAC T
2493 Telserup3	ACA TTG AAC TTC CCC CTA CTT GTA CAA CTC ATC CAT

7.2 Constructs

Table 12 Overview of constructs made during this Thesis.

Construct (vector + insert)	Vector (AB marker)	Restriction enzyme (supplier) and buffer	Template for PCR insert	Primer pair	TM[1]
pVTOP + L-iScarlet-mNeonGreen	pVTOP (KanR)	SalI (ThermoScientific) Orange Buffer	pERnew-L-GUS a	2293-Xfragdn1 2295-Xfragup2	57°C/ 71°C
			pMK-T_iScarlet-mNeonGreen	2300-ScarletNeon1(dn1) 2301-ScarletNeon1(up1)	65°C/ 72°C
pVTOP + M-iScarlet-mNeonGreen	pVTOP (KanR)	SalI (ThermoScientific) Orange Buffer	pERnew-M-GUS a	2293-Xfragdn1 2295-Xfragup2	57°C/ 71°C
			pMK-T_iScarlet-mNeonGreen	2300-ScarletNeon1(dn1) 2301-ScarletNeon1(up1)	65°C/ 72°C
pVTOP + R-iScarlet-mNeonGreen	pVTOP (KanR)	SalI (ThermoScientific) Orange Buffer	pERnew-R-GUS a	2293-Xfragdn1 2295-Xfragup2	57°C/ 71°C
			pMK-T_iScarlet-mNeonGreen	2300-ScarletNeon1(dn1) 2301-ScarletNeon1(up1)	65°C/ 72°C
pVTOP + L-Wirtz_mCherry-sfGFP	pVTOP (KanR)	SalI (ThermoScientific) Orange Buffer	pERnew-L-GUS a	2293-Xfragdn1 2294-Xfragup1	57°C/ 71°C
			pBIN AR_S5_tFT	2298-Wirtzdn1 2299-Wirtzup1	60°C/ 72°C
pVTOP + M-Wirtz_mCherry-sfGFP	pVTOP (KanR)	SalI (ThermoScientific) Orange Buffer	pERnew-M-GUS a	2293-Xfragdn1 2294-Xfragup1	57°C/ 71°C
			pBIN AR_S5_tFT	2298-Wirtzdn1 2299-Wirtzup1	60°C/ 72°C
pVTOP + R-Wirtz_mCherry-sfGFP	pVTOP (KanR)	SalI (ThermoScientific) Orange Buffer	pERnew-R-GUS a	2293-Xfragdn1 2294-Xfragup1	57°C/ 71°C
			pBIN AR_S5_tFT	2298-Wirtzdn1 2299-Wirtzup1	60°C/ 72°C
pVTOP + L-Dagdas_YFP-mCherry	pVTOP (KanR)	SalI (NEB) NEBuffer 3.1	pERnew-L-GUS a	2293-Xfragdn1 2294-Xfragup1	57°C/ 71°C
			pGD YFP-mCherry	2296-Dagdasdn1 2297-Dagdasup1	72°C
pVTOP + M-Dagdas_YFP-mCherry	pVTOP (KanR)	SalI (ThermoScientific) Orange Buffer	pERnew-M-GUS a	2293-Xfragdn1 2294-Xfragup1	57°C/ 71°C
			pGD YFP-mCherry	2296-Dagdasdn1 2297-Dagdasup1	72°C

pVTOP + R-Dagdas_YFP-mCherry	pVTOP (KanR)	SalI (NEB) NEBuffer 3.1	pERnew-R-GUS a	2293-Xfragdn1 2294-Xfragup1	57°C/ 71°C
			pGD YFP-mCherry	2296-Dagdasdn1 2297-Dagdasup1	72°C
pBIBpOpTev-c1 + L-iScarlet-mNeonGreen	pBIBpOpTev-c1 (KanR)	XhoI (NEB) CutSmart buffer	pVTOP + L-iScarlet-mNeonGreen	2488 Telserdn1 2489 Telserup1	72°C
pBIBpOpTev-c1 + M-iScarlet-mNeonGreen	pBIBpOpTev-c1 (KanR)	XhoI (NEB) CutSmart buffer	pVTOP + M-iScarlet-mNeonGreen	2488 Telserdn1 2489 Telserup1	72°C
pBIBpOpTev-c1 + R-iScarlet-mNeonGreen	pBIBpOpTev-c1 (KanR)	XhoI (NEB) CutSmart buffer)	pVTOP + R-iScarlet-mNeonGreen	2488 Telserdn1 2489 Telserup1	72°C
pNIGEL + L-iScarlet-mNeonGreen	pNIGEL07 (AmpR)	NcoI/SmaI (NEB) CutSmart buffer	pVTOP + L-iScarlet-mNeonGreen	2492 Telserdn3 2493 Telserup3	72°C
pNIGEL + M-iScarlet-mNeonGreen	pNIGEL07 (AmpR)	NcoI/SmaI (NEB) CutSmart buffer	pVTOP + M-iScarlet-mNeonGreen	2492 Telserdn3 2493 Telserup3	72°C
pNIGEL + R-iScarlet-mNeonGreen	pNIGEL07 (AmpR)	NcoI/SmaI (NEB) CutSmart buffer	pVTOP + R-iScarlet-mNeonGreen	2492 Telserdn3 2493 Telserup3	72°C
pBIN AR + L-iScarlet-mNeonGreen	pBIN AR_S5_tFT	Asp718 (Roche)/ BamHI (ThermoScientific) Buffer B	pVTOP + L-iScarlet-mNeonGreen	2490 Telserdn2 2491 Telserup2	72°C
pBIN AR + M-iScarlet-mNeonGreen	pBIN AR_S5_tFT	Asp718 (Roche)/ BamHI (ThermoScientific) Buffer B	pVTOP + M-iScarlet-mNeonGreen	2490 Telserdn2 2491 Telserup2	72°C
pBIN AR + R-iScarlet-mNeonGreen	pBIN AR_S5_tFT	Asp718 (Roche)/ BamHI (ThermoScientific) Buffer B	pVTOP + R-iScarlet-mNeonGreen	2490 Telserdn2 2491 Telserup2	72°C
YCplac22 + short F-box fragment (Ufo1)	YCplac22 + PRT1	NdeI (NEB) CutSmart buffer	L3	2451-PGK-Fbxdn1 2453-PGK-Fbxsup2	55°C/ 72°C
YCplac22 + long F-box fragment (Ufo1)	YCplac22 + PRT1	NdeI (NEB) CutSmart buffer	L3	2451-PGK-Fbxdn1 2452-PGK-Fbxlup1	55°C/ 72°C
YCplac22 + long Ufo1 + BIGfragment	YCplac22 + long Ufo1	AfeI (NEB) CutSmart buffer	pACYC177 + cDNA_BIG_At3g02260, fragment1+2+3+4, 466bp deletion	2478-BIGfrUFO1dn 2479-BIGfrUFO1up	45°C/ 72°C
YCplac22 + BIGfragment	YCplac22	NdeI (NEB) CutSmart buffer	pACYC177 + cDNA_BIG_At3g02260, fragment1+2+3+4, 466bp deletion	2476-BIGfrNdedn 2477-BIGfrNdeup	45°C/ 72°C

YCplac22 + long Ufo1 + UBR domain (PRT6)	YCplac22 + long Ufo1	AfeI (NEB) CutSmart buffer	Δ9BLRp_pGAD_T_7	2470-UFO1UBRdn 2471-UFO1UBRup	62°C/ 72°C
YCplac22 + long Ufo1 + short cand16 (F-box)	YCplac22 + long Ufo1	AfeI (NEB) CutSmart buffer	AD-c16(short)	2469-UFO1c16sup 2486-UFO1lc16dn	45°C/ 69°C
YCplac22 + long Ufo1 + long cand16 (F-box)	YCplac22 + long Ufo1	AfeI (NEB) CutSmart buffer	At3g12350.2 F-box (c16) cDNA from RIKEN	2468-UFO1c16lup 2486-UFO1lc16dn	45°C/ 69°C
pACYC177 + fragment1_BIG_CDS	pACYC177	BamHI (ThermoScientific)/ AatII (ThermoScientific) Tango buffer	pAGM1311 + pcTK20	2407-BIG1234-177up 2406-BIG1-177dn	63°C/ 72°C
pACYC177 + fragment1+2_BIG_CDS	pACYC177 + fragment 1_BIG_CDS	AatII (ThermoScientific)/ BpiI (NEB) Tango buffer/ 2.1 NEBuffer	pAGM1311 + pcTK21a	2407-BIG1234-177up 2408-BIG2-177dn	57°C/ 72°C
pACYC177 + fragment1+2+3_BIG_CDS	pACYC177 + fragment1+2_BIG_CDS	AatII (ThermoScientific)/ BpiI (NEB) Tango buffer/ 2.1 NEBuffer	pAGM1311 + pcTK22a	2407-BIG1234-177up 2409-BIG3-177dn	68°C/ 72°C
pACYC177 + fragment1+2+3+4_BIG_CDS	pACYC177 + fragment1+2+3_ BIG_CDS	AatII (ThermoScientific)/ BpiI (NEB) Tango buffer/ 2.1 NEBuffer	pAGM1311 + pcTK23b	2407-BIG1234-177up 2410-BIG4-177dn	70°C/ 72°C
pACYC177 + BIG_CDS_complete	pACYC177 + fragment1+2+3+4_BIG_ CDS	PshAI (NEB)/ SmaI (NEB) CutSmart buffer	pACYC177 + fragment1+2+3+4_BIG_CDS	2460-CYCSma2226up 2461-CYCBam3320dn	68°C/ 72°C
			PCR fragment with primer pair 2454-BIGstartdn1 and 2455-BIG1822up, template: cDNA	2406-BIG1-177dn 2456-BIGcDNAPshup2	68°C/ 72°C
YCplac22 + BIG_CDS	pACYC177 + fragment1+2+3+4_BIG_ CDS	SmaI (NEB)/ AatII (ThermoScientific) CutSmart buffer/ Tango buffer	pACYC177 + PRT1	2462-BIG_YCpstart 2463-BIG_YCpend	57°C/ 71°C

[1] if the inserts were amplified in a two step PCR reaction, the first 5 cycles were run at the lower, the last 30 cycles on the higher annealing temperature.